CHAPTER 14

Clock and Serial Data Communications Channel Measurements

Many of today's electronic devices make use of high-speed asynchronous serial links for data communications such as USB, Firewire, PCI-Express, XAUI, SONET, SAS, and so on. Such devices make use of a serializer-deserializer transmission scheme called SerDes. Older devices operated on a synchronous clocking system such as the recommended standard 232 serial bus, referred to as RS232, or the small computer system interface, known as SCSI. While such synchronous buses are being used less as a means to communicate between two separate devices, buses internal to most devices remain for the most part dependent on a synchronous clocking scheme. The goal of this chapter is describe the various data communication schemes used today and how such systems are characterized and tested in production.

This chapter will begin by describing the attributes of both synchronous clock signals and those signals transmitted asynchronous over a serial channel. In the case of synchronous clock signals, both time- and frequency-domain descriptions of performance are described. This includes various time-domain jitter metrics, like periodic jitter and cycle-to-cycle jitter, and frequency-domain metrics, like phase noise. Our readers encountered phase noise for RF systems back in Chapters 12 and 13. It is pretty much the same for clocks. For asynchronous systems, the ultimate measure of performance is bit error rate (BER). The student will learn how to calculate the necessary test time to assure a desired level of BER performance and learn about several techniques that are used in production to reduce this test time. The latter approaches are largely based on jitter decomposition methods, and this chapter will explore four common methods found in production test. Unique to this chapter is the extensive application of probability theory to quantify the use of these jitter decomposition methods. This chapter will conclude with a discussion of several DSP-based test techniques used to quantify jitter transmission from the system input to its output. This includes a discussion about jitter transfer function test and a jitter tolerance test.

14.1 SYNCHRONOUS AND ASYNCHRONOUS COMMUNICATIONS

When two devices exchange data, there is a flow of information between the two. Typically, this information is transmitted in the form of a set of binary bits referred to as a symbol. As this

Figure 14.1. Synchronous clock distribution between two D-type registers.

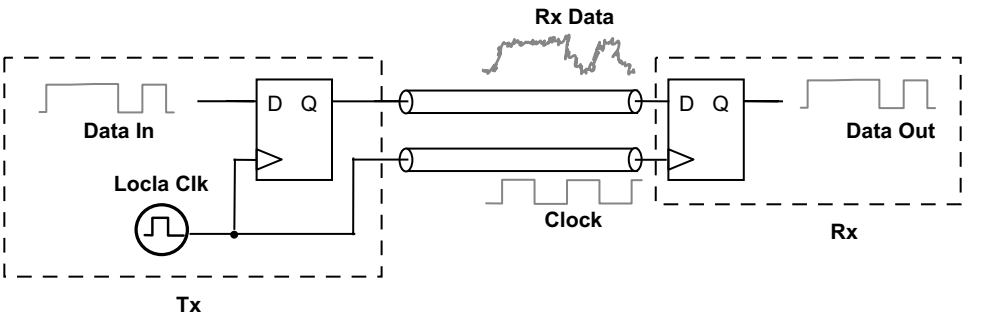

Figure 14.2. An asynchronous data communication link involving two D-type registers.

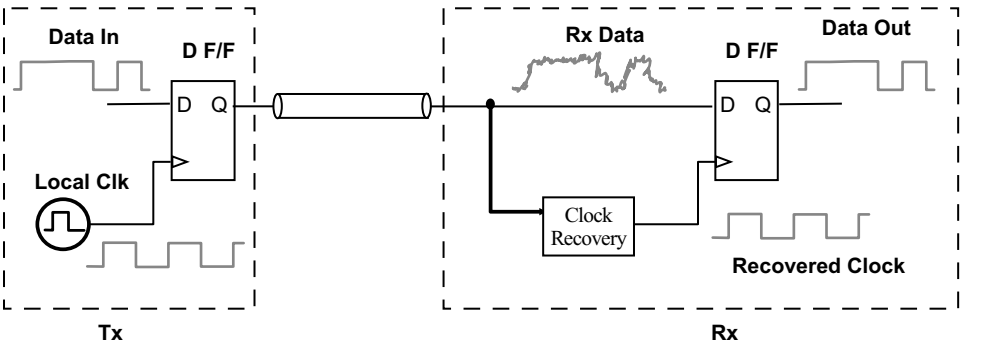

information is transmitted in sequence, the receiver must have the means to extract the individual symbols. As symbols arrive as a continuous stream of bits, one has to be able to separate one symbol from another. In asynchronous communications, each symbol is separated by the equivalent of a tag so that one knows exactly when the symbol arrives at its destination. In synchronous communications, both the sender and receiver are synchronized with a separate clock signal, thereby providing all necessary timing information at both ends.

Figure 14.1 illustrates a typical synchronous system involving two D-type registers physically separated from one another via a transmission line. One-bit data are exchanged between the two registers through the action of the falling or rising edge of the clock signal. The clock signal is used to specify when a specific bit is to be transmitted and received. Due to the physical distance between the sender and the receiver, and the fact that the clock signal travels at about one-half light speed on a PCB (equivalent to 3.3 ns/m or 2 ns/ft), the timing information is not the same at all locations. This results in timing differences between the clock signal at the transmit and receive ends, commonly referred to as clock skew. Ultimately, clock skew limits the maximum rate at which symbols can be exchanged between the transmitter and the receiver.

Conversely, an asynchronous system involving two D-type registers does not share a common clock signal (Figure 14.2). Rather, the timing information associated with the clock signal is embedded in the data stream and recovered by the receiver by a clock recovery (CR) circuit. While the system is more complicated than a synchronous system, no clock skew occurs. This enables faster data exchange rates. For this reason alone, asynchronous data communications is fast becoming the dominant method of exchanging information between electronic devices.

While asynchronous systems avoid the problem of clock skew, both synchronous and asynchronous systems suffer from the effects of circuit noise. While the source of noise is identical to that which we studied previously, here we are interested in the effect of noise on the timing information that is associated with a data communication link. Deviation from the reference signal is referred to as clock jitter.

14.2 TIME-DOMAIN ATTRIBUTES OF A CLOCK SIGNAL

A clock signal is used in both synchronous and asynchronous systems in one form or another. Deviations from its ideal behavior affect the overall performance of the data communication system.

Mathematically, we can define the transmit clock with frequency f_o as

$$c_{Tx}(t) = \text{sgn}\left[\cos\left(2\pi f_o t\right)\right] \tag{14.1}$$

where sgn( ) is the sign function and is defined as follows

$$\text{sgn}(x) = \begin{cases} 1, & x > 0 \\ 0, & x = 0 \\ -1, & x < 0 \end{cases} \tag{14.2}$$

The clock signal is assumed to be symmetrical with a zero DC offset and a 1-V signal amplitude. Of course, any offset and amplitude can be incorporated into the model of the clock by introducing the appropriate terms.

If the clock signal experiences a time delay as it travels from one point to another, say on a PCB, then we can model the received clock signal by incorporating a time delay T_D in Eq. (14.1) according to

$$c_{Rx}(t) = \text{sgn}\left\{\cos\left[2\pi f_o\left(t - T_D\right)\right]\right\} \tag{14.3}$$

From a system timing perspective, the time at which the rising edge of a clock signal crosses the logic level threshold, represented here by the 0-V level, can be deduced from Eq. (14.3) by equating it to 0 and solving for the zero crossing times. This is illustrated in Figure 14.3 for both the transmit and received clock signals. Following this logic, we can write

$$T_{ZC}(n) = \frac{2\pi n + 2\pi f_o T_D}{2\pi f_o} = \frac{n}{f_o} + T_D \tag{14.4}$$

where n represents the nth clock cycle associated with the transmit clock. In the manner written here, clock skew alters the zero crossing point by a constant amount T_D. However, in practice, T_D varies from system to system and from device to device, hence we must treat T_D as a random variable. Let us assume that T_D is a Gaussian random variable with mean value T_D and standard deviation σT_D; then we can write the mean value and standard deviation of the zero crossing point as

$$\begin{aligned} \mu_{ZC} &= \mu_{T_D} \\ \sigma_{ZC} &= \sigma_{T_D} \end{aligned} \tag{14.5}$$

Figure 14.3. Zero crossing times associated with a clock signal.

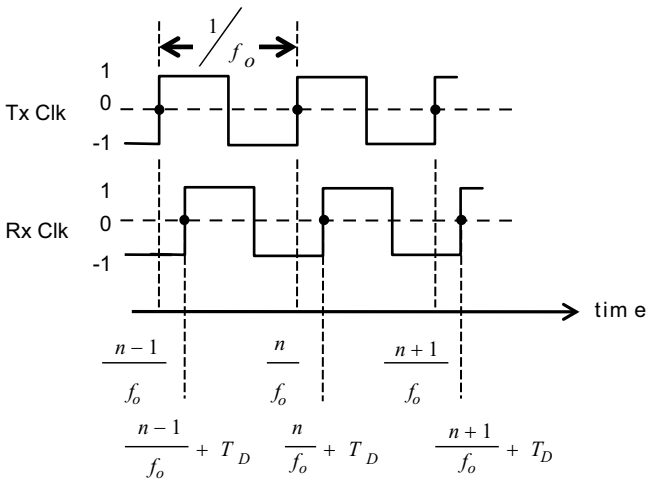

Figure 14.4. Illustrating the effects of noise on the received clock signal when compared against that which was transmitted.

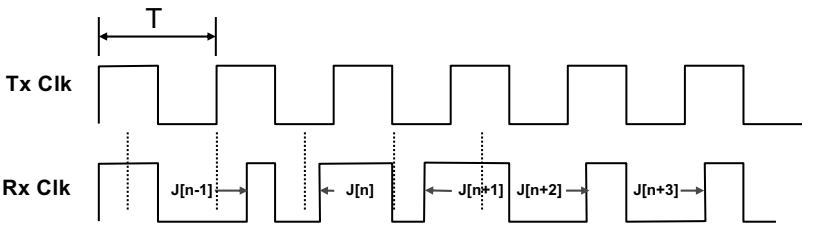

Since the standard deviation is nonzero, it indicates that the zero crossing times will vary and in some way act to reduce the amount of time available for the logic circuits to react to incoming signals, thereby increasing the probability of logic errors.

In addition to clock skew, noise is always present in any electronic circuit. While noise may arise from many different sources, the effect of noise on a synchronous or asynchronous system is to alter the zero crossing point. This is depicted in Figure 14.4, where a received signal is compared to a transmitted signal minus any physical delays for ease of comparison. Here we see that the zero crossing of the received clock varies with respect to that which was transmitted. If we denote the time difference between the transmit and received zero crossings as $J(n)$, then we can gather a set of data and perform some data analysis to better understand the underlying noise mechanism. For ease of discussion, we shall refer to $J(n)$ as the instantaneous time jitter associated with the received signal. Conversely, we can convert this jitter term into a phase-difference jitter term, that is,

$$\phi[n] = 2\pi f_o \times J[n] = 2\pi \times \frac{J[n]}{T} \tag{14.6}$$

In the study of jitter one finds several ways to interpret jitter behavior. The most common approach is to construct a histogram of the instantaneous jitter and observe the graphical behavior

Figure 14.5. Typical jitter histogram and its corresponding density function.

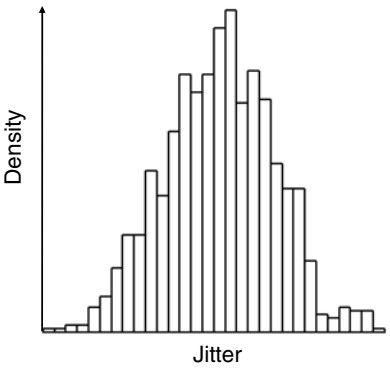

Figure 14.6. The histogram and PDF associated with a random noise and a sinusoidal signal.

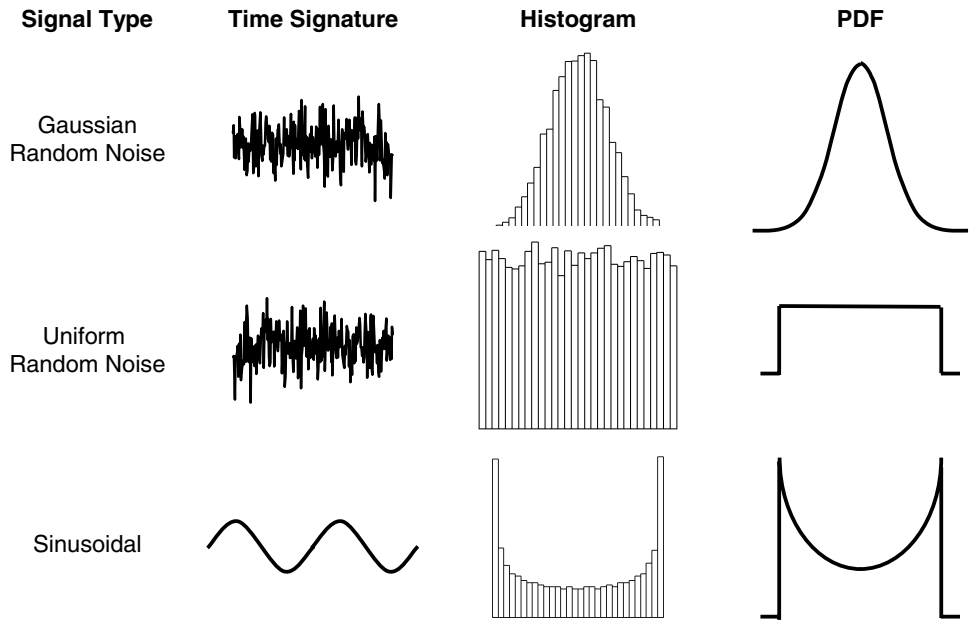

that results (see Figure 14.5). By comparing it to known shapes, one can deduce the nature of the underlying source of jitter, at least in a qualitative manner. For example, Figure 14.6 illustrates the histogram as well as its corresponding PDF for several known signal types such as a Gaussian random noise signal, a uniform random noise signal, and a sinusoidal signal. It is reasonable to assume that the distribution shown in Figure 14.5 was obtained from a noise source with a Gaussian distribution and not one from a signal involving a uniform random noise signal or a signal with a sinusoidal component.

To obtain a more quantitative measure of jitter, one can extract statistical measures[1] from the captured data such as the mean and standard deviation. For instance, if N samples of the instantaneous jitter is captured, then we can calculate the mean according to

$$\mu_J = \frac{1}{N}\sum_{n=1}^{N} J[n] \tag{14.7}$$

and the standard deviation as

$$\sigma_J = \sqrt{\frac{1}{N}\sum_{n=1}^{N}\left\{J[n]-\mu_J\right\}^2} \tag{14.8}$$

Here the mean value would refer to the symmetric timing offset associated with the data set. If the data represent the jitter associated with a received signal, then the mean value represents the clock skew mentioned earlier. Often we are also interested in the peak-to-peak jitter, which is computed as follows:

$$pp_J = \max\left\{J[1], J[2]\cdots J[N]\right\} - \min\left\{J[1], J[2]\cdots J[N]\right\} \tag{14.9}$$

Due to the statistical nature of a peak-to-peak estimator, it is always best to repeat the peak-to-peak measurement and average the set of values, rather than work with any one particular value. A peak-to-peak metric is a biased estimator and will increase in value as the number of points collected increases. This stems from the fact that a Gaussian random variable has a theoretically infinite peak-to-peak value, although obtaining such a value would require infinite samples. We often to refer to such random variables as being unbounded since they theoretically have no limit.

There are other types of analysis that can be performed directly on the time jitter sequence. For instance, one may be interested in how the period of the clock varies as a function of time. This removes any time offset or skew. Mathematically, this is defined as

$$J_{PER}[n] = J[n] - J[n-1] \tag{14.10}$$

where we denote $J_{PER}[n]$ as the period jitter for the nth clock cycle. For a large enough sample set, we can calculate the mean and standard deviation of the period jitter. We can also define a cycle-to-cycle time jitter metric as follows:

$$J_{CC}[n] = J_{PER}[n] - J_{PER}[n-1] \tag{14.11}$$

Substituting Eq.(14.10) into Eq.(14.11), we can write the cycle-to-cycle jitter in terms of the time jitter as

$$J_{CC}[n] = J[n] - 2J[n-1] + J[n-2] \tag{14.12}$$

Mean and standard deviation can be computed when a significant number of samples of cycle-to-cycle jitter are captured.

Sometimes jitter metrics are used that go beyond comparing adjacent edges or periods and instead look at the difference between a multiple number of edges or periods that have passed.

Such metrics are referred to as *N*-period or *N*-cycle jitter. Let us assume that *N* is the number of periods of the clock signal that separate the edges or periods, then we can write the new metrics as

$$J_{N,PER}\left[n\right] = J\left[n+N-1\right] - J\left[n-1\right] \tag{14.13}$$

and

$$J_{N,CC}\left[n\right] = J_{PER}\left[n+N-1\right] - J_{PER}\left[n-1\right] \tag{14.14}$$

Phase, period, and cycle-to-cycle jitter provide information about clock behavior at a localized point in time. *N*-period or *N*-cycle jitter metrics track the effects of jitter that accumulate over time, at least, over the *N* period observation interval.

Time jitter, period jitter, and cycle-to-cycle jitter are related quantities. They are related through the backwards difference operator, a functionanalogous to differentiation for continuous functions. Assuming that time jitter has a uniform frequency distribution, period jitter will have a high-pass nature that increases at rate of 20 dB/decade across the frequency spectrum. Cycle-to-cycle jitter will also have a high-pass behavior but will increase at a much faster rate of 40 dB/dec. In both cases, low-frequency jitter components will be greatly attenuated and will not have much influence on the jitter metric. This may lead to incorrect decisions about jitter, so one must be careful in the use of these jitter metrics.

Metrics that provide insight into the low-frequency variation of jitter involve a summation or integration process as opposed to a differencing or differentiation operation. One such metric is known as accumulated jitter or long-term jitter. Accumulated jitter involves collecting the statistics of time jitteras a function of the number of cycles that has passed from the reference point. In order to identify the reference point, as well the time instant the time jitter is captured, we write $J[n,k]$ where n is the sampling instant and k is the number of clock delays that has passed from the reference point. Figure 14.7a illustrates the time jitter captured as a function of clock period delay, k. For each delay, we compute the statistics of the jitter, that is,

$$\begin{aligned} \mu_J\left[k\right] &= \frac{1}{N}\sum_{n=0}^{N} J\left[n,k\right] \\ \sigma_J\left[k\right] &= \sqrt{\frac{1}{N}\sum_{n=0}^{N}\left[J\left[n,k\right]-\mu_J\left(k\right)\right]^2} \qquad \text{for } k = 0,\ldots,\frac{N}{2} \end{aligned} \tag{14.15}$$

Accumulated jitter refers to the behavior of the standard deviation $\sigma_j[k]$ as a function of the delay index, k, as illustrated in Figure 14.7b. This particular jitter accumulation plot would be typical of a PLL. It is useful for identifying low-frequency jitter trends associated with the clock signal. The concept of accumulated jitter is related to the autocorrelation function of random signals. As a word of caution, the length of each jitter sequence must be the same for each delay setting to ensure equal levels of uncertainty.Moreover, the length of each sequence must be no longer than the fastest time constant associated with the jitter sequence. For instance, if the jitter sequence has a noise bandwidth of 1 MHz, then the time over which a set of points are collected should be no longer than 1 μs.

Figure 14.7. Accumulated jitter: (a) illustrating the sampling instant as function of the number of clock period delays from the reference point. (b) Jitter standard deviation as a function of delay index, *k*.

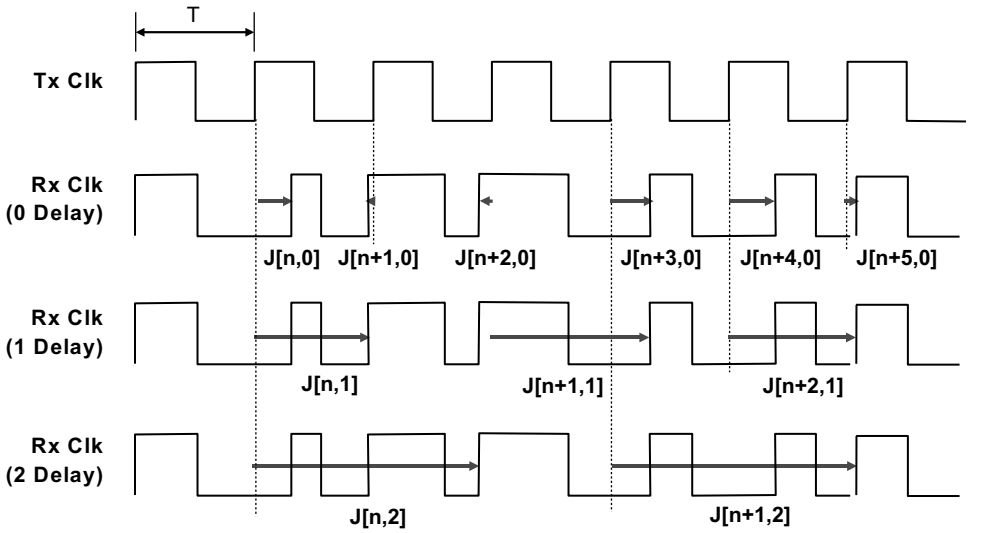

(a)

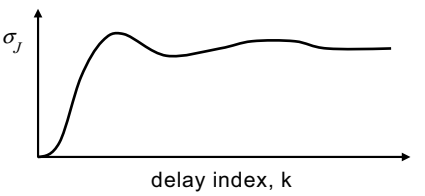

(b)

Exercises

14.1. A set of 8 samples was extracted from a received signal with respect to a reference clock having the following instantaneous time jitter values: [1 ps, 1 ps, -2 ps, 3 ps, 1 ps, 0 ps, -1 ps, 5 ps]. What is the mean, standard deviation and peak-to-peak values?

ANS. $\mu = 1\times 10^{-12}$, $\sigma = 2.06\times 10^{-12}$, $pp = 7\times 10^{-12}$.

14.2. Compute the period jitter and cycle-to-cycle jitter from time jitter samples of exercise 15.1.

ANS. J_{PER} = [0 ps, –3.5 ps, –2 ps, –1 ps, –1.6 ps]; J_{CC} = [–3.8 ps, –7 ps, 1 ps, 0 ps, 7 ps].

14.3 FREQUENCY-DOMAIN ATTRIBUTES OF A CLOCK SIGNAL

While time-domain measures of a clock signal are commonly used to describe its behavior, a power spectral density (PSD) description or phase noise $\pounds(\Delta f)$ is also used. The reader was introduced to this approach back in Sections 12.3.3 and 13.4 for RF circuits. The same approach extends to clock signals in almost the exact same way.[2,3]

Figure 14.8. (a) PSD of an ideal clock signal. (b) PSD of a jittered clock signal.

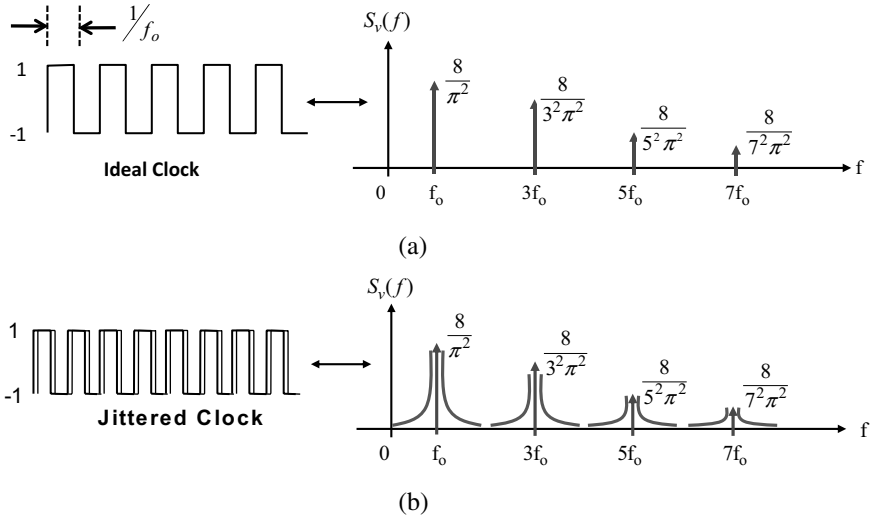

The PSD of an ideal clock signal $S_v(f)$ expressed in units of V^2 per Hz is illustrated in Figure 14.8a. Here the clock signal is decomposed into a set of monotonically decreasing sized impulses that are odd multiples of the clock frequency f_o. The impulses indicate that each harmonic contributes a constant level of power to the spectrum of the clock signal. When random jitter is present with the clock signal, it modifies the spectrum of the clock signal by adding sidebands about each harmonic as shown in Figure 14.8b. This spectrum is the result of noise in the clock circuitry phase modulating the output signal. We learned in Section 12.3.3 that the resulting PSD follows a Lorentzian distribution.

The instantaneous phase difference ϕ between the first harmonic of the clock signal located at f_o and a signal occupying a 1-Hz bandwidth offset from this harmonic by some frequency Δf has a PSD described by

$$S_\phi(\Delta f) = 2\frac{S_v(f_o+\Delta f)}{S_v(f_o)} \quad \frac{\text{rad}^2}{\text{Hz}} \tag{14.16}$$

As we learned in Section 12.3.3, $s_\phi(\Delta f)$ is related to the 1139IEEE standard definition for phase noise £(Δf) according to

$$£(\Delta f)\big|_{\text{dBc/Hz}} \triangleq 10\log_{10}\left[\frac{S_\phi(\Delta f)}{2}\right] = 10\log_{10}\left[\frac{S_v(f_o+\Delta f)}{S_v(f_o)}\right] \tag{14.17}$$

The term dBc is a shorthand notation for "decibels with respect to carrier." In the context of clock signals, the carrier is the fundamental harmonic of the clock.

In many measurement situations involving a spectrum analyzer, the PSD displayed on the screen of the instrument is not in terms of V^2 per Hz but rather V^2 per resolution bandwidth in Hz. The resolution bandwidth (BW) represents the equivalent noise bandwidth of the front-end filter of the spectrum analyzer. To get the correct PSD level, one must scale the instrument PSD

EXAMPLE 14.1

Below is a PSD plot of the voltage level associated with a clock generator captured by a spectrum analyzer with a center frequency of 1.91 GHz and a resolution bandwidth of 200 kHz. Each frequency division represents 1-MHz span. What is the phase noise £(*f*) at a 1-MHz offset from the 1.91-GHz fundamental tone of this clock signal?

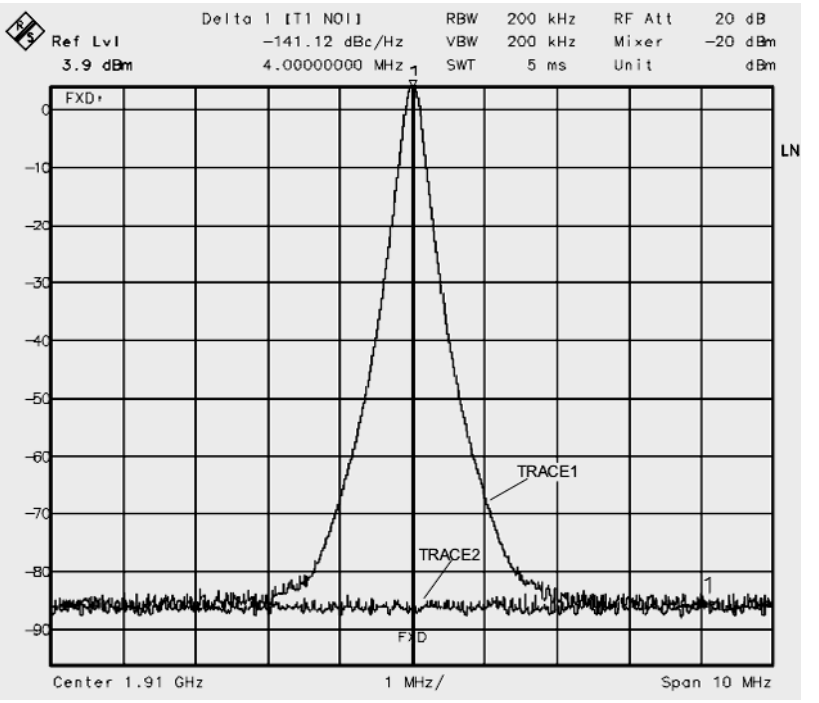

Solution:

As the carrier at 1.91 GHz has a signal level of 3.9 dBm and the PSD at 1 MHz offset from the carrier is –68 dBm, the phase noise metric [Eq. (14.19)] is computed as follows:

$$£\,(1\text{ MHz}) = -68\text{ dBm} - 3.9\text{ dBm} - 3.9\text{ dBm} - 10\log_{10}(200 \times 10^3) = -124.9\frac{\text{dBc}}{\text{Hz}}$$

Hence, the phase noise at a 1-MHz frequency offset is –124.9 dBc/Hz.

Exercises

14.3. The PSD of the voltage level of a 10-MHz clock signal is described by $S_v(f) = 10^{-8}/10^4 + (f - 10^7)^2 + 0.5 \times \delta(f - 10^7)$ in units of V2/Hz. What is the RMS noise level associated with this clock signal over a 1000-Hz bandwidth center around the first harmonic of the clock signal?

ANS. $V_{rms} = \sqrt{\int_{10\text{MHz}-500\text{Hz}}^{10\text{MHz}+500\text{Hz}} \frac{10^{-8}}{10^4 + (f - 10^7)^2}\, df} =$ 1.66×10^{-5} V

14.4. The PSD of the voltage level of a 10-MHz clock signal is described by $S_v(f) = 10^{-8}/10^4 + (f - 10^7)^2 + 0.5 \times \delta(f - 10^7)$ in units of V2/Hz. What is the phase noise of the clock at 1000-Hz offset in dBc/Hz?

ANS. $£(1\,\text{kHz}) = -137.0$ dBc/Hz.

by dividing by the factor BW. In terms of the phase noise metric, £(Δf), the expression would become

$$£(\Delta f)\big|_{\text{dBc/Hz}} = 10\log_{10}\left[\frac{1}{BW}\frac{S_v(f_o + \Delta f)}{S_v(f_o)}\right] \tag{14.18}$$

More often than not, the data read off a spectrum analyzer is in terms of dBm, hence we convert Eq. (14.18) into the following equivalent form

$$£(\Delta f)\big|_{\text{dBc/Hz}} = P_{SSB}\big|_{\text{dBm}} - P_{carrier}\big|_{\text{dBm}} \tag{14.19}$$

where we define $P_{\text{carrier}}\big|_{\text{dBm}} = 10\log_{10}\left[S_v(f_o)\right]$ and $P_{SSB}\big|_{\text{dBm}} = 10\log_{10}[S_v(f_o + \Delta f)] - 10\log_{10}(BW)$, both in units of dBm.

In the study of jitter, one often comes across different measures of the underlying noise mechanisms associated with a clock signal. In the previous section, measures such as a time-jitter sequence $J[n]$ or a period jitter sequence $J_{PER}[n]$ were introduced. In all cases, these sampled quantities are related to one another through a linear operation. For instance, from Eq. (14.6) the phase-difference sequence is related to the time-jitter sequence through the proportional constant $2\pi/T$, where T is the period of the clock signal. Correspondingly, the PSD of the time-jitter sequence can be expressed in terms of the PSD of the phase jitter according to

$$S_J(\Delta f)\big|_{\text{s}^2/\text{Hz}} = \left(\frac{T}{2\pi}\right)^2 S_\phi(\Delta f)\ \frac{\text{s}^2}{\text{Hz}} \tag{14.20}$$

Normalizing by the period T, we can express the jitter PSD in terms of the unit interval (denoted as UI) and write Eq. (14.20) as

$$S_J(\Delta f)\big|_{\text{UI}^2/\text{Hz}} = \left(\frac{1}{2\pi}\right)^2 S_\phi(\Delta f)\ \frac{\text{UI}^2}{\text{Hz}} \tag{14.21}$$

We can also relate the phase noise £(Δf) to the PSD of the jitter sequence expressed in s^2/Hz or in UI^2/Hz by substituting Eq. (14.20) or Eq.(14.21) into Eq.(14.16) above.

To obtain the PSD associated with the phase signal, we can perform an FFT analysis of the samples of the instantaneous phase jitter signal. Following the procedure outlined in Section 9.3.3,

we first calculate the RMS value of the spectral coefficients of the DTFS representation of the phase error signal, that is,

$$c_{k,RMS} = \begin{cases} \left|\Phi\left[k\right]\right|, & k = 0 \\ \sqrt{2}\left|\Phi\left[k\right]\right|, & k = 1,\ldots,N/2-1 \\ \dfrac{\left|\Phi\left[k\right]\right|}{\sqrt{2}}, & k = N/2 \end{cases} \tag{14.22}$$

where the N-point variable Φ is obtain from the N-point FFT analysis from the phase-jitter sequence ϕ expressed in radians as follows:

$$\Phi = \frac{\text{FFT}\left\{\phi\left[n\right]\right\}}{N} \tag{14.23}$$

As a phase signal may consist of both periodic signals (e.g., spurs) and noise, we must handle the two types of signals differently. Specifically, $S_\phi[k]$ of the random noise component expressed in rad^2-per-Hz is given by

$$S_\phi\left[k\right] = c_{k,RMS}^2 \times \frac{N}{F_s} \quad \frac{\text{rad}^2}{\text{Hz}} \tag{14.24}$$

whereas the power associated with any periodic component in the spectrum of the phase signal expressed in rad^2 is given by

$$S_\phi\left[k_{tone}\right] = c_{k,RMS}^2 \quad \text{rad}^2 \tag{14.25}$$

Here $k = k_{tone}$ represents the bin location of the tone. As these tonal components are not known *a priori*, the user must decide if a periodic component is present and its corresponding bin location. If the number of samples is increased, the PSD level of the random component will remain the same, however, a periodic component will increase in amplitude, thereby revealing its periodic nature. To summarize, the $S_\phi[k]$ of the phase signal can be described as

$$S_\phi\left[k\right] = \begin{cases} c_{k,RMS}^2 \times \dfrac{N}{F_s} & \dfrac{\text{rad}^2}{\text{Hz}}, \quad k = 0,\ldots,N/2, \quad k \neq \text{tone BIN} \\ c_{k,RMS}^2 & \text{rad}^2, \quad k = \text{tone BIN} \end{cases} \tag{14.26}$$

Because the phase noise PSD sequence will change with different sample sets, it is customary to average K-sets of the PSD on a frequency-by-frequency basis and obtain an average PSD behavior defined as follows

$$\hat{S}_\phi\left[k\right] = \frac{1}{K}\sum_{i=1}^{K} S_{\phi,i}\left[k\right] \tag{14.27}$$

where the subscript i indicates the ith-PSD obtain from Eq. (14.26). These short-term PSDs are commonly referred to as periodograms.

EXAMPLE 14.2

The following plot of a 512-point phase-difference sequence was obtained from a heterodyning process for capturing the phase errors associated with a clock signal:

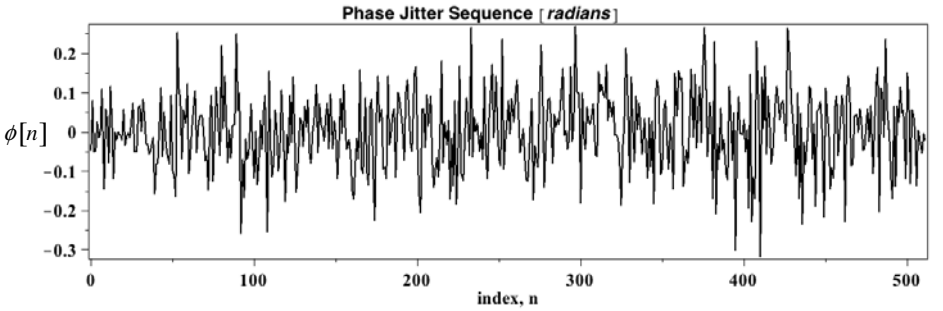

The samples were obtained with a digitizer operating at a 10 MHz sampling rate. The continuous-time phase signal passes through a 1-MHz low-pass filter prior to digitization. What is the phase noise £(Δf) at a frequency offset of about 40 kHz for this particular sample set?

Solution:
Because the sampling rate is 10 MHz and 512 points have been collected, the frequency resolution of the PSD will be

$$\frac{F_s}{N} = \frac{10 \times 10^6}{512} = 19531.25 \text{ Hz}$$

Hence we can find the offset in the second bin of the PSD of phase error signal at about 39.0625 kHz. The PSD of the phase signal is found by sequencing through Eqs. (14.22) to (14.26), resulting in the following PSD plot of $S_\phi[k]$:

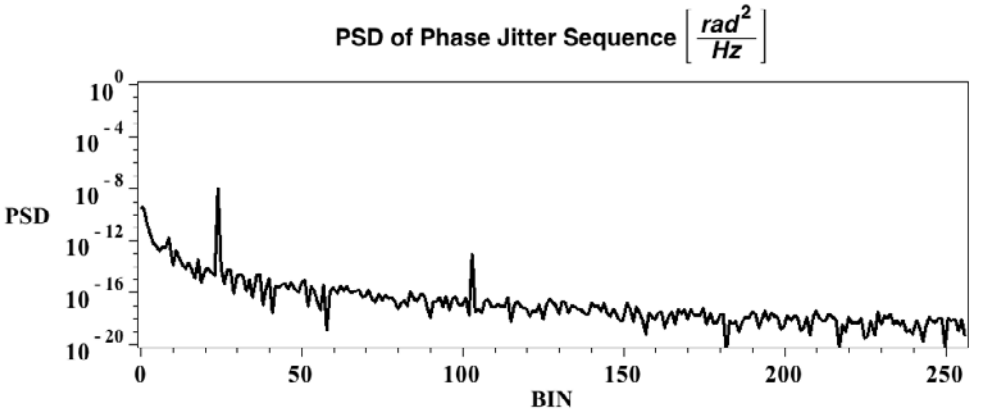

Here we see that spurious tones are present in bins 24 and 103 corresponding to frequencies of 468.75 kHz and 2.0117 MHz. In order to remove the statistical variation in the PSD, we repeated the sampling process an additional 10 times and then averaged the PSD. The resulting smoothed

PSD for the phase noise is as follows:

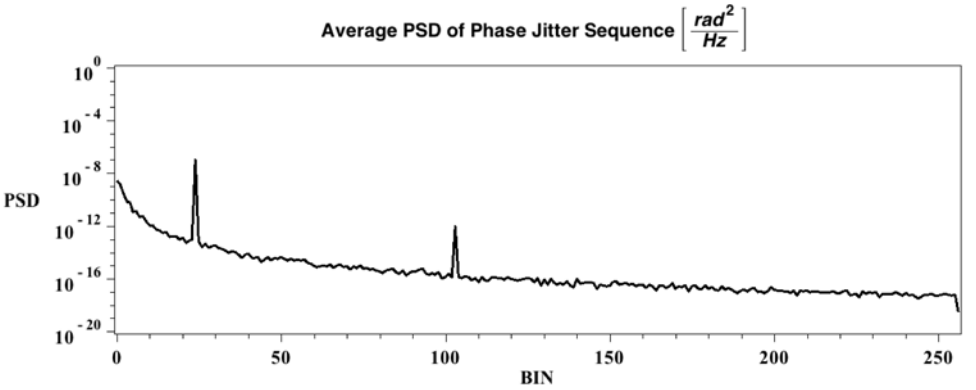

From the information contained in bin 2, we obtain

$$\hat{S}_{\phi}[2] = 2.66 \times 10^{-10} \quad \frac{\text{rad}^2}{\text{Hz}}$$

Subsequently, we compute the phase noise metric at a 39.0625 kHz offset from the carrier as follows:

$$\pounds(39.0625\ \text{kHz}) = 10\log_{10}\left[\frac{2.66 \times 10^{-10}}{2}\right] = -98.8 \quad \frac{\text{dBc}}{\text{Hz}}$$

Exercises

14.5. The PSD of the instantaneous phase of a 10 MHz clock signal is described by $S_{\phi}(f) = 10^{-8}/10^4 + f^2$ in units of rad²/Hz. What is the PSD of the corresponding jitter sequence in UI²/Hz?

ANS. $S_J(f) = \left(\frac{1}{2\pi}\right)^2 \frac{10^{-8}}{10^4 + f^2} \quad \frac{\text{UI}^2}{\text{Hz}}$

14.6. The PSD of the instantaneous phase of a 10-MHz clock signal is described by $S_{\phi}(f) = 10^{-8}/10^4 + f^2$ in units of rad²/Hz. What is the phase noise of the clock at a 1000-Hz offset in dBc/Hz?

ANS. $\pounds = -143.1$ dBc/Hz.

14.4 COMMUNICATING SERIALLY OVER A CHANNEL

Serial communication is the process of sending data one symbol at a time, sequentially, over a communication channel. In order to retrieve the symbols that were sent, some form of synchronization between the transmitter and the receiver is required. This is typically performed with the aid of a clock signal combined with the data. In this section, we shall create a model of the communication channel, provide measures of transmission quality, and describe various methods to test for system behavior. Many of the methods used to describe system behavior are extension of the methods introduced for clock signals.

14.4.1 Ideal Channel

A simple model of a serial communication system is shown in Figure 14.9 consisting of a transmitter, an ideal channel with T_D time delay, and a receiver. For sake of argument, we will assume that the symbol being transmitted is either a binary 0 or 1. With an ideal channel, the data that are transmitted is delivered to the receiver in the exact same form that it was transmitted. That is, if a binary 1 were sent at time instant TS_1, then at the receiver a binary 1 would arrive at time $TS_1 + T_D$. If another symbol were sent some time instant later, say TS_2, then this symbol would arrive at the receiver at time $TS_2 + T_D$. It is fair to say that at the receiver end, there is a 50% probability that the received symbol is a 1 if we assume that there is a 50% probability that a 1 was transmitted. Likewise, a binary 0 will arrive with identical probability since there are only two possible outcomes.

In practice, a signal cannot be sent in zero time, because this would require infinite bandwidth. A better model of system behavior is one where the transmitter sends a pulse of some finite width duration T and height 1 or 0, depending on the bit being sent, as depicted in Figure 14.10. At the receiver end, a process must be in place to decide whether a 0 or a 1 was transmitted at the appropriate time. To gain insight into this process, consider overlaying k durations of the received signal into one full bit period T, as illustrated in Figure 14.11a. It is customary to normalize the time axis by the bit duration and refer to the normalized bit period as the unit interval, UI. On doing so, the resulting diagram is called an *eye diagram* and is used extensively in data communication studies. We can just as easily express the horizontal axis of the eye diagram in terms of denormalized time as shown in Figure 14.11b. For our convenience throughout this chapter we shall work with the denormalized eye diagram.

An eye diagram is a two-dimensional diagram where the vertical axis represents the range of possible signals that can appear at the receiver end and the horizontal axis represents the range of times modulo the bit duration T that also appears at the receiver end. For any bit of information that is transmitted, two pieces of information must be transmitted: the bit level and the time at which bit is sent. At the receiver end, these two pieces of information must be extracted from the incoming signal. A decision-making process involving two decision thresholds performs this operation. One threshold V_{TH} is used to determine if the receive level is a logically high or low

Figure 14.9. Asynchronous communications through an ideal channel with ideal signaling.

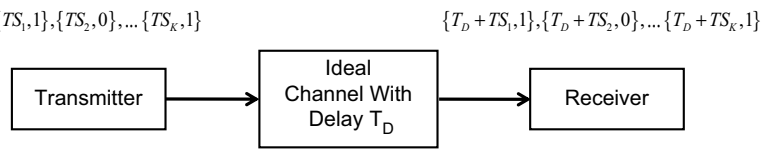

Figure 14.10. Asynchronous communications using finite width pulses.

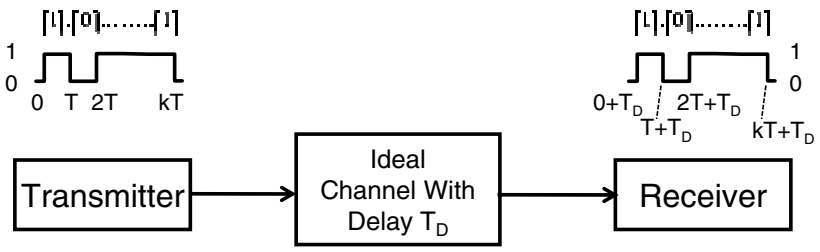

Figure 14.11. Illustrating the creation of an eye diagram from the received signal: (a) normalized eye diagram (b) denormalized eye diagram.

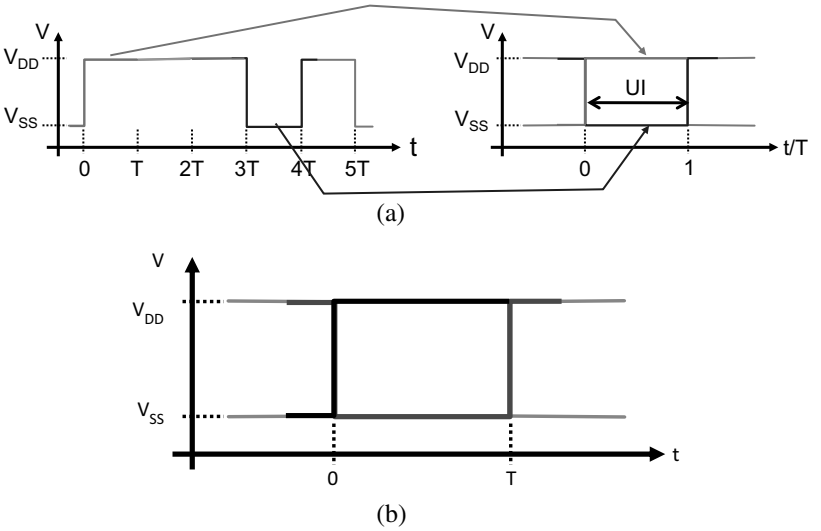

Figure 14.12. Illustrating the decision level thresholds associated with an eye diagram.

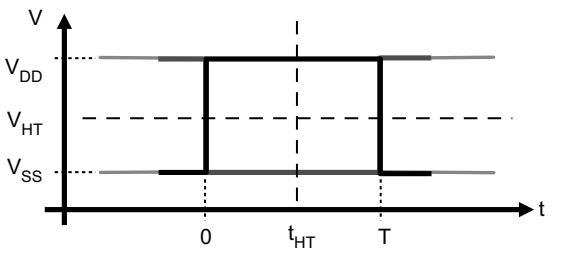

level and the other threshold t_{TH} is used to set the bit sample time (between 0 and T). To maximize the likelihood of making the correct decision, the decision point lies in the middle of the range of possible values as shown in the eye diagram of Figure 14.12.

At this point in our discussion it is interesting to make some general statement about the events that are taking place at the receiver. From the eye diagram we see that received signal crosses the logic threshold V_{TH} at two points: $t = 0$ and $t = T$. If we assume that a logical 0 or 1 is equally likely, then the probability that either a 0–1 transition or 1–0 transition occurs is also equally likely at a 50% probability level. Hence we can model the PDF of the time at which a signal crosses the logic threshold (also referred to as the zero-crossing) with two equal-sized delta functions at $t = 0$ and $t = T$, each having a magnitude of 50% as shown in Figure 14.13a. Likewise, we can model the PDF of the voltage level that appears at the receiver in a similar manner as shown in Figure 14.13b. These two plots correspond to the fact that perfect square waves appear at the receiver. In a real serial communication system, such perfection is a very long way off.

14.4.2 Real Channel Effects

Transmitted signals experience interference and dispersion effects as the signal propagates through the channel to the receiver. As a result, the receive signal contains additional noise not sent by

Figure 14.13. A PDF interpretation of the received signal: (a) as measured along the voltage decision axis defined by $V = V_{TH}$. (b) as measured along the time decision axis defined by $t = t_{TH}$.

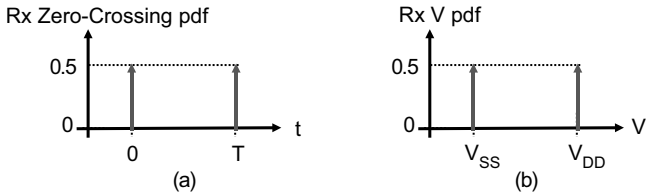

Figure 14.14. Real channel effects; (a) A pulse experiencing an additive noise effect. (b) A pulse experiencing a spreading effect due to the dispersion nature of the channel.

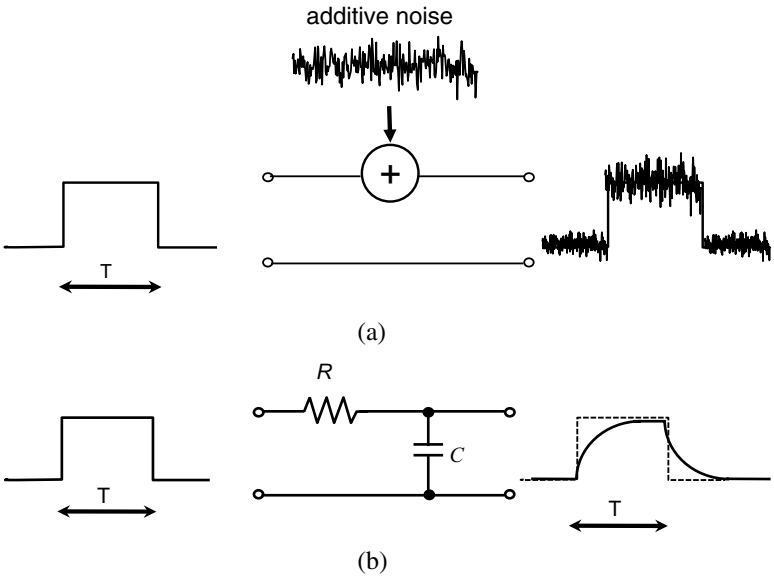

the transmitter, and the signal experiences a spreading effect due to the dispersion of the channel (e.g., high-frequency attenuation effects, as well as a delay dependent on frequency). We model the additive noise with a summing block placed in series with the channel, as illustrated in Figure 14.14a. A simple model that captures the basic idea of dispersion is that shown in Figure 14.14b. Here the channel is model as a simple RC circuit. A square pulse of duration T applied to one end of the RC line comes out of the other end as an exponential type pulse with a duration that extends beyond time T. It is this pulse spreading effect that can lead to a bit interfering with the next bit. When this occurs, it is referred to as *inter-symbol interference* (ISI).

Noisy Channel

Let us begin our investigation of real channels by modeling the effects of additive noise on the received signal. We shall assume that the noise is Gaussian distributed. A pulse train passing through a channel would experience additive noise and may appear as that shown in Figure 14.15a. The eye diagram corresponding to this pulse train would be that shown in Figure 14.15b. Also drawn alongside the eye diagram are the corresponding PDFs associated with each decision axis, that is, $V = V_{TH}$ and $t/T = \mathrm{UI}_{TH}$. In contrast to the PDFs along the decision axis for the ideal channel shown in Figure 14.13, here we see that additive noise modified the PDF of the voltage

Figure 14.15. (a) Pulse train subject to additive channel noise. (b) Corresponding eye diagram and its PDFs along the decision-making axes ($V = V_{TH}$ and $t/T = t_{TH}$).

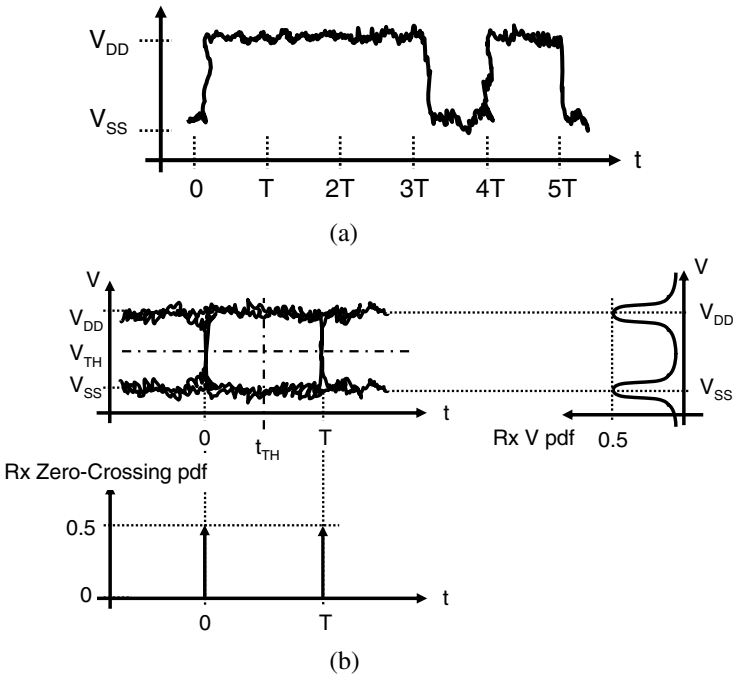

that appears at the received at the sampling instant UI_{TH} but has no effect on the PDF corresponding to the zero-crossing times. Moreover, the PDF of the noise level appears to be the convolution of the delta functions with a Gaussian distribution with zero mean and some arbitrary standard deviation, σ_N.

Dispersive Channel

In this subsection we shall consider the effects of a dispersive channel on the behavior of a transmitted square pulse train. The eye diagram corresponding to a pulse train subject to channel dispersive effects is illustrated in Figure 14.16. Here we see that the channel impairments alter the distributions of the received signal along both decision axes. We model these impairments as discrete lines in the PDF rather than as a continuous PDF because these effects are deterministic and dependent on the data pattern transmitted as well as the channel characteristics. This effect is commonly referred to as *data-dependent jitter* (DDJ). Due to the physical nature of a channel, the distribution along each decision axes is bounded by some peak-to-peak value. Unless the eye opening along the $t = UI_{TH}$ axis is closed, DDJ will have little effect on the bit error rate. However, when the effects of the channel noise is incorporated alongside the dispersive effects, we would find an increased bit error rate (over and above the bit error rate that would correspond to the additive noise effect alone). The reason for this stems from the way the different channel effects combine. From a probability point of view, assuming that the PDFs for the different channels impairments are independent, they would combine through a convolution operation as shown in Figure 14.18. The net effect is a wider PDF extending over a larger range on both decision axes, that is, closing the eye opening. Also, we note that the PDFs no longer follow a Gaussian distribution.

Figure 14.16. (a) Pulse train subject to channel dispersion or ISI. (b) Corresponding eye diagram and its PDFs along the decision-making axes ($V = V_{TH}$ and $t/T = t_{TH}$).

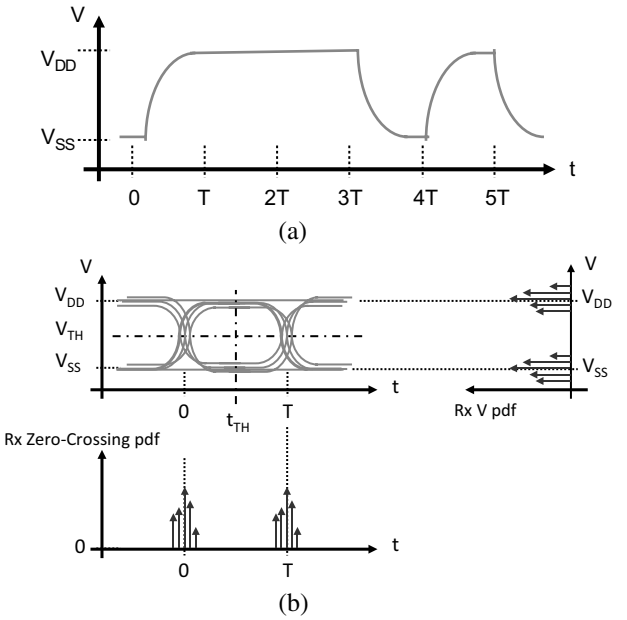

Figure 14.17. (a) Pulse train subject to channel dispersion and additive Gaussian noise. (b) Corresponding eye diagram and its PDFs along the decision-making axes ($V = V_{TH}$ and $t = t_{TH}$).

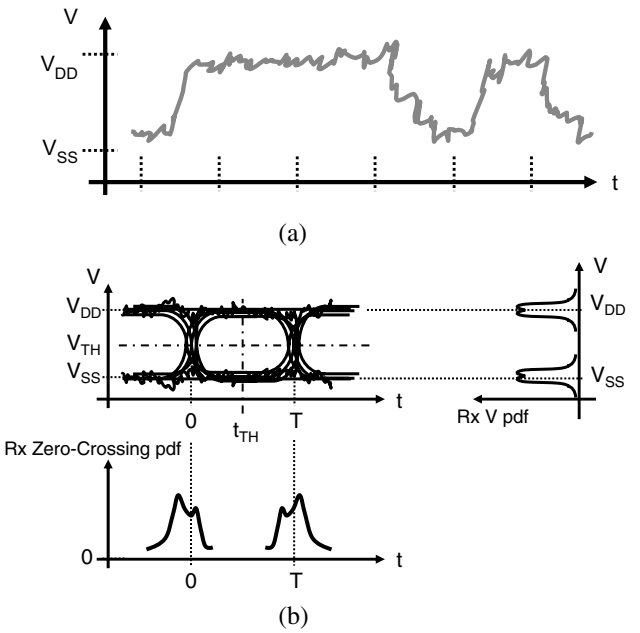

Figure 14.18. Independent PDFs are combined by a convolution operation.

EXAMPLE 14.3

Determine the convolution of two impulse functions centered at V_{SS} and V_{DD} with a Gaussian function with zero mean and σ_N standard deviation.

Solution:
Mathematically, the two functions are written as follows:

$$f(v) = \frac{1}{2}\delta(v - V_{SS}) + \frac{1}{2}\delta(v - V_{DD})$$

$$g(v) = \frac{1}{\sigma_N\sqrt{2\pi}} e^{-v^2/2\sigma_N^2}$$

The convolution of two PDFs is defined by the following integral equation,

$$f(v) \otimes g(v) \triangleq \int_{-\infty}^{\infty} f(v - \tau)\, g(\tau)\, d\tau$$

where τ is just an immediate variable used for integration. Substituting the above two functions, we write

$$f(v) \otimes g(v) = \int_{-\infty}^{\infty} \left[\frac{1}{2}\delta(v - V_{SS} - \tau) + \frac{1}{2}\delta(v - V_{DD} - \tau)\right]\left[\frac{1}{\sigma_N\sqrt{2\pi}} e^{-\tau^2/2\sigma_N^2}\right] d\tau$$

Next, using the sifting property of the impulse function, we write the above integral as

$$f(v) \otimes g(v) = \frac{1}{\sigma_N 2\sqrt{2\pi}} e^{-(v-V_{SS})^2/2\sigma_N^2} + \frac{1}{\sigma_N 2\sqrt{2\pi}} e^{-(v-V_{DD})^2/2\sigma_N^2}$$

Hence, the convolution of two impulse functions center at V_{SS} and V_{DD}, and a Gaussian distribution with zero mean and standard deviation σ_N are two Guassian distributions with mean V_{SS} and V_{DD} having a standard deviation σ_N.

Figure 14.19. Illustrating the effects on the zero-crossing levels: (a) duty-cycle distortion and (b) periodic-induced jitter, without any noise present.

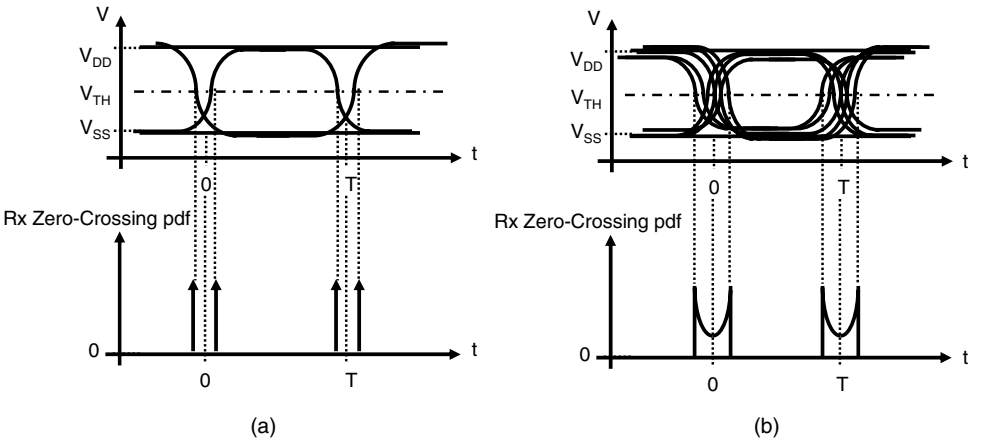

In many practical situations we encounter problems that involve the convolution of two Gaussian distributions. As such, one can easily show the convolution of two Gaussian distributions is another Gaussian distribution, whose mean value is the sum of individual mean values and whose variance is the sum of individual variances, that is,

$$\begin{aligned} \mu_T &= \mu_1 + \mu_2 \\ \sigma_T^2 &= \sigma_1^2 + \sigma_2^2 \end{aligned} \tag{14.28}$$

where the two Gaussian distributions are described by parameters $N(\mu_1, \sigma^2{}_1)$ and $N(\mu_2, \sigma^2{}_2)$.

Transmitter Limitations

The transmitter also introduces signal impairments that show up at the receiver—specifically, duty-cycle distortion (DCD) and periodic induced jitter (PJ). Duty-cycle distortion is caused by the unsymmetrical rise and fall times of the driver located in the transmitter as represented by the eye diagram shown in Figure 14.19a. As can be seen from this figure, a logic 1 bit value has a shorter bit duration than a logic 0 bit value relative to the zero crossing point. In essence, DCD can be considered as a shift in the time of the rising and falling edge of the data bit. DCD is a deterministic effect because it depends only on the driver characteristic together with the logic pattern that is transmitted. Fortunately, its effect on the zero-crossing levels is small and bounded.

Sometimes one finds a periodic component of jitter showing up at the receiver end. This is typically caused by some periodic interference located at the transmitter or picked up via the channel. Such effects include crosstalk from adjacent power nets and noise from switching power supplies. Its effect on the zero-crossing levels is bounded. Figure 14.19b illustrates a single sine wave component and its effect on the zero-crossing PDF as shown in Figure 14.19b. Through the application of the Fourier series more complicated periodic components can be also be described.

Jitter Classifications

Figure 14.20 provides a quick summary of the breakdown of the various jitter components described in the previous subsection. At the top of the tree, we list the total jitter (TJ), which is

Figure 14.20. A summary of the different components of jitter.

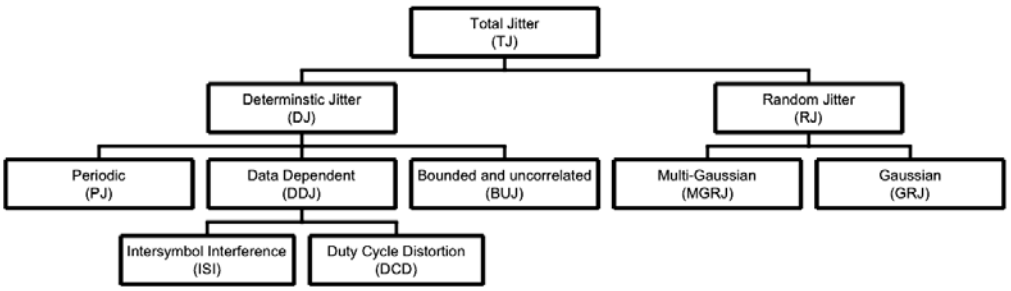

Figure 14.21. A simple receiver arrangement.

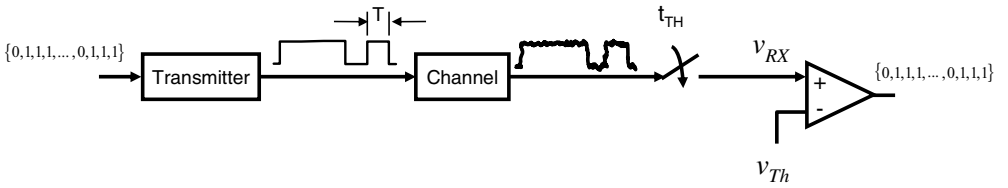

broken down into two parts: deterministic (DJ) and random (RJ) jitter. The deterministic jitter component is further broken down into period jitter PJ, data-dependent jitter DDJ, and a catch-all category called bounded and uncorrelated jitter denoted by BUJ. We further divide DDJ into intersymbol interference (ISI) and duty-cycle distortion (DCD) components.The BUJ component includes tones that are unrelated to the input data sequence, as well as uncorrelated noise-like signals. In essence, it is a catch-all quantity that accounts for unexplained effects. Random jitter is divided into single or multi-Gaussian distributions, denoted as MGRJ or GRJ, respectively.

The entire jitter classification is further divided between whether the jitter is bounded or unbounded—that is, varies with sample set. As a general rule, bounded parameters will be specified with a min–max value or a peak-to-peak value, whereas unbounded parameters have no limit so instead are specified with anRMS or standard deviation parameter.

14.4.3 Impact of Decision Levels on Receiver Performance

In this section we shall investigate the effects that jitter has on the performance of a simple receiver arrangement as a function of the decision levels t_{TH} and V_{TH}. Consider the simple receiver arrangement shown in Figure 14.21 consisting of a switch in series with the channel and a comparator with reference level V_{TH}. The series switch is used to sample the incoming signal at the appropriate time designated by t_{TH}. The resulting sampled level is then applied to a comparator where a decision of being logical 0 or 1 is made based on a comparison with the voltage threshold level V_{TH}. Let us consider the effect of each decision level—first separately, then combined.

Received Voltage Decision Level, VTH

Let us assume that the channel has corrupted the received signal v_{Rx} in such a way that a logical 0 level, denote V_{Logic0}, has a Gaussian distribution with mean value V_{Logic0} and standard deviation σ_N. Likewise, a logical 1 level, denoted V_{Logic1}, is also Gaussian distributed with mean value V_{Logic1} and

Figure 14.22. Modeling the PDF of the received voltage signal and identifying the regions of the PDF that contributes to the probability of error.

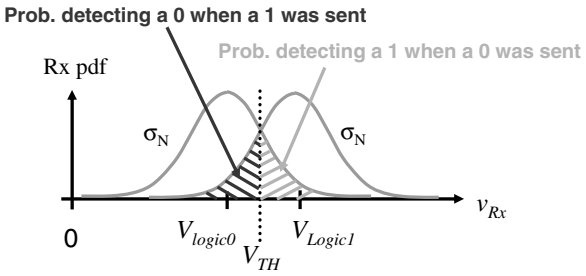

standard deviation σ_N. Superimposing these two distributions along the same axis we obtain the decision diagram shown in Figure 14.22. The dotted vertical line indicates the voltage threshold V_{TH}. The portion of the distribution centered around V_{Logic0} but above V_{TH} represents the probability that logic 1 is detected when logic 0 was sent. Mathematically, we write

$$P\left(V_{Rx} > V_{TH} \mid Tx = 0\right) = \int_{V_{TH}}^{\infty} pdf_{Rx,Logic0} dv_{Rx} = 1 - \Phi\left(\frac{V_{TH} - V_{Logic0}}{\sigma_N}\right) \tag{14.29}$$

Conversely, the portion of the distribution centered around V_{Logic1} but below V_{TH} represents the probability that logic 0 is detected when logic 1 was sent. This allows us to write

$$P\left(V_{Rx} < V_{TH} \mid Tx = 1\right) = \int_{-\infty}^{V_{TH}} pdf_{Rx,Logic1} dv_{Rx} = \Phi\left(\frac{V_{TH} - V_{Logic1}}{\sigma_N}\right) \tag{14.30}$$

Assuming the probability of transmitting a logic 0 and a logic 1 is 1/2, respectively, then we can write the total probability that a single bit is received in error as

$$P_e\left(V_{TH}\right) = \frac{1}{2} \times P\left(V_{Rx} > V_{TH} \mid Tx = 0\right) + \frac{1}{2} \times P\left(V_{Rx} < V_{TH} \mid Tx = 1\right) \tag{14.31}$$

Substituting Eqs. (14.29) and (14.30) into Eq.(14.31), we write

$$P_e\left(V_{TH}\right) = \frac{1}{2} - \frac{1}{2} \times \Phi\left(\frac{V_{TH} - V_{Logic0}}{\sigma_N}\right) + \frac{1}{2} \times \Phi\left(\frac{V_{TH} - V_{Logic1}}{\sigma_N}\right) \tag{14.32}$$

The following example will help illustrate the application of this formula.

EXAMPLE 14.4

A logic 0 is transmitted at a nominal level of 0 V and a logic 1 is transmitted at a nominal level of 2.0 V. Each logic level has equal probability of being transmitted. If a 150-mV RMS Gaussian noise signal is assumed to be present at the receiver, what is the probability of making an single trial bit error if the detector threshold is set at 1.0 V.

Solution:
According to Eq.(14.32), together with the numbers described above, we write

$$P_e(V_{TH}) = \frac{1}{2} - \frac{1}{2} \times \Phi\left(\frac{V_{TH} - V_{Logic0}}{\sigma_N}\right) + \frac{1}{2} \times \Phi\left(\frac{V_{TH} - V_{Logic1}}{\sigma_N}\right)$$

$$P_e(1.0) = \frac{1}{2} - \frac{1}{2} \times \Phi\left(\frac{1.0 - 0}{0.15}\right) + \frac{1}{2} \times \Phi\left(\frac{1.0 - 2.0}{0.15}\right)$$

$$\therefore P_e(1.0) = 1.31 \times 10^{-11}$$

Therefore the probabilitry of a single bit error is 1.31×10^{-11}. Alternatively, if 1.31×10^{11} bits are sent in one second, then one can expect about 1 error to be made during this transmisison.

EXAMPLE 14.5

For the system conditions described in Example 14.4, compute the probability of error as a function of the threshold voltage V_{TH} beginning at 0 V and extending to 2 V.

Solution:
Using Eq. (14.32), together with the data from Example 14.7, we can write the probability of error as a function of the threshold voltage V_{TH} as follows:

$$P_e(V_{TH}) = \frac{1}{2} - \frac{1}{2} \times \Phi\left(\frac{V_{TH} - 0}{0.15}\right) + \frac{1}{2} \times \Phi\left(\frac{V_{TH} - 2.0}{0.15}\right)$$

Numericially, we iterate V_{TH} through this formula beginning at 0 V and ending at 2 V with a 10 mV step, resulting in the P_e plot shown below:

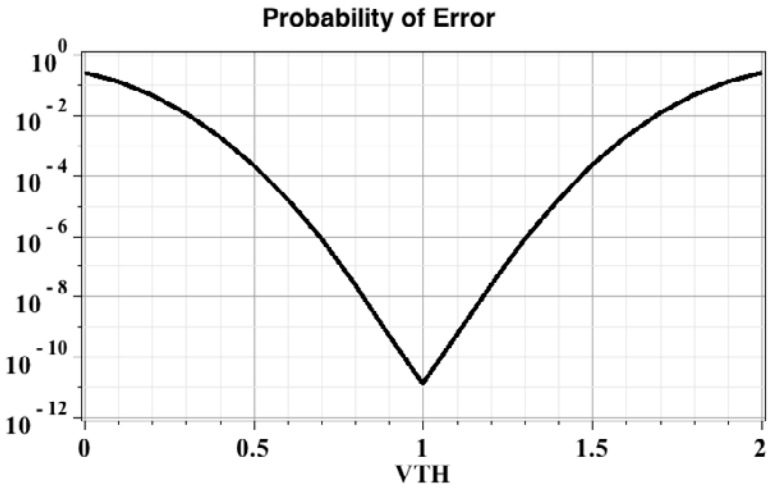

Here we the P_e plot is minumum at about the 1-V threshold level, a level midway between the logic 0 and logic 1 level. Also, we see the Pe is symmetrical about this same threhold level. The above plot is commonly referred to as a *bathtub plot* on account of its typical shape. (Albeit, this particular plot looks more like a valley associated with a mountain range than a bathtub. This is simply a function of the numerical values used for this example.)

Exercises

14.7. A logic 0 is transmitted at a nominal level of 0 V and a logic 1 is transmitted at a nominal level of 1.0 V. A logic 0 level is three times as likely to be transmitted as a logic 1 level. If a 100-mV RMS Gaussian noise signal is assumed to be present at the receiver, what is the probability of making an single trial bit error if the detector threshold is set at 0.6 V? What about if the detector threshold is set at 0.35 V?

ANS.
$P_e = 15.8 \times 10^{-6}$;
$P_e = 116.3 \times 10^{-6}$.

Up to this point in the discussion, we have assumed that the distribution of the received signal is modeled as a Gaussian random variable. We learned in the previous section that this is rarely the case on account of the channel dispersion effects as well as circuit asymmetries associated with the transmitter.From a mathematical perspective, this does not present any additional complication to quantifying the probability of error provided that the PDFs of the received signal is captured in some numerical or mathematical form described in the general way by the following expression:

$$P_e\left(V_{TH}\right) = \frac{1}{2} \times \int_{V_{TH}}^{\infty} pdf_{Rx,Logic0} dv_{Rx} + \frac{1}{2} \times \int_{-\infty}^{V_{TH}} pdf_{Rx,Logic1} dv_{Rx} \quad \textbf{(14.33)}$$

Received Zero-Crossing Decision Level, t_{TH}

Let us now turn our attention to the performance of the receiver from the perspective of the normalized sampling instant represented by t_{TH}. Let us begin by assuming that the distribution of zero crossings around the $(n-1)$th-bit transition and the nth-bit transition are both Gaussian distributed with standard deviation σ_{ZC}. Such a situation is depicted in Figure 14.23. Once again, on account of channel effects (i.e., additive noise and dispersion), a zero-crossing edge intended for the $(n-1)$ th sampling instant may find itself occurring after the sampling instant defined by t_{TH}, resulting in a synchronization error that may lead to a bit error. Of course, the reverse is also possible whereby the intended zero-crossing corresponding to the nth-bit arrives before the sampling instant, resulting in a potential bit error. Following the same theoretical development pose earlier for the received voltage signal, we can state that the probability of error due to a sampling timing error is

$$P_e\left(t_{TH}\right) = P\left(\text{bit transition}\right) \times P\left(t > t_{TH} \middle| \text{bit} = n-1\right) + P\left(\text{bit transition}\right) \times P\left(t < t_{TH} \middle| \text{bit} = n\right) \quad \textbf{(14.34)}$$

Figure 14.23. Modeling the PDF of the received zero-crossing time and identifying the regions of the PDF that contributes to the probability of error.

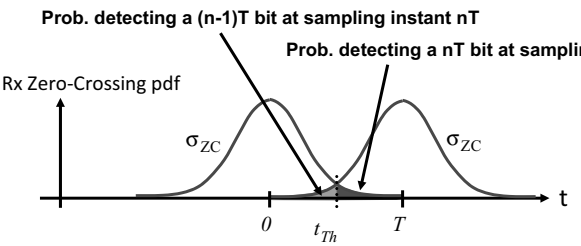

Since we assumed that a 0 and 1 are equally likely to occur, it is reasonable to assume that a bit transition is also equally likely, hence we write the probability of error as

$$P_e(t_{TH}) = \frac{1}{2} \times \int_{t_{TH}}^{\infty} pdf_{TJ,n-1} dt + \frac{1}{2} \times \int_{-\infty}^{t_{TH}} pdf_{TJ,n} dt \tag{14.35}$$

where the subscript *TJ*, *n* signifies the PDF of the total jitter around the *n*th bit transition. Because the PDFs are Gaussian in nature, we can replace the integral expressionsby normalized Gaussian CDF functions and write

$$P_e(t_{TH}) = \frac{1}{2} - \frac{1}{2} \times \Phi\left(\frac{t_{TH} - 0}{\sigma_{ZC}}\right) + \frac{1}{2} \times \Phi\left(\frac{t_{TH} - T}{\sigma_{ZC}}\right) \tag{14.36}$$

Interesting enough, the above formula has a very similar form as that for the received voltage signal probability of error shown in Eq. (14.32). Let us look at an example using this approach.

EXAMPLE 14.6

Data are transmitted to a receiver at a data rate of 1 Gbits/s through a channel that causes the zero crossings to vary according to a Gaussian distribution with zero mean and a 70-ps standard deviation. What is the probability of error of a single event if the sampling instant is set midway between bit transitions?

Solution:

As the data rate is 1 Gbits/s, the spacing between bit transistions is 1 ns. Hence the sampling instant will be set at 500 ps or 0.5 UI. From Eq. (14.36), the P_e is

$$P_e(t_{TH}) = \frac{1}{2} - \frac{1}{2} \times \Phi\left(\frac{t_{TH} - 0}{\sigma_{ZC}}\right) + \frac{1}{2} \times \Phi\left(\frac{t_{TH} - T}{\sigma_{ZC}}\right)$$

$$P_e(500\text{ ps}) = \frac{1}{2} - \frac{1}{2} \times \Phi\left(\frac{500\text{ ps} - 0}{70\text{ ps}}\right) + \frac{1}{2} \times \Phi\left(\frac{500\text{ ps} - 1000\text{ ps}}{70\text{ ps}}\right)$$

$$\therefore P_e(500\text{ ps}) = 4.57 \times 10^{-13}$$

Therefore the probability of a single bit error is 4.57×10^{-13}.

Combined Effect of Varying Received Voltage Level Decision V_{TH} and Zero-Crossing Decision Level, t_{TH}

The previous two subsections look at the impact of the decision levels on the probability of error assuming Gaussian random variables. Let us combine these two effects assuming that the two sets of random variables are independent. In practice, one would expect that some correlation between the signal around the zero crossing and the voltage level appearing at the comparator input. However, away from the zero-crossing point, the signal saturates at one of its logic level; hence in this region one would expect little correlation between voltage level and the zero-crossing point.

Exercises

14.8. Data are transmitted to a receiver at a data rate of 100 Mbits/s through a channel that causes the zero crossings to vary according to a Gaussian distribution with zero mean and a 100-ps standard deviation. What is the probability of error of a single event if the sampling instant is set at 0.3UI? Repeat for a threshold of 0.75UI?

ANS. $P_e = 4.93 \times 10^{-10}$; $P_e = 1.43 \times 10^{-7}$.

Regardless of whether or not we obtain complete independence, this analysis helps to illustrate the dependence of the decision levels on the eye opening. Consider the total probability of error as

$$P_e\left(t_{TH}, V_{TH}\right) = P_e\left(t_{TH}\right) + P_e\left(V_{TH}\right) \tag{14.37}$$

Substituting Eqs. (14.32) and (14.36), we write the above expression as

$$\begin{aligned} P_e\left(t_{TH}, V_{TH}\right) = 1 - \frac{1}{4} \times \Phi\left(\frac{V_{TH} - V_{Logic0}}{\sigma_N}\right) + \frac{1}{4} \times \Phi\left(\frac{V_{TH} - V_{Logic1}}{\sigma_N}\right) \\ - \frac{1}{4} \times \Phi\left(\frac{t_{TH} - 0}{\sigma_{ZC}}\right) + \frac{1}{4} \times \Phi\left(\frac{t_{TH} - T}{\sigma_{ZC}}\right) \end{aligned} \tag{14.38}$$

14.5 BIT ERROR RATE MEASUREMENT

All communication systems experience some form of transmission error. We learned previously about the various ways in which errors (e.g., additive noise, dispersion, etc.) arise in a communication system. We modeled these effects as variations in the decision points using different probability density functions and used them to compute theprobability of a single error during transmission, denoted by P_e. In this section we shall consider a cumulative measure of transmission quality called the bit error ratio or which is sometimes referred to as the bit error rate. We shall use either term interchangeably and we will often use the acronym BER.

The bit error ratio (BER) is defined as the average number of transmission errors, denoted by μ_{N_e}, divided by the total number of bits sent in a specified time interval, denoted N_T, that is,

$$\text{BER} = \frac{\mu_{N_E}}{N_T} \tag{14.39}$$

According to our earlier development, if N_T bits were transmitted to a receiver, then according to our probability model, we would expect the average number of bit errors to given by

$$\mu_{N_E} = N_T P_e \tag{14.40}$$

which leads to the simple observation that BER is equivalent to P_e, that is,

$$\text{BER} = P_e \tag{14.41}$$

Figure 14.24. BER test setup.

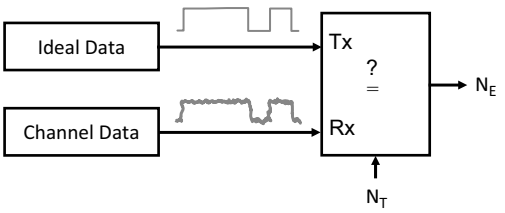

The test setup for measuring a BER is that shown in Figure 14.24. It consists of a block that compares the logic state of the data appearing at its two input port: Tx and Rx. One input contains the ideal data or the transmitted data, and the other input contains the received data. The compare block captures data over some specified time interval or over some total count N_T from which the number of transmission errors N_E is identified. While one may be tempted to compute the BER using the measured N_E, this would be incorrect as BER is defined in terms of the average N_E or as denoted in Eq. (14-39) by μ_{N_e}. Subsequently, a series of identical measurements must be made in order to extract the average value. However, we learned from Chapter 5, specifically Section 5.3, that extracting the average value from a finite-sized population of random variables will always have some level of uncertainty associated with it. If we were to assume that the error count is Gaussian distributed with parameters $N(\mu_{N_e}, \sigma_{N_e})$, then one could bound the variation in the BER value with a 99.7% confidence level as

$$\frac{\mu_{N_E} - 3\sigma_{N_E}}{N_T} \le \text{BER} \le \frac{\mu_{N_E} + 3\sigma_{N_E}}{N_T} \tag{14.42}$$

Clearly, the higher the number of bits transmitted (N_T), the smaller the expected range in possible measured BER values. While this conclusion is true in general, transmission bit errors do not obey Gaussian statistics, rather they follow more closely a binomial distribution.We saw this distribution back in Chapter 4, Section 4.3. There the binomial distribution is the discrete probability distribution of the number of successes in a sequence of N independent yes/no experiments, each of which yields a success with probability p. Following this train of thought, if N_T bits are transmitted, then the probability of having N_E errors in the received bit set assuming the errors are independent with probability of error P_e can be written as

$$P[X = N_E] = \begin{cases} \dfrac{N_T!}{N_E!(N_T - N_E)!} P_e^{N_E} (1 - P_e)^{N_T - N_E}, & N_E = 0, \ldots, N_T \\ 0, & \text{otherwise} \end{cases} \tag{14.43}$$

The binomial distribution has the following mean and standard deviation:

$$\begin{aligned} \mu &= N_T P_e \\ \sigma &= \sqrt{N_T P_e (1 - P_e)} \end{aligned} \tag{14.44}$$

The cumulative distribution function CDF of the binomial distributioncan be described by

$$P[X \le N_E] = \sum_{k=0}^{N_E} P[X = k] = \sum_{k=0}^{N_E} \left(\frac{N_T!}{k!(N_T - k)!} \right) P_e^k (1 - P_e)^{N_T - k} \tag{14.45}$$

which can be further simplified when N_T BER < 10 using the Poisson approximation as

$$P\left[X \le N_E\right] \approx \sum_{k=0}^{N_E} \frac{1}{k!}\left(N_T \text{BER}\right)^k e^{-N_T BER} \tag{14.46}$$

The transmission test problem is one where we would like to verify that the system meets a certain BER level while at the same time we remain confident that the test results are repeatable to some statistical level of certainty.[4] Mathematically, we can state this as a conditional probability whereby we assume that the single bit error probability P_e is equal to the desired BER, and we further set the probability of N_E bit errors to a confidence parameter α as follows:

$$P\left[X \le N_E \middle| P_e = \text{BER}\right] = \alpha \tag{14.47}$$

The meaning of what BER refers to should now be clear; every bit received has a probability of being in error equal to the BER. The parameter α represents the probability of receiving N_E errors or less. For a very large α, the probability of receiving N_E or fewer errors is very likely. However, a small α signifies the reverse, a very unlikely situation. Hence, focusing in on the unlikely situation provides us with a greater confidence that the assigned conditions will be met. It is customary to refer to (1 – α) as the confidence level (CL) expressed in percent, that is,

$$\text{CL} = 1 - \alpha \tag{14.48}$$

Combining Eq. (14.46) with Eq. (14.47), together with the appropriate parameter substitutions, we write

$$P\left[X \le N_E \middle| P_e = \text{BER}\right] = \sum_{k=0}^{N_E} \frac{1}{k!}\left(N_T \text{BER}\right)^k e^{-N_T BER} = 1 - \text{CL} \tag{14.49}$$

To help the reader visualize the relationship provided by Eq.(14.49), Figure 14.25 provides a contour plot of the confidence levels corresponding to the probability of 2 errors or less as a function of BER and N_T. This plot provides important insight into the tradeoffs between CL, BER and bit length N_T. For example, if 10^{12} bits are transmitted and 2 or less data errors are received, then with 95% confidence level we can conclude that the BER ≤ 10^{-11}. Likewise, if after 10^{11} bits are received with 2 or less data errors, we can conclude with very little confidence (5%) that the BER ≤ 10^{-11}.

Exercises

14.9. Data are transmitted with a single-bit error probability of 10^{-12}. If 2×10^{12} bits are transmitted, what is the probability of no bit errors, one bit error, two bit errors, and five bit errors? What is the average number of errors expected?

ANS. $P[N_E = 0] = 0.135$; $P[N_E = 1] = 0.271$; $P[N_E = 2] = 0.271$; $P[N_E = 5] = 0.036$; $\mu = 2$.

14.10. Data are transmitted at a rate of 10 Gbps over a channel with a single-bit error probability of 10^{-11}. If 10^{12} bits are transmitted, what is the probability of less than or equal to one bit error, less than or equal to two bit errors, and less thanor equal to 10 bit errors.

ANS. $P[N_E \le 1] = 0.000499$; $P[N_E \le 2] = 0.00277$; $P[N_E \le 10] = 0.583$.

Figure 14.25. The confidence level for a probability of 2 errors or less as a function of BER and bit length, N_T.

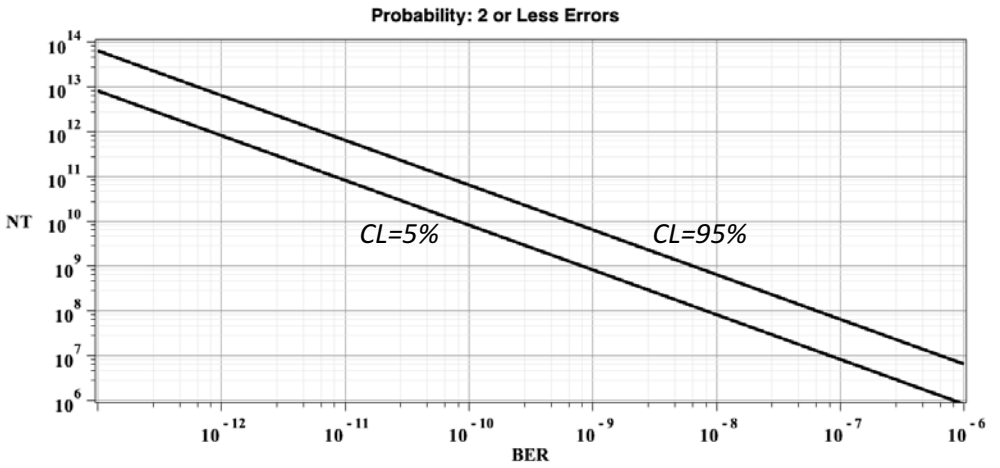

Equation (14.49) provides us with the opportunity to compute the number of bits N_T that need to be transmitted such that the desired level of BER is reached to a desired level of confidence CL. As N_T represents the minimum bit length that must pass with errors N_E or less, we shall designate this bit length as $N_{T,\min}$. Next, we rearrange Eq. (14.49) and solve for $N_{T,\min}$ as

$$N_{T,\min} = \frac{1}{\text{BER}} \ln\left[\sum_{k=0}^{N_E} \frac{1}{k!}\left(N_T \text{BER}\right)^k\right] - \frac{1}{\text{BER}} \ln\left(1-\text{CL}\right) \tag{14.50}$$

Using numerical methods, $N_{T,\min}$ can be solved for specific values of BER and CL. To achieve a high level of confidence, typically, one must collect at least 10 times the reciprocal of the desired BER. For example, if a BER of 10^{-12} is required, then one can expect that at least 10^{13} samples will be required.

It is interesting to note that Eq.(14.50) reveals a tradeoff between the confidence level of the test and the bit length $N_{T,\min}$, which in turn is related to test time, T_{test}. When Consider substituting $N_E = 0$ into Eq. (14.50), one finds

$$N_{T,\min} = -\frac{\ln\left(1-\text{CL}\right)}{\text{BER}} \tag{14.51}$$

Since the test time T_{test} is given by

$$T_{test} = \frac{N_{T,\min}}{F_S} \tag{14.52}$$

we find after substituting into Eq. (14.51),

$$T_{test} = -\frac{\ln\left(1-\text{CL}\right)}{F_S \times \text{BER}} \tag{14.53}$$

The higher the confidence level CL, the longer the time required for completing the test.

EXAMPLE 14.7

A system transmission test is to be run whereby a BER < 10^{-10} is to be verified. How many samples should be collected such that the desired BER is met with a CL of 99% when no more than 2 errors are deemed acceptable.What is the total test time if the data rate is 2.5 Gbps?

Solution:
Using Eq. (14.50), we write

$$N_{T,\min} = \frac{1}{10^{-10}} \ln\left[\sum_{k=0}^{2} \frac{1}{k!}\left(N_T 10^{-10}\right)^k\right] - \frac{1}{10^{-10}} \ln\left(1-0.99\right)$$

Here we have a transcendental expression in terms of $N_{T,\min}$ only, as N_E was set to 2. Using a computer program, we solve for $N_{T,\min}$ and get

$$N_{T,\min} = \frac{1}{10^{-10}} \ln\left[1+\frac{1}{1!}10^{-10}N_{T,\min} + \frac{1}{2!}\left(10^{-10}N_{T,\min}\right)^2\right] - \frac{1}{10^{-10}} \ln\left(1-0.99\right) = 8.41 \times 10^{12} \text{ bits}$$

If after 8.41×10^{12} bits we have 2 bit errors or less, then we can conclude that BER < 10^{-10} with a confidence level of 99%. The time required to perform this test at a data rate of 2.5 Gpbs is

$$T_{test} = \frac{N_{T,\min}}{F_S} = \frac{8.41\times 10^{12} \text{ bits}}{2.5 \text{ Gbits/s}} = 3362.4 \text{ s}$$

Therefore, 3363.4 s is required to perfom this test. This is almost one hour of testing one part only!

BER tests are extremely time-consuming and very expensive to run in production. A second test limit can be derived that measures the confidence that the bit sequence will have more bit errors than the desired amount. Hence, once identified, the test can be terminated and declared a failure, thereby saving test time.

Consider the probability of achieving more bit errors than desired with confidence CL; that is, we write

$$P\left[\, X > N_E \,\middle|\, P_e = \text{BER}\right] = 1 - P\left[\, X \le N_E \,\middle|\, P_e = \text{BER}\right] = 1 - \text{CL} \tag{14.54}$$

Substituting the appropriate CDF, we write

$$P\left[\, X > N_E \,\middle|\, P_e = \text{BER}\right] = 1 - \sum_{k=0}^{N_E} \frac{1}{k!}\left(N_T \text{BER}\right)^k e^{-N_T BER} = 1 - \text{CL} \tag{14.55}$$

Following the same set of steps as before, we write a transcendental expression in terms of the bit length N_T. Because this bit length represents the maximum number of bits that can pass before exceeding a given number of errors, N_E, we designate this bit length as $N_{T,\max}$ and write

$$N_{T,\max} = \frac{1}{\text{BER}} \ln\left[\sum_{k=0}^{N_E} \frac{1}{k!}\left(N_T \text{BER}\right)^k\right] - \frac{1}{\text{BER}} \ln\left(\text{CL}\right) \tag{14.56}$$

Figure 14.26. A flow diagram illustrating the test process for performing an efficient BER test.

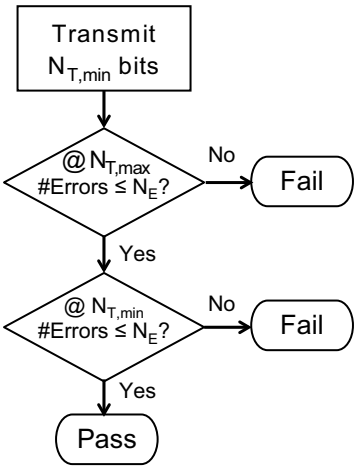

If the number of observed errors is greater than N_E after $N_{T,\max}$ bits have been collected, the test can be declared a failure. Otherwise, we continue the test until all $N_{T,\min}$ bits are transmitted. A flow diagram illustrating the test process is shown in Figure 14.26.

EXAMPLE 14.8

A system transmission test is to be run whereby a BER < 10^{-10} is to be verified at a confidence level of 99% when 2 or less bit errors are deemed acccptable. What are the minumum and maximum bit lengths required for this test? Also what is the minimum and maximum time for this test if the data rate is 2.5 Gbps? Does testing for a fail part prior to the end of the test provide significant test time savings?

Solution:
From the previous example, we found the minumum bit length to be

$$N_{T,\min} = \frac{1}{10^{-10}} \ln\left[1 + \frac{1}{1!}10^{-10}N_{T,\min} + \frac{1}{2!}\left(10^{-10}N_{T,\min}\right)^2\right] - \frac{1}{10^{-10}}\ln(1 - 0.99) = 8.41 \times 10^{12} \text{ bits}$$

and the maximum bit length is found from

$$N_{T,\max} = \frac{1}{10^{-10}} \ln\left[1 + \frac{1}{1!}10^{-10}N_{T,\max} + \frac{1}{2!}\left(10^{-10}N_{T,\max}\right)^2\right] - \frac{1}{10^{-10}}\ln(0.99) = 4.36 \times 10^{11} \text{ bits}$$

The test time for any one test will be

$$T_{test,\max} = \frac{N_{T,\min}}{F_S} = \frac{8.41 \times 10^{12} \text{ bits}}{2.5 \text{ Gbits/s}} = 3362.4 \text{ s}$$

or

$$T_{test,\min} = \frac{N_{T,\max}}{F_S} = \frac{4.36 \times 10^{11} \text{ bits}}{2.5 \text{ Gbits/s}} = 1524.3 \text{ s}$$

Therefore we can save almost 50% of the test time on a bad part by introducing a second test.

Exercises

14.11. A system transmission test is to be run whereby a BER < 10^{-11} is to be verified at a confidence level of 95% when 4 or less bit errors are deemed acceptable. What is the minimum bit length required for this test?

ANS. $N_{T,\min} = 9.15 \times 10^{11}$.

14.12. A system transmission test is to be run whereby a BER < 10^{-11} is to be verified at a confidence level of 95% when 2 or less bit errors are deemed acceptable. What is the maximumbit length required for this test?

ANS. $N_{T,\max} = 8.18 \times 10^{10}$.

14.5.1 PRBS Test Patterns

BER testing uses predetermined stress patterns comprising of a bit sequence of logical ones and zeros generated by a pseudorandom binary sequence (PRBS). The sequence is made up of 2^P bits that are generated from a core routine involving *P*-bits. In many PRBS sequences, the zero state is avoided, reducing the sequence to $2^P - 1$ unique patterns. There are many different pattern types, largely dependent on the system application and its data rates.[5,6] The bit sequence is pseudorandom because the pattern is not truly random, rather it is deterministic and repeats itself, unlike that which would be produced by a truly random source like white noise. The patterns must be long enough to simulate random data at the data rate being tested. If the pattern is too short, it will repeat rapidly and may confuse the clock recovery circuitry, which will prevent the receiver from synchronizing on the data.

Linear feedback shift registers (LFSRs) make extremely good pseudorandom pattern generators. An LFSR consists of a shift-register involving *P* flip-flops or stages, together with an exclusive-OR feedback function operating on the flip-flop outputs. Finite field mathematics in base 2 is used to derive PBRS patterns. Any LFSR can be represented as a polynomial in variable *X* referred to as the generator polynomial, *G*(*X*), given by

$$G(X) = X^P + g_{P-1}X^{P-1} + g_{P-2}X^{P-2} + \cdots + g_2X^2 + g_1X^1 + 1 \qquad \textbf{(14.57)}$$

The generalized Fibonacci implementation of an LFSR consists of a simple shift register in which a binary-weighted modulo-2 sum of the flip-flop outputs is fed back to the input as shown in Figure 14.27. (The modulo-2 sum of two 1-bit binary numbers yields 0 if the two numbers are identical, and 1 if they differ, e.g., 0 + 0 = 0, 0 + 1 = 1, 1 + 1 = 0.) For any given flip-flop output except the first flip-flop, the weight g_i is either 0, meaning "no connection," or 1, meaning it is fed back. The 0th flip-flop weight is always 1 and the output of the XOR operation feeds into the D-input of the $(P - 1)$th stage. The most economical manner in which to realize an LFSR with a generator polynomial of *P*th-order involves those *P*th-order polynomials with minimum number of nonzero coefficients. In addition, the generator polynomial G(X) must also be made primitive, that is, it cannot be factor into smaller terms. When this condition is met, the LFSR will produce a maximal length sequence, that is, a pattern with period equal to $2^P - 1$. Table 14.1 lists some primitive generator polynomials of degrees 2 to 33.

Figure 14.28 illustrates the implementation of a four-stage LFSR with generator polynomial,

$$G(X) = X^4 + X + 1 \qquad \textbf{(14.58)}$$

Here the first and second flip-flop outputs are feedback to the shift register input through a single XOR operation. As each flip-flop delays their input by one clock cycle, we can write the following equations for each flip-flop output at time index n as

Figure 14.27. A generalized N-stage LFSR based on the Fibonacci implementation.

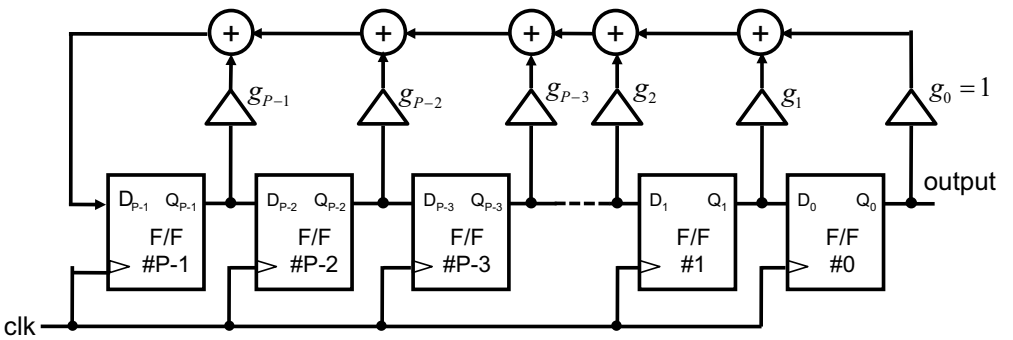

Figure 14.28. A 4-stage linear feedback shift register.

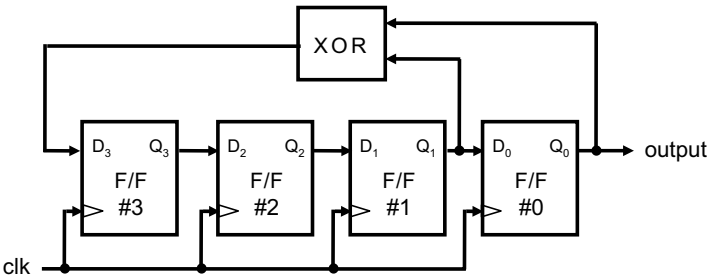

Table 14.1. Some Primitive LFSR Generator Polynomials of Degrees 2 to 33

Degree	Generator Polynomial	Degree	Generator Polynomial
2	X^2+X+1	18	$X^{18}+X^7+1$
3	X^3+X+1	19	$X^{19}+X^5+X^2+X+1$
4	X^4+X+1	20	$X^{20}+X^3+1$
5	X^5+X^2+1	21	$X^{21}+X^2+1$
6	X^6+X+1	22	$X^{22}+X+1$
7	X^7+X^3+1	23	$X^{23}+X^5+1$
8	$X^8+X^6+X^5+X^3+1$	24	$X^{24}+X^7+X^2+X+1$
9	X^9+X^4+1	25	$X^{25}+X^3+1$
10	$X^{10}+X^3+1$	26	$X^{26}+X^6+X^2+X+1$
11	$X^{11}+X^2+1$	27	$X^{27}+X^5+X^2+X+1$
12	$X^{12}+X^6+X^4+X+1$	28	$X^{28}+X^3+1$
13	$X^{13}+X^4+X^3+X+1$	29	$X^{29}+X^2+1$
14	$X^{14}+X^{10}+X^6+X+1$	30	$X^{30}+X^{23}+X^2+X+1$
15	$X^{15}+X+1$	31	$X^{31}+X^3+1$
16	$X^{16}+X^{12}+X^3+X+1$	32	$X^{32}+X^{22}+X^2+X+1$
17	$X^{17}+X^3+1$	33	$X^{33}+X^{13}+1$

$$\begin{aligned} F_3[n] &= L_{XOR}[n-1] \\ F_2[n] &= F_3[n-1] \\ F_1[n] &= F_2[n-1] \\ F_0[n] &= F_1[n-1] \end{aligned} \tag{14.59}$$

where L_{XOR} is the output of the XOR gate. We can describe the XOR output as a summing operation over a finite field of mod 2 with inputs F_1 and F_0 as follows:

$$L_{XOR}[n] = F_1[n] + F_0[n] \mod 2 \tag{14.60}$$

Substituting the above equation into Eq. (14.59)and solving for the output $F_o[n]$, we write

$$F_0[n] = F_0[n-3] + F_0[n-4] \mod 2 \tag{14.61}$$

Including the initial register values, we further write

$$F_0[n] = \begin{cases} F_0[0], & n=0 \\ F_1[0], & n=1 \\ F_2[0], & n=2 \\ F_3[0], & n=3 \\ F_0[n-3] + F_0[n-4] \mod 2, & n=4,5,\cdots \end{cases} \tag{14.62}$$

The above time difference equation (mod 2) provides the complete pattern sequence from an initial state or seed. The following example will illustrate this procedure.

EXAMPLE 14.9

Derive the first 15 bits associated with the four-stage LFSR shown in Figure 14.28, assuming that the shift register is initialized with seed 1011 (from left to right).

Solution:
According to Eq. (14.62), we write

$$F_0[n] = \begin{cases} 1 & n=0 \\ 1 & n=1 \\ 0 & n=2 \\ 1 & n=3 \\ F_0[n-3] + F_0[n-4] \mod 2, & n=4,5,\ldots \end{cases}$$

Next, stepping through n from 4 to 19, we get the following 15 bits:

0, 1, 1, 1, 1, 0, 0, 0, 1, 0, 0, 1, 1, 0, 1

If the sequence is allowed to run longer, one would observe the following repeating pattern:

1, 1, 0, 1,0, 1, 1, 1, 1, 0, 0, 0, 1, 0, 0, 1, 1, 0, 1, 0, 0, 1, 0, 0, 1, 1, 0, 1,
0, 1, 1, 1, 1, 0, 0, 0, 1, 0, 0, 1, 1, 0, 1, 0, 1, 1, 1, 1, 0, 0, 0, 1, 0, 0, 1, 1, 0, 1, ...

In general, for any *P*th-order generator polynomial described by Eq. (14.57) the output of the XOR gate can be written in terms of state of each flip-flop output at sampling instant *n* as

$$\mathrm{XOR}\left[n\right] = g_{P-1}F_{P-1}\left[n\right] + g_{P-2}F_{P-2}\left[n\right] + \cdots + g_kF_k\left[n\right] + \cdots + g_1F_1\left[n\right] + F_0\left[n\right] \tag{14.63}$$

Correspondingly, we can write the state of the output of the 0th flip-flop in terms of its passed state as

$$F_0\left[n\right] = g_{P-1}F_0\left[n-1\right] + g_{P-2}F_0\left[n-2\right] + \cdots + g_kF_0\left[n-\left(P-k\right)\right] + \cdots + g_1F_0\left[n-\left(P-1\right)\right] + F_0\left[n-P\right] \tag{14.64}$$

The next example will help to illustrate the use of these generalized equations, as well as describe how the initial seed is incorporated into the PRBS generation.

EXAMPLE 14.10

An LFSR of degree 8 is required. Write a short routine that generates the complete set of unique bits associated with this sequence. Initialize the LSFR using the seed 00000001, where the first bit corresponds to the state of the 7th flip-flop and the last bit is associated with the state of the 0th flip-flop.

Solution:

The generator polynomial for a PRBS of degree 8 (Table 14.1) is

$$G(X) = X^8 + X^6 + X^5 + X^3 + 1$$

Comparing this expression to the general form of the generating polynomial of degree $P = 8$, we determine

$$G(X) = X^8 + g_7X^7 + g_6X^6 + g_5X^5 + g_4X^4 + g_3X^3 + g_2X^2 + g_1X^1 + 1$$

$$g_7 = 0,\ \ g_6 = 1,\ \ g_5 = 1,\ \ g_4 = 0,\ \ g_3 = 1,\ \ g_2 = 0,\ \ g_1 = 0$$

Subsequently, the recursive equation that governs the output behavior of the LSFR as desribed by Eq. (14.64) can be written as

$$F_0\left[n\right] = F_0\left[n-\left(8-6\right)\right] + F_0\left[n-\left(8-5\right)\right] + F_0\left[n-\left(8-3\right)\right] + F_0\left[n-8\right]$$

which reduces to

$$F_0\left[n\right] = F_0\left[n-2\right] + F_0\left[n-3\right] + F_0\left[n-5\right] + F_0\left[n-8\right]$$

Subsequently, we can write the following routine involving a programming for loop and the array varaible *F* as

```
# initialize the output using the given seed value
F[7] = 0 : F[6] = 0 : F[5] = 0 : F[4] = 0 : F[3] = 0 : F[2] = 0 : F[1] = 0 : F[0] = 1:
# cycle through the leading flip-flop recursive equation
for n = 8 to 262,
        F[n] = F[n-2] + F[n-3] + F[n-5] + F[n-8]
end
```

Cycling through this routine will provide all 255 unique bits of this sequence corresponding to the initial conditions provided by the seed number.

Exercises

14.13. An LFSR has primitive generator polynomial $G(X) = X^{19} + X^5 + X^2 + X + 1$. How many bits are associated with this repeating pattern?	ANS. $2^{19} - 1$.
14.14. An LFSR has primitive generator polynomial $G(X) = X^{19} + X^5 + X^2 + X + 1$. Write the expression for the XOR operation assuming the output is taken from the 0th flip-flop.	ANS. XOR= $F_5 + F_2 + F_1 + F_0$; XOR is fed into the D-input of the #18 flip-flop.
14.15. Determine the first 15 unique bits associated with a four-stage LFSR with generator polynomial $G(X) = X^4 + X + 1$ with initial seed 0001.	ANS. 1, 0, 0, 1, 1, 0, 1, 0, 1, 1, 1, 1, 0, 0, 0.

14.6 METHODS TO SPEED UP BER TESTS IN PRODUCTION

A BER test generally takes a very long time to execute to any reasonable level of accuracy. There have been numerous attempts to reduce the amount of test time required to perform a BER test, such as the scan testapproach and the jitter decomposition technique. In all cases, these approaches reduce test time at the expense of accuracy. Their use in practice is therefore limited and application-dependent.

14.6.1 Amplitude-Based Scan Test

The amplitude-based scan test method attempts to estimate the BER of a system component in minutes rather than hours or days. It does so by measuring the amount of signal power andnoise power present in a system, assuming, the underlying statistics of the noise is Gaussian. In the statistical literature, this class of estimation is known as importance sampling. In the optical networking literature, the amplitude-based scan test method is referred to as the Q-factor test method.[11]

The amplitude-based scan test method further assumes that no periodic or pattern dependent jitter is present. Generally, a repeating 1010 pattern is used to excite the system rather than a PRBS pattern. This ensures that no ISI is present.

Recall from Section 14.4.3 that the probability of single bit error P_e as a function of the threshold voltage V_{TH} for a receiver is given by Eq. (14.32). Assuming that each bit has the same probability of error, we can set the BER as a function of V_{TH} and write

$$\mathrm{BER}\left(V_{TH}\right) = \frac{1}{2} - \frac{1}{2} \times \Phi\left(\frac{V_{TH} - V_{Logic0}}{\sigma_N}\right) + \frac{1}{2} \times \Phi\left(\frac{V_{TH} - V_{Logic1}}{\sigma_N}\right) \tag{14.65}$$

The minimum BER occurs when the threshold voltage V_{TH} is set equal to the average voltage representing the two logic levels, i.e.,

$$V^*_{TH} = \frac{V_{Logic0} + V_{Logic1}}{2} \tag{14.66}$$

Hence the minimum BER is found by substituting Eq. (14.66) into (14.65), together with the mathematical identity,

$$\Phi\left(-x\right) = 1 - \Phi\left(x\right) \tag{14.67}$$

and write Eq. (14.65) as

$$\mathrm{BER}\left(V_{TH}^{*}\right)=1-\Phi\left(\frac{V_{Logic1}-V_{Logic0}}{\sigma_N}\right) \tag{14.68}$$

The amplitude-based scan test strategy can now be identified. The goal is to identify the three unknown parameters of the BER expression found in Eq. (14.65) then using the ideal sampling point defined by Eq. (14.66), compute the corresponding BER. Moreover, as these three quantities are the same at any BER level, we can identify them at relatively large BER values (low performance) and save enormous test time in the process.

The procedure works by moving the receiver threshold level V_{TH} closer to the logic 1 voltage level such that the BER performanceis reduced, say, to some value between10^{-4} and 10^{-10} where the test time is short. Let us assume at this instant that the BER is set at some level near 10^{-9}. According to Eq. (14-65), with $V_{TH} = V_{TH,1}$, we can write

$$\mathrm{BER}\left(V_{TH,1}\right)=\frac{1}{2}-\frac{1}{2}\times\Phi\left(\frac{V_{TH,1}-V_{Logic0}}{\sigma_N}\right)+\frac{1}{2}\times\Phi\left(\frac{V_{TH,1}-V_{Logic1}}{\sigma_N}\right) \tag{14.69}$$

We further recognize that probability of error due to the noise centered on the logic 0 level is now insignificant at this BER level, hence we can write

$$\mathrm{BER}\left(V_{TH,1}\right)\approx\frac{1}{2}\times\Phi\left(\frac{V_{TH,1}-V_{Logic1}}{\sigma_N}\right) \tag{14.70}$$

Next, move the threshold level again such that the BER is reduced to say 10^{-6}. This means moving the threshold level even closer towards the logic 1 voltage level. We now have a second equation in terms of $V_{TH,2}$ and the revised BER level, i.e.,

$$\mathrm{BER}\left(V_{TH,2}\right)\approx\frac{1}{2}\times\Phi\left(\frac{V_{TH,2}-V_{Logic1}}{\sigma_N}\right) \tag{14.71}$$

We now have two linear equations in two unknowns, from which we can easilysolve $V_{Logic,1}$ and σ_N as follows:

$$V_{Logic1}=\frac{V_{TH,2}\times\Phi^{-1}\left[2\mathrm{BER}\left(V_{TH,1}\right)\right]-V_{TH,1}\times\Phi^{-1}\left[2\mathrm{BER}\left(V_{TH,2}\right)\right]}{\Phi^{-1}\left[2\mathrm{BER}\left(V_{TH,2}\right)\right]-\Phi^{-1}\left[2\mathrm{BER}\left(V_{TH,1}\right)\right]}$$
$$\sigma_N=\frac{V_{TH,2}-V_{TH,1}}{\Phi^{-1}\left[2\mathrm{BER}\left(V_{TH,2}\right)\right]-\Phi^{-1}\left[2\mathrm{BER}\left(V_{TH,1}\right)\right]} \tag{14.72}$$

assuming

$$V_{TH,1}<V_{TH,2}$$
$$\mathrm{BER}\left(V_{TH,1}\right)<\mathrm{BER}\left(V_{TH,2}\right)$$

We repeat the above procedure, but this time we move closer to the other logic level using the same BER levels, and we obtain another set of equations assuming $V_{TH,4} < V_{TH,3}$ and BER ($V_{TH,3}$) < BER ($V_{TH,4}$), that is,

$$\begin{aligned} \text{BER}\left(V_{TH,3}\right) &\approx \frac{1}{2} - \frac{1}{2} \times \Phi\left(\frac{V_{TH,3} - V_{Logic0}}{\sigma_N}\right) \\ \text{BER}\left(V_{TH,4}\right) &\approx \frac{1}{2} - \frac{1}{2} \times \Phi\left(\frac{V_{TH,4} - V_{Logic0}}{\sigma_N}\right) \end{aligned} \tag{14.73}$$

These two equations can then be solved for unknown parameters, $V_{Logic,0}$ and $\sigma_{N,}$ as follows:

$$\begin{aligned} V_{Logic0} &= \frac{V_{TH,3} \times \Phi^{-1}\left[1 - 2\text{BER}\left(V_{TH,4}\right)\right] - V_{TH,4} \times \Phi^{-1}\left[1 - 2\text{BER}\left(V_{TH,3}\right)\right]}{\Phi^{-1}\left[1 - 2\text{BER}\left(V_{TH,4}\right)\right] - \Phi^{-1}\left[1 - 2\text{BER}\left(V_{TH,3}\right)\right]} \\ \sigma_N &= \frac{V_{TH,3} - V_{TH,4}}{\Phi^{-1}\left[1 - 2\text{BER}\left(V_{TH,4}\right)\right] - \Phi^{-1}\left[1 - 2\text{BER}\left(V_{TH,3}\right)\right]} \end{aligned} \tag{14.74}$$

Here we have two expressions for the standard deviation of the noise. Based on our initial assumptions, these should both be equal. If they are not, we can simply average the two estimate of the standard deviation of the underlying noise process and use the average value in our estimates of this model parameter, that is,

$$\sigma_N = \frac{\sigma_{N,0} + \sigma_{N,1}}{2} \tag{14.75}$$

Conversely, we can create a new theory of BER performance based on two different Gaussian distributions with zero means and standard deviations of $\sigma_{N,0}$ and $\sigma_{N,1}$ and solve for the BER performance as

$$\text{BER}\left(V_{TH}\right) = \frac{1}{2} - \frac{1}{2} \times \Phi\left(\frac{V_{TH} - V_{Logic0}}{\sigma_{N,0}}\right) + \frac{1}{2} \times \Phi\left(\frac{V_{TH} - V_{Logic1}}{\sigma_{N,1}}\right) \tag{14.76}$$

The optimum threshold level V^*_{TH} tor minimum level of BER can then be found to occur at

$$V^*_{TH} = \frac{\sigma_{N,0} V_{Logic1} + \sigma_{N,1} V_{Logic0}}{\sigma_{N,0} + \sigma_{N,1}} \tag{14.77}$$

In order visualize the order of variables, Figure 14.29 illustrate the arrangement of threshold voltages with respect to the BER level. It is important that the reader maintains the correct order; otherwise the estimated BER will be incorrect.

To perform numerical calculations, we need to find the inverse value of the Gaussian CDF function for very small values. Appendix B, found at the back of the book, provides a short table of some of the important values of this inverse function. One can also make use of the approximation to the Gaussian CDF when x is large but negative:

$$\Phi\left(x\right) \approx \frac{1}{\left(-x\right)\sqrt{2\pi}} e^{-\frac{1}{2}x^2}, \quad x \ll 0 \tag{14.78}$$

Figure 14.29. Highlighting the notation of the threshold voltages with respect to the BER level.

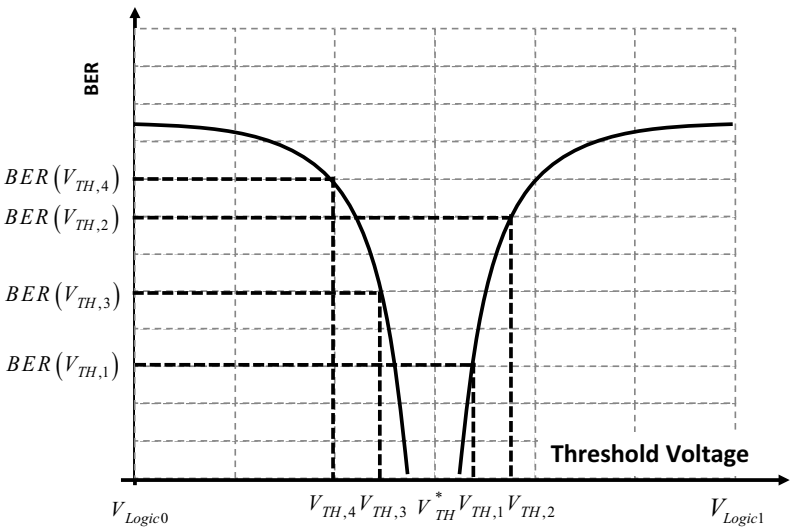

EXAMPLE 14.11

A system transmission test is to be run whereby a BER < 10^{-12} is to be verified using the amplitude-based scan test method. The following BER measurements were made at the following four threshold levels:

Voltage Threshold Levels	BER Measurement
0.70	0.5 x 10^{-6}
0.90	0.5 x 10^{-9}
1.20	0.5 x 10^{-9}
1.35	0.5 x 10^{-6}

Does this system have the capability to meet the BER requirements and what is the optimum threshold level? Assume that the noise is asymmetrical.

Solution:

Following the reference system of equations we write

$$\text{BER}\,(V_{TH,1}) = 0.5\times10^{-9} \text{ @ } V_{TH,1}=1.20, \qquad \text{BER}\,(V_{TH,2}) = 0.5\times10^{-6} \text{ @ } V_{TH,2}=1.35,$$
$$\text{BER}\,(V_{TH,3}) = 0.5\times10^{-9} \text{ @ } V_{TH,3}=0.90, \qquad \text{BER}\,(V_{TH,4}) = 0.5\times10^{-6} \text{ @ } V_{TH,4}=0.70,$$

Substituting the above parameters into Eq. (14.72), we get

$$V_{Logic1} = \frac{1.35\times\Phi^{-1}\left[10^{-9}\right] - 1.20\times\Phi^{-1}\left[10^{-6}\right]}{\Phi^{-1}\left[10^{-6}\right] - \Phi^{-1}\left[10^{-9}\right]}$$
$$\sigma_{N,1} = \frac{1.35 - 1.20}{\Phi^{-1}\left[10^{-6}\right] - \Phi^{-1}\left[10^{-9}\right]}$$

Using the relationship for $\Phi^{-1}(x)$ from the table in Appendix B, specifically, $\Phi^{-1}(10^{-6}) = -4.7534$ and $\Phi^{-1}(10^{-9}) = -5.9978$, we find

$$V_{Logic1} = \frac{1.35 \times \Phi^{-1}\left[10^{-9}\right] - 1.20 \times \Phi^{-1}\left[10^{-6}\right]}{\Phi^{-1}\left[10^{-6}\right] - \Phi^{-1}\left[10^{-9}\right]} = \frac{1.35 \times (-5.9978) - 1.20 \times (-4.7534)}{(-4.7534) - (-5.9978)} = 1.923 \text{ V}$$

$$\sigma_{N,1} = \frac{1.35 - 1.20}{\Phi^{-1}\left[10^{-6}\right] - \Phi^{-1}\left[10^{-9}\right]} = \frac{1.35 - 1.20}{(-4.7534) - (-5.9978)} = 0.1205 \text{ V}$$

Likewise, for the other logic level parameters with $\Phi^{-1}(1 - 10^{-6}) = 4.7534$ and $\Phi^{-1}(1 - 10^{-9}) = 5.9978$, we write

$$V_{Logic0} = \frac{0.90 \times \Phi^{-1}\left[1-10^{-6}\right] - 0.70 \times \Phi^{-1}\left[1-10^{-9}\right]}{\Phi^{-1}\left[1-10^{-6}\right] - \Phi^{-1}\left[1-10^{-9}\right]} = \frac{0.90 \times 4.7534 - 0.70 \times 5.9978}{4.7534 - 5.9978} = -0.064 \text{ V}$$

$$\sigma_{N,0} = \frac{0.90 - 0.70}{\Phi^{-1}\left[1-10^{-6}\right] - \Phi^{-1}\left[1-10^{-9}\right]} = \frac{0.90 - 0.70}{4.7534 - 5.9978} = 0.1607 \text{ V}$$

The optimum threshold level is

$$V^*_{TH} = \frac{\sigma_{N,0} V_{Logic1} + \sigma_{N,1} V_{Logic0}}{\sigma_{N,0} + \sigma_{N,1}} = \frac{0.1607 \times 1.923 - 0.1205 \times (-0.064)}{0.1607 + 0.1205} = 1.071 \text{ V}$$

Finally, we compute the minimum BER from

$$BER\left(V^*_{TH}\right) = \frac{1}{2} - \frac{1}{2} \times \Phi\left(\frac{1.071 + 0.064}{0.1607}\right) + \frac{1}{2} \times \Phi\left(\frac{1.071 - 1.923}{0.1205}\right) = \frac{1}{2} - \frac{1}{2} \times \Phi(7.06) + \frac{1}{2} \times \Phi(-7.06)$$

Using the identity

$$\Phi(7.06) = 1 - \Phi(-7.06)$$

The above expression reduces to

$$\text{BER}\left(V^*_{TH}\right) = \Phi(-7.06)$$

Using the table in Appendix B, we note that is $\Phi(-7.06)$ is bounded by $\Phi(-7.06) = 10^{12}$; hence we estimate the minumum BER as

$$\text{BER}\left(V^*_{TH}\right) < 10^{-12}$$

Alternatively, we can make use of the approximation in Eq. (14.78) and estimate $\Phi(-7.06)$ as

$$\Phi(-7.06) \approx \frac{1}{7.06\sqrt{2\pi}} e^{-\frac{1}{2}(-7.06)^2} = 8.22 \times 10^{-13}$$

We can therefore conclude that the system meets the BER requirements (just barely, though).

A variant of the amplitude-based scan test technique is one that captures a histogram of the voltage level around each logic level at the center of the eye diagram. A digital sampler or digital sampling oscilloscope is often used to capture these histograms, from which its mean (logic voltage level) and standard deviation can be found. Subsequently, the optimum threshold and minimum BER can be found by combining Eq. (14.77) with Eq. (14.76). The following example will illustrate this approach.

EXAMPLE 14.12

A digital sampling oscilloscope obtained the following eye diagram while observing the characteristics of a 1-Gbps digital signal. Histograms were obtain using the built-in function of the scope at a sampling instant midway between transitions (i.e., at the maximum point of eye opening). Detailed analysis revealed that each histogram is Gaussian. One histogram has a mean value of 100 mV and a standard deviation of 50 mV. The other has a mean of 980 mV and a standard deviation of 75 mV. What is the theoretical minimum BER associated with this system?

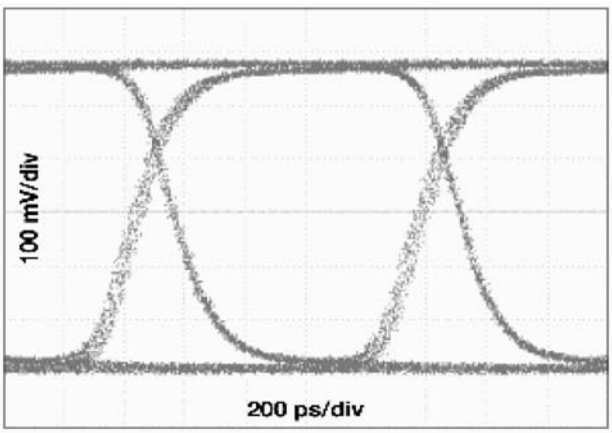

Solution:
Restating the given information in terms of the parameters used in the text above, we write

$$V_{Logic0} = 100 \text{ mV}, \qquad V_{Logic1} = 980 \text{ mV}$$
$$\sigma_{N,0} = 50 \text{ mV}, \qquad \sigma_{N,1} = 75 \text{ mV}$$

Substituting the above parameters into the expression for the optiumum thresold level given in Eq. (14.77), we write

$$V^*_{TH} = \frac{\sigma_{N,0} V_{Logic1} + \sigma_{N,1} V_{Logic0}}{\sigma_{N,0} + \sigma_{N,1}} = \frac{0.050 \times 0.980 + 0.075 \times 0.100}{0.050 + 0.075} = 0.452 \text{ V}$$

from which we write the minimum BER as

$$\text{BER}\left(V^*_{TH}\right) = \frac{1}{2} - \frac{1}{2} \times \Phi\left(\frac{0.452 - 0.100}{0.050}\right) + \frac{1}{2} \times \Phi\left(\frac{0.452 - 0.980}{0.075}\right)$$

resulting in

$$\mathrm{BER}\left(V^{*}_{TH}\right) = \Phi\left(-7.04\right) = 9.61\times 10^{-13}$$

Here we see that the theoretical minumum BER is slightly less than 10^{-12}.

Exercises

14.16. A system transmission test is to be run whereby a BER < 10^{-12} is to be verified using the amplitude-based scan test method. The threshold voltage of the receiver was adjusted to the following levels: 0.7, 1.0, 3.1 and 3.3 V. Also, the corresponding BER levels were measured: 5 x 10^{-6}, 5 x 10^{-9}, 5 x 10^{-9}, and 5 x 10^{-6}. What are the levels of the received logic values? Does the system meet the BER requirements if the receiver threshold is set at 2.0 V?

ANS. $V_{Logic,0} = -249.7$ mV;
$V_{Logic,1} = 3.933$ mV;
$\mathrm{BER}(2.0\ \mathrm{V}) = 1.3\times 10^{-24}$.

14.17. A digital system is designed to operate at 25 Gbps and have a nominal logic 1 level of 0.9 V and a logic 0 at 0.1 V. If the threshold of the receiver is set at 0.6 V and the noise present at the receiver is 100 mV RMS, select the levels of the amplitude scan test method so that the system can be verified for a BER < 10^{-12} at a confidence level of 99.7% and that the total test time is less than 50 ms.

ANS.
$V_{TH,1} = 0.680$ V @ $\mathrm{BER}_1 = 10^{-8}$,
$V_{TH,2} = 0.716$ V @ $\mathrm{BER}_2 = 10^{-6}$,
Test Time =46.9 ms.

14.18. A time jitter sequence is described by $s[n] = 1\times \sin^2(14\pi/1024\, n)$ for n = 0,1,..., 1023. What is the mean, sigma and kurtosis of this data set? Is the data set Gaussian?

ANS.
$\mu = 0.5$, $\sigma = 0.354$, $k = 1.5$.
No, as $k \neq 3$.

The application of the amplitude-based scan test technique assumes that the histogram around each voltage level is Gaussian. One often needs to assure oneself that this assumption is realistic with the data set that are collected. Simply looking at the histogram plot to see if the distribution accurately follows a Gaussian is difficult because the subtleties in the tails are not easy to observe. A kurtosis metric or a normal probability plot can be used (see Section 4.2.4).

The validity of the amplitude-based scan test technique or *Q*-factor method has been called into question,[11] largely on account of its ability to accurately predict system behavior at very low BER from measurements made at much larger BER levels. While system impairments may be dominated by Gaussian noise behavior at large BER levels, one really doesn't know if such behavior continues at low BER levels unless one measures it. The converse is also true: When jitter impairments are present, the amplitude-based scan test technique predicts the minimum BER at a much higher level than a direct BER measurement would find—again, skewing the results. Even with these drawbacks, the amplitude-based scan test technique is a widely used method.

14.6.2 Time-Based Scan Test

The BER depends on the voltage noise present in the system as well as the noise associated with the sampling instant. We can repeat the BER analysis of the previous subsection, but this time let us write the BER in terms of the sampling instant assuming that the jitter distribution is Gaussian with zero mean and standard deviation σ_{RJ}. As previously stated for the amplitude-based scan test method, this test would be conducted with an altering 1010 pattern to ensure that no ISI is present.

In Section 14.4.3 we derived the BER in terms of the denormalized sampling instant as

$$\mathrm{BER}\left(t_{TH}\right)=\frac{1}{2}-\frac{1}{2}\times\Phi\left(\frac{t_{TH}-0}{\sigma_{RJ}}\right)+\frac{1}{2}\times\Phi\left(\frac{t_{TH}-T}{\sigma_{RJ}}\right) \tag{14.79}$$

Here we recognize that the BER expression contains one unknown σ_{RJ}; hence we can make a single measurement and solve for this unknown. Furthermore, we recognize that if we sample close to either edge of a bittransition, we can approximate Eq.(14.79) by the following:

$$\mathrm{BER}\left(t_{TH}\right)\approx\begin{cases}\dfrac{1}{2}-\dfrac{1}{2}\times\Phi\left(\dfrac{t_{TH}}{\sigma_{RJ}}\right) & 0\le t_{TH}\ll\dfrac{T}{2}\\[2ex] \dfrac{1}{2}\times\Phi\left(\dfrac{t_{TH}-T}{\sigma_{RJ}}\right) & \dfrac{T}{2}\ll t_{TH}\le T\end{cases} \tag{14.80}$$

Assuming that we set the sampling instant at $t_{TH,1}$ much less than $T/2$, then after making a single BER measurement we can write an expressionrelating this measurement as

$$\mathrm{BER}\left(t_{TH,1}\right)=\frac{1}{2}-\frac{1}{2}\times\Phi\left(\frac{t_{TH,1}}{\sigma_{RJ}}\right) \tag{14.81}$$

We can then solve for σ_{RJ} and write

$$\sigma_{RJ}=\frac{t_{TH,1}}{\Phi^{-1}\left[1-2\times\mathrm{BER}\left(t_{TH,1}\right)\right]} \tag{14.82}$$

To estimate the location of the sampling instant, first assume a specific level of noise present and the level of BER that is expected, then rearrange Eq. (14.81) and write

$$t_{TH,1}=\sigma_{RJ}\times\Phi^{-1}\left[1-2\times\mathrm{BER}\left(t_{TH,1}\right)\right] \tag{14.83}$$

For instance, if we estimate that 10 ps of RJ is present on the digital signal and we want to make a BER measurement at a 10^{-6} level, we estimate the sampling time to be

$$t_{TH,1}=10^{-11}\times\Phi^{-1}\left[1-2\times10^{-6}\right]\approx 46.1\ \mathrm{ps}$$

Once σ_{RJ} is determined, we substitute this result back into Eq. (14.79) and solve for the system BER at the appropriate sampling instant, typically the middle of the data eye.

EXAMPLE 14.13

The BER performance of a digital reciever was measured to be 10^{-14} at a bit rate of 600 Mbps having a sampling instant at one-half the bit duration. Due to manufacturing errors, the sampling instant can vary by a ±20% from its ideal position. Assuming an underlying noise component that is Gaussian in nature, what is the range of BER performance expected during production?

Solution:
As the ideal sampling instant is set at one-half the clock period, for a 600-MHz bit rate, this corresponds to a 0.833-ns sampling instant. Using Eq. (14.82), we can solve for the standard deviation of the underlying noise process as follows

$$\mathrm{BER}\left(\frac{T}{2}\right) = 10^{-14} = \frac{1}{2} - \frac{1}{2} \times \Phi\left(\frac{T}{2\sigma_{RJ}}\right) + \frac{1}{2} \times \Phi\left(-\frac{T}{2\sigma_{RJ}}\right)$$

which reduces to the following when the identity is substituted:

$$\mathrm{BER}\left(\frac{T}{2}\right) = 10^{-14} = \Phi\left(-\frac{T}{2\sigma_{RJ}}\right)$$

Rearranging, we write

$$\sigma_{RJ} = \frac{1/600 \times 10^{6}}{-2 \times \Phi^{-1}\left(10^{-14}\right)} = \frac{1/600 \times 10^{6}}{-2 \times -7.651} = 1.09 \times 10^{-10} \text{ s}$$

Next, given that the sampling instant can vary by ±20% from its ideal position of 8.33×10^{-10} s, we write

$$\frac{1/600 \times 10^{6}}{2}\left(1 - 0.2\right) \le t_{TH} \le \frac{1/600 \times 10^{6}}{2}\left(1 + 0.2\right)$$

or when simplified as

$$6.66 \times 10^{-10} \le t_{TH} \le 1 \times 10^{-9}$$

As the BER performance varies in a symmetrical manner about the $T/2$ sampling instant, the BER performance level is the same at either extreme. Selecting $t_{TH} = 1 \times 10^{-9}$s, the BER performance we can expect is

$$\mathrm{BER}\left(10^{-9}\right) = \frac{1}{2} - \frac{1}{2} \times \Phi\left(\frac{10^{-9} - 0}{1.09 \times 10^{-10}}\right) + \frac{1}{2} \times \Phi\left(\frac{10^{-9} - 1/600 \times 10^{6}}{1.09 \times 10^{-10}}\right) = \frac{1}{2} - \frac{1}{2} \times \Phi\left(9.18\right) - \Phi\left(-6.12\right) \approx \Phi\left(-6.12\right)$$

Through the application of a computer program (MATLAB, Excel, etc.) we find

$$\mathrm{BER}\left(10^{-9}\right) = 2.33 \times 10^{-10}$$

Therefore during a production test, we can expect the BER performance to vary between 10^{-14} and 2.33 x 10^{-10}.

Exercises

14.19. A digital sampling oscilloscope was used to determine the zero crossings of an eye diagram. At 0 UI, the histogram is Gaussian distributed with zero mean and a standard deviation of 5 ps. At the unit interval, the histogram is again Gaussian distributed with zero mean value and a standard deviation of 8 ps. If the unit interval is equal to 100 ps, what is the expected BER associated with this system at a normalized sampling instant of 0.5 UI?

ANS. $\text{BER} = 1.03 \times 10^{-10}$

14.6.3 Dual-Dirac Jitter Decomposition Method

System transmission is often evaluated under various stressed conditions in order to better evaluate its behavior under typical operating conditions. System test specifications are often written to include BER tests for various types of PRBS input patterns. The amplitude or time-based scan test methods previously described are not suitable for this test, as the PRBS pattern introduces a data-dependent jitter component (as explained in Section 14.4.2). In other words, the underlying assumption that the noise associated with the received signal follows Gaussian statistics no longer holds. Instead, the method of jitter decomposition is used to evaluate the system transmission BER in production. The basic idea behind this method is to separate the random jitter (RJ) components from the deterministic jitter (DJ) components, write an expression for the BER in terms of these jitter terms, and then, in much the same way as the scan test approach, make measurements of BER at different sampling instants then solve for the unknown jitter terms.

Let us begin by assuming that the total jitter distribution is non-Gaussian and consisting of two parts: one random with PDF denoted by pdf_{RJ} and the other deterministic with PDF pdf_{DJ}. As we learned in Section 14.4.2, the PDF of the total jitter can be written as the convolution of the two separate parts, that is.,

$$pdf_{TJ} = pdf_{RJ} \otimes pdf_{DJ} \tag{14.84}$$

We further learned that the DJ component could consist of many parts, including PJ, DDJ and DCD jitter components. One can extend the above theory for each of these separate noise components by expanding the convolution operation across all noise elements, for example,

$$pdf_{TJ} = pdf_{RJ} \otimes pdf_{PJ} \otimes pdf_{ISI} \otimes pdf_{DCD} \tag{14.85}$$

Keeping the situation here more manageable, we shall consider the situation described by Eq. (14.84) and leave the more general case to some later examples.

We shall begin by describing the dual-Dirac jitter decomposition method[8] where the RJ noise component is assumed to follow Gaussian statistics with zero mean and standard deviation σ_{RJ} and the DJ component follows a distribution that has a dual-impulse or dual-Dirac behavior with parameter μ_{DJ}. Mathematically, we write these two PDFs as follows:

$$pdf_{RJ} = \frac{1}{\sigma_{RJ} 2\sqrt{2\pi}} e^{-t^2/2\sigma_{RJ}^2} \tag{14.86}$$

$$pdf_{DJ} = \frac{1}{2}\delta\left(t - \frac{\mu_{DJ}}{2}\right) + \frac{1}{2}\delta\left(t + \frac{\mu_{DJ}}{2}\right) \tag{14.87}$$

Figure 14.30. A multi-mode Gaussian representation of the total jitter distribution.

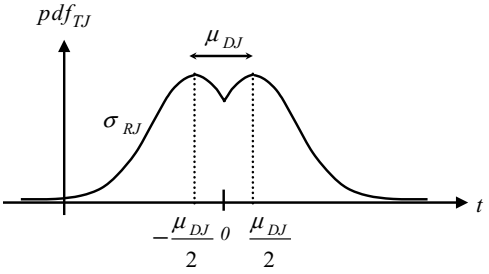

and denote the DJ and RJ measurement metrics as

$$\begin{aligned} DJ &= \mu_{DJ} \\ RJ &= \sigma_{RJ} \end{aligned} \tag{14.88}$$

Through the convolution operation listed in Eq. (14.84), we can describe the total jitter PDF for any bit transition as

$$pdf_{TJ} = \frac{1}{2} \times \frac{1}{\sigma_{RJ}\sqrt{2\pi}} e^{-\left(t+\mu_{DJ}/2\right)^2 / 2\sigma_{RJ}^2} + \frac{1}{2} \times \frac{1}{\sigma_{RJ}\sqrt{2\pi}} e^{-\left(t-\mu_{DJ}/2\right)^2 / 2\sigma_{RJ}^2} \tag{14.89}$$

We illustrate this PDF in Figure 14.30, where it consists of two Gaussians distributions centered at $t = -\mu_{DJ}/2$ and $t = \mu_{DJ}/2$. It is important to recognize that the peaks associated with each Gaussian distribution are offset from one another by the parameter μ_{DJ}. Moreover, this offset is independent of the number of samples collected, as it is deterministic in nature. In practice, this fact is often used to identify the amount of DJ present with a jittery signal. In essence, the dual-Dirac modeling method is attempting to fit two Gaussian distributions with symmetrical mean values and equal standard deviation to the random portion of the digital signal.

Following the development of Section 14.4.3, the BER is computed as follows

$$\mathrm{BER}\left(t_{TH}\right) = \frac{1}{2} \times \int_{(n-1)T+t_{TH}}^{\infty} pdf_{TJ}\big|_{t=(n-1)T}\, dt + \frac{1}{2} \times \int_{-\infty}^{nT-t_{TH}} pdf_{TJ}\big|_{t=nT}\, dt \tag{14.90}$$

where $pdf_{TJ}\big|_{t=(n-1)T}$ and $pdf_{TJ}\big|_{t=nT}$ represents the total jitter of $(n-1)$-th and nth consecutive bit transitions. t_{TH} is the sampling instance within the unit-interval bit period T. Substituting Eq. (14.89) into Eq. (14.90) and working through the integration, we find the BER can be written in terms of the Gaussian CDF and sampling instant t_{TH} as follows:

$$\begin{aligned} \mathrm{BER}\left(t_{TH}\right) = {} & \frac{1}{4} \times \left[2 - \Phi\left(\frac{t_{TH} + \mu_{DJ}/2}{\sigma_{RJ}} \right) - \Phi\left(\frac{t_{TH} - \mu_{DJ}/2}{\sigma_{RJ}} \right) \right] \\ & + \frac{1}{4} \times \left[\Phi\left(\frac{t_{TH} - T + \mu_{DJ}/2}{\sigma_{RJ}} \right) + \Phi\left(\frac{t_{TH} - T - \mu_{DJ}/2}{\sigma_{RJ}} \right) \right] \end{aligned} \tag{14.91}$$

Because only two of the four terms contribute to the overall BER in a region, we can simplify the above equation and write

$$\text{BER}(t_{TH}) = \begin{cases} \frac{1}{4}\times\left[2-\Phi\left(\frac{t_{TH}+\mu_{DJ}/2}{\sigma_{RJ}}\right)-\Phi\left(\frac{t_{TH}-\mu_{DJ}/2}{\sigma_{RJ}}\right)\right] & 0 \le t_{TH} \ll T/2 \\ \frac{1}{4}\times\left[\Phi\left(\frac{t_{TH}-T+\mu_{DJ}/2}{\sigma_{RJ}}\right)+\Phi\left(\frac{t_{TH}-T-\mu_{DJ}/2}{\sigma_{RJ}}\right)\right] & T/2 \ll t_{TH} \le T \end{cases} \quad \textbf{(14.92)}$$

The following example will be used to illustrate how the dual-Dirac jitter decomposition method is applied to a practical situation.

EXAMPLE 14.14

A digital system operates with a 1-GHz clock. How much RJ can be tolerated by the system if the BER is to be less than 10^{-10} and the DJ is no greater than 10 ps? Assume that the sampling instant is in the middle of the data eye having a unit time interval of 1 ns.

Solution:

Substituting the given information, that is, T = 1000 ps, t_{TH} = 500 ps, μ_{DJ} 10 ps, and BER (t_{TH}) 10^{-10} into Eq. (14.91), we write

$$BER(t_{TH}) \le 10^{-10}$$

or

$$\frac{1}{4}\times\left[2-\Phi\left(\frac{500\text{ ps}+5\text{ ps}}{\sigma_{RJ}}\right)-\Phi\left(\frac{500\text{ ps}-5\text{ ps}}{\sigma_{RJ}}\right)\right] + \frac{1}{4}\times\left[\Phi\left(\frac{500\text{ ps}-1000\text{ ps}+5\text{ ps}}{\sigma_{RJ}}\right)+\Phi\left(\frac{500\text{ ps}-1000\text{ ps}-5\text{ ps}}{\sigma_{RJ}}\right)\right] \le 10^{-10}$$

which, when simplified, becomes

$$\Phi\left(\frac{-495\text{ ps}}{\sigma_{RJ}}\right)+\Phi\left(\frac{-505\text{ ps}}{\sigma_{RJ}}\right) \le 2\times10^{-10}$$

Because this expression is transdental and nonlinear, we simply vary for σ_{RJ} until the left-hand side of the above expression is less than 10^{-10} and declare the largest value of σ_{RJ} as the largest RJ jitter that the system can tolerate. On doing this, we obtain the following listing of results:

σ_{RJ}(ps)	BER
60	4.93 x10^{-17}
70	5.19 x10^{-13}

σ_{RJ}(ps)	BER
78.5	1.00 x 10^{-10}
80	2.21 x 10^{-10}
90	1.45 x 10^{-8}
100	2.96 x 10^{-7}

As is evident from the table, the system can tolerate a random component of jitter of less having a standard deviaiton of less than 78.5 ps in order to ensure a BER of less than or equal to 10^{-10}.

Returning to Eq. (14.91), it is evident that the BER expression is a function of two unknown parameters, μ_{DJ} and σ_{RJ}. These two parameters can be identified by making two measurements of the BER under two separate sampling instants, say $t_{TH,1}$ and $t_{TH,2}$, both less than $T/2$, resulting in the following two equations:

$$\left(\quad\right) - \qquad \Big/ \qquad \Big/$$

$$\left(\quad\right) - \qquad \Big/ \qquad \Big/$$

$$\begin{aligned} \text{BER } t_{TH,1} &\approx \frac{1}{4}\times\left[1-\Phi\left(\frac{t_{TH,1}-\mu_{DJ}/2}{\sigma_{RJ}}\right)\right] \\ \text{BER}\left(t_{TH,2}\right) &\approx \frac{1}{4}\times\left[1-\Phi\left(\frac{t_{TH,2}-\mu_{DJ}/2}{\sigma_{RJ}}\right)\right] \end{aligned} \tag{14.94}$$

The two unknown parameters can then be easily solved as follows:

$$\begin{aligned} \sigma_{RJ} &= \frac{t_{TH,1}-t_{TH,2}}{\Phi^{-1}\left[1-4\times\text{BER}\left(t_{TH,1}\right)\right]-\Phi^{-1}\left[1-4\times\text{BER}\left(t_{TH,2}\right)\right]} \\ \mu_{DJ} &= \frac{2\times t_{TH,2}\times\Phi^{-1}\left[1-4\times\text{BER}\left(t_{TH,1}\right)\right]-2\times t_{TH,1}\times\Phi^{-1}\left[1-4\times\text{BER}\left(t_{TH,2}\right)\right]}{\Phi^{-1}\left[1-4\times\text{BER}\left(t_{TH,1}\right)\right]-\Phi^{-1}\left[1-4\times\text{BER}\left(t_{TH,2}\right)\right]} \end{aligned} \tag{14.95}$$

The following example will help to illustrate the application of this theory.

Figure 14.31. (a) The zero-crossing distribution around two consecutive bit transitions; shaded area indicate bit error probability. (b) Individual Gaussian distribution around each bit transition. (c) BER as a function of sampling instant ($t=t_{TH}$).

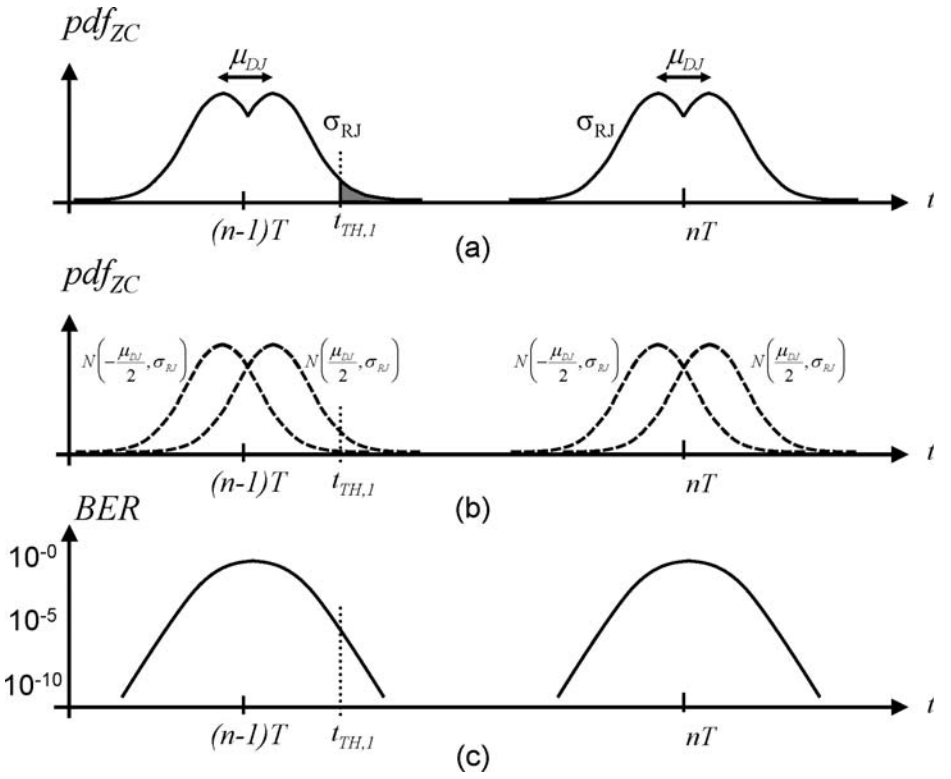

EXAMPLE 14.15

A system transmission test is to be run whereby a BER < 10^{-12} is to be verified using the jitter-decomposition test method. The system operates with a 1-GHz clock and the following BER measurements are at two different sampling instances: BER = 0.25 x 10^{-4} at 300 ps, and BER = 0.25 x 10^{-6} at 350 ps. Assume the digital system operates with a sampling instant in the middle of the data eye. Does the system meet spec?

Solution:
Following the reference system of equations, we write

$$BER(t_{TH,1}) = 0.25 \times 10^{-4} \text{ @ } t_{TH,1} = 300 \times 10^{-12}$$

$$BER(t_{TH,2}) = 0.25 \times 10^{-6} \text{ @ } t_{TH,2} = 350 \times 10^{-12}$$

Assuming the BERs were obtained on the tail of a single Gaussian, we substitute the above parameters into Eq.(14.95) and write

$$\sigma_{RJ} = \frac{300\times10^{-12} - 350\times10^{-12}}{\Phi^{-1}\left[1-10^{-4}\right] - \Phi^{-1}\left[1-10^{-6}\right]}$$

$$\mu_{DJ} = \frac{2\times350\times10^{-12}\times\Phi^{-1}\left[1-10^{-4}\right] - 2\times300\times10^{-12}\times\Phi^{-1}\left[1-10^{-6}\right]}{\Phi^{-1}\left[1-10^{-4}\right] - \Phi^{-1}\left[1-10^{-6}\right]}$$

Using the relationship for $\Phi^{-1}(1 - x)$ from the table in Appendix B, specifically, $\Phi^{-1}(1 - 10^{-4}) = 3.7190$, and $\Phi^{-1}(1 - 10^{-6}) = 4.7534$, we solve to obtain $\mu_{DJ} = 240.5$ ps and $\sigma_{RJ} = 48.3$. In order to ensure that our simiplified model of BER behavior is reasonable in the region where the samples of BER were obtained, we compare

$$\mathrm{BER}(t_{TH}) = \frac{1}{4}\times\left[2 - \Phi\left(\frac{t_{TH}+120.2\text{ ps}}{48.3\text{ ps}}\right) - \Phi\left(\frac{t_{TH}-120.2\text{ ps}}{48.3\text{ ps}}\right)\right]$$

with

$$\mathrm{BER}(t_{TH}) = \frac{1}{4}\times\left[1 - \Phi\left(\frac{t_{TH}-120.2\text{ ps}}{48.3\text{ ps}}\right)\right]$$

as shown below:

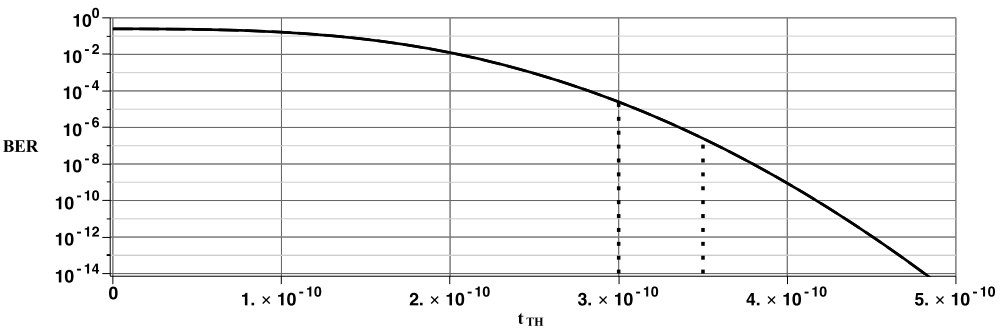

Clearly, we see that the two curves are identical in the region over the range of sampling instants chosen. Hence our initial assumption is correct and we are confident that our calculation of DJ and RJ are correct. Substituting these two parameters into Eq. (14.91) we obtain an expresson of the BER across the entire eye diagram as as a function of the sampling instant t_{TH} as

$$\mathrm{BER}(t_{TH}) = \frac{1}{4}\times\left[1 - \Phi\left(\frac{t_{TH}+240.5\text{ ps}}{48.3\text{ ps}}\right)\right] + \frac{1}{4}\times\left[1 - \Phi\left(\frac{t_{TH}-240.5\text{ ps}}{48.3\text{ ps}}\right)\right]$$
$$+\frac{1}{4}\times\Phi\left(\frac{t_{TH}-1000\text{ ps}+240.5\text{ ps}}{48.3\text{ ps}}\right) + \frac{1}{4}\times\Phi\left(\frac{t_{TH}-1000\text{ ps}-240.5\text{ ps}}{48.3\text{ ps}}\right)$$

Finally, we solve for the BER at a samping instant in the middle of the data eye, (i.e., t_{TH} = 0.5 ns), and obtain

$$\text{BER (5 ns)} = 9.8 \times 10^{-16}$$

Therefore we conclude the BER is less than 10^{-12} and the system meets spec. We should note that if the 1-Gaussian model of BER behavior differs from the 2-Gaussian behavior, then we must solve the RJ and DJ parameters directly from the 2-Gaussian model of BER behavior. We encourage our readers to attempt the exercise below.

Exercises

14.20. A system transmission test is to be run whereby a BER < 10^{-14} is to be verified using the dual-Dirac jitter-decomposition test method. The system operates with a 25-GHz clock and the following BER measurements are made at two different sampling instances: BER = 0.25 x 10^{-4} at 9 ps, and BER = 0.25 x 10^{-6} at 11 ps. Assume the digital system operates with a sampling instant in the middle of the data eye. Does the system meet spec?

ANS.
$\text{BER}(T/2) = 1.26 \times 10^{-21}$;
RJ = 1.9 ps; DJ = 3.6 ps.
Yes, the system meets spec.

Total Jitter Definition

Transmission specifications, such as fiber channel, Infini-band, and XAUI, often include a test metric called total jitter (denoted TJ), in addition to the test limits for DJ and RJ. While DJ and RJ are model parameters derive indirectly through the application of several BER measurements, TJ is derived directly from these two parameters.

To understand the definition of TJ, let us first consider the eye diagram shown in Figure 14.32a. Here we highlight the size of the eye opening along the time axis. Intuitively, the larger the

Figure 14.32. Illustrating the definition of total jitter (TJ) based on eye opening: (a) Eye diagram and (b) corresponding BER versus sampling instant ($t = t_{TH}$).

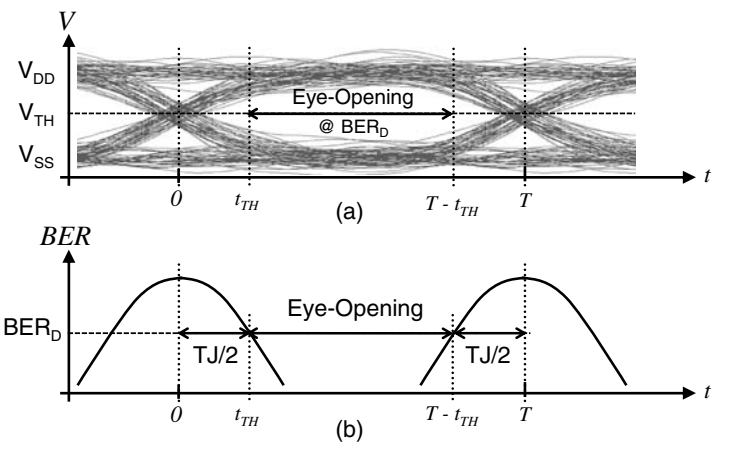

eye opening, the better the quality of the signal transmission, because there would be less chance of obtaining a bit error. Under ideal conditions, the maximum eye opening is equal to the bit duration, *T*. The difference between the ideal and actual eye opening is defined as the total jitter, TJ, that is,

$$\text{TJ} \triangleq \text{Ideal eye opening} - \text{Actual eye opening} \tag{14.96}$$

While we could define the eye opening based on the signal transitions that bound the open area encapsulatedby the data eye, we need to account for the random variations that will occur. Specifically, the edges of the eye opening along the time axis are defined based on an expected probability that a transition will go beyond a specific time instant, which we learned previously is equivalent to the BER. Figure 14.32(b) illustrates the BER as function of the sampling instant, and provides a manner in which to quantify TJ, that is,

$$\text{TJ} = 2 \times t_{TH} \tag{14.97}$$

At relative low BER levels, we can approximate the BER as

$$\text{BER}\left(t_{TH}\right) \approx \frac{1}{4} \times \left[1 - \Phi\left(\frac{t_{TH} - \mu_{DJ}/2}{\sigma_{RJ}}\right)\right] \tag{14.98}$$

Rearranging, we can write the sampling instant t_{TH} in terms of the desired BER, denoted by BER_D, as follows:

$$t_{TH} = \sigma_{RJ} \times \Phi^{-1}\left[1 - 4 \times \text{BER}_D\right] + \frac{\mu_{DJ}}{2} \tag{14.99}$$

Substituting the above expression into Eq. (14.97), we obtain the commonly used definition for TJ, that is,

$$\text{TJ} = 2 \times \sigma_{RJ} \times \Phi^{-1}\left[1 - 4 \times \text{BER}_D\right] + \mu_{DJ} \tag{14.100}$$

EXAMPLE 14.16

A system transmission test was run and the RJ and DJ components were found to be 13 ps and 64.6 ps, respectively. What is the TJ component at a BER level of 10^{-12}?

Solution:
Substituting RJ and DJ into Eq. (14.100), we write

$$\text{TJ} = 2 \times 13 \text{ ps} \times \Phi^{-1}\left[1 - 4 \times 10^{-12}\right] + 64.6 \text{ ps}$$

Using the data provided in the Table of Appendix B, we find $\Phi^{-1}[1 - 4 \times 10^{-12}]$, allowing us to write

$$\text{TJ} = 2 \times 13 \text{ ps} \times 6.839 + 64.6 \text{ ps} = 242.4 \text{ ps}$$

Exercises

14.21. A system transmission test was run where the RJ component was found to be 25 ps and the TJ component at a BER level of 10^{-14} was found to be 400 ps. What is DJ? ANS. DJ = 26.48 ps.

14.22. A system transmission test was run where the DJ component was found to be 5 ps and the TJ component at a BER level of 10^{-12} was found to be 120 ps. What is RJ? ANS. RJ = 8.4 ps.

14.6.4 Gaussian Mixture Jitter Decomposition Method

The dual-Dirac jitter composition method just described in the last subsection is a special case of fitting a set of independent Gaussian distributions to an arbitrary distribution, albeit without the physical understanding associated with the PDF convolution method. Assuming that the total jitter distribution consists of G independent Gaussian distributions with mean values of μ_i and standard deviation σ_i for $i = 1, ..., G$, we can write the PDF for the TJ as

$$pdf_{TJ} = \frac{\alpha_1}{\sigma_1\sqrt{2\pi}} e^{-(t-\mu_1)^2/2\sigma_1^2} + \frac{\alpha_2}{\sigma_2\sqrt{2\pi}} e^{-(t-\mu_2)^2/2\sigma_2^2} + \cdots + \frac{\alpha_{N_G}}{\sigma_G\sqrt{2\pi}} e^{-(t-\mu_G)^2/2\sigma_G^2} \tag{14.101}$$

where the terms α_i are weighting terms. Subsequently, we can substitute Eq.(14-101) into Eq. (14.90) and write the BER at sampling instant t_{TH} as

$$\begin{aligned} \mathrm{BER}(t_{TH}) = {} & \frac{\alpha_1}{2} \times \left[1 - \Phi\left(\frac{t_{TH} - \mu_1}{\sigma_1} \right) \right] + \frac{\alpha_2}{2} \times \left[1 - \Phi\left(\frac{t_{TH} - \mu_2}{\sigma_2} \right) \right] + \ldots + \frac{\alpha_G}{2} \times \left[1 - \Phi\left(\frac{t_{TH} - \mu_G}{\sigma_G} \right) \right] \\ & + \frac{\alpha_1}{2} \times \Phi\left(\frac{t_{TH} - T - \mu_1}{\sigma_1} \right) + \frac{\alpha_2}{2} \times \Phi\left(\frac{t_{TH} - T - \mu_2}{\sigma_2} \right) + \ldots + \frac{\alpha_G}{2} \times \Phi\left(\frac{t_{TH} - T - \mu_G}{\sigma_G} \right) \end{aligned} \tag{14.102}$$

We depict a three-term Gaussian mixture in Figure 14.33. In part (a) we illustrate the total jitter distribution as a function of eye position, followed by the individual Gaussian mixture in part (b) and then the corresponding BER as a function of sampling instant in part (c). A specific sampling instance t_{TH} is identified in all three diagrams of Figure 14.33, highlighting a specific bit error probability and its impact on the BER. It is important to recognizefrom this figure that the distributions and BER function can be asymmetrical with respect to the ideal bit transition instant ($t = (n–1)T$ and $t = nT$).

For low BER levels, we can approximate Eq. (14.102) using two Gaussian distributions taken from the Gaussian mixture of Eq. (14.101) as follows:

$$\mathrm{BER}(t_{TH}) \approx \begin{cases} \dfrac{\alpha_{tail+}}{2} \times \left[1 - \Phi\left(\dfrac{t_{TH} - \mu_{tail+}}{\sigma_{tail+}} \right) \right], & 0 \ll t_{TH} \le \dfrac{T}{2} \\ \dfrac{\alpha_{tail-}}{2} \times \Phi\left(\dfrac{t_{TH} - T - \mu_{tail-}}{\sigma_{tail-}} \right), & \dfrac{T}{2} \le t_{TH} \ll T \end{cases} \tag{14.103}$$

where tail+ and tail– is a integer number from 1 to G, and tail+ can also be equal to tail–. Because the tails of a general distribution depends on both the mean values and the standard deviations of

the Gaussian mixture, some effort must go into to identifying the dominant Gaussian function in each tail region of the total jitter distribution. A simple approach is to evaluate the BER contribution of each Gaussian term at some distance away from each edge transition of the eye diagram.

In terms of extracting the RJ and DJ metrics from the total jitter, we note that in the general case, DJ is defined as the distance between the two Gaussians that define the tail regions of the total distribution, that is,

$$\mathrm{DJ} \triangleq \mu_{DJ} = \mu_{tail+} - \mu_{tail-} \tag{14.104}$$

Likewise, RJ is defined as the average value of the standard deviations associated with the tail distributions[9], that is,

$$\mathrm{RJ} \triangleq \sigma_{RJ} = \frac{\sigma_{tail-} + \sigma_{tail+}}{2} \tag{14.105}$$

In addition to these two definitions, we can also write an equation for the TJ metric using the notation indicated in Figure 14.33c, specifically

$$\mathrm{TJ} = T - \left(t_{TH,2} - t_{TH,1}\right) \tag{14.106}$$

where $t_{TH,1}$ and $t_{TH,2}$ correspond to the sampling instant at the desired BER level, BER_D, given by

$$\begin{aligned} t_{TH,1} &= \sigma_{tail+} \times \Phi^{-1}\left[1 - \frac{2}{\alpha_{tail+}}\mathrm{BER}_D\right] + \mu_{tail+} \\ t_{TH,2} &= \sigma_{tail-} \times \Phi^{-1}\left[\frac{2}{\alpha_{tail-}}\mathrm{BER}_D\right] + T + \mu_{tail-} \end{aligned} \tag{14.107}$$

Substituting into Eq. (14.106) and simplifying, we obtain

$$\mathrm{TJ} = \sigma_{tail+} \times \Phi^{-1}\left[1 - \frac{2}{\alpha_{tail+}}\mathrm{BER}_D\right] + \sigma_{tail-} \times \Phi^{-1}\left[1 - \frac{2}{\alpha_{tail-}}\mathrm{BER}_D\right] + \mu_{tail+} - \mu_{tail-} \tag{14.108}$$

Looking back at the dual-Dirac jitter decomposition methods of Section 14.6.3, these three definitions of DJ, RJ and TJ are consistent with the definitions given there when $\mu_{tail+} = -\mu_{tail-}$, $\sigma_{tail+} = \sigma_{tail-}$ and $\alpha_{tail+} = \alpha_{tail-} = 0.5$.

Finally, the random component of the jitter has a PDF that can be described by

$$pdf_{RJ} = \frac{1}{\sigma_{RJ}\sqrt{2\pi}} e^{-t^2/2\sigma_{RJ}^2} \tag{14.109}$$

The remaining task at hand is to determine the model parameters μ_{tail-}, μ_{tail+}, σ_{tail-}, σ_{tail+} and the weighting coefficients, α_{tail-} and α_{tail+}. While one may be tempted to go off and measure five different BER values at six different sampling times and attempt to solve for the six unknowns using some form of nonlinear optimization, much care is needed in selecting the sampling instants. It is imperative that samples are derived only from the outer tails of the total jitter distribution to avoid any contributions from the other Gaussians. This generally means sampling at very low BER levels, driving up test time. This approach is the basis of the Tail-Fit™ algorithm of Wavecrest™. At the heart of this method is the chi-square (χ^2) curve-fitting algorithm. Interested readers can refer to reference 14.

Exercises

14.23. The jitter distribution at the transmit side of a communication channel can be described by a Gaussian mixture model with parameters:

$\mu_1 = -100$ ps, $\sigma_1 = 50$ ps, $\alpha_1 = 0.3$
$\mu_2 = -1$ ps, $\sigma_2 = 60$ ps, $\alpha_2 = 0.4$
$\mu_3 = 50$ ps, $\sigma_3 = 50$ ps, $\alpha_3 = 0.3$

What is the RJ, DJ, and TJ at a BER of 10^{-14} assuming a bit rate of 100 Mbps? Which indiviudal distribution set the tail regions of the total jitter?

ANS.

RJ = 55 ps, DJ = 99 ps,
TJ = 915.6 ps.

The positive tail is set by $N(\mu_2,\sigma_2)$ and the negative tail is set by $N(\mu_1,\sigma_1)$

Figure 14.33. (a) An asymmetrical zero-crossing distributions around two consecutive bit transitions; shaded area indicate bit error probability. (b) Individual Gaussian distribution around each bit transition. (c) BER as a function of sampling instant ($t = t_{TH}$).

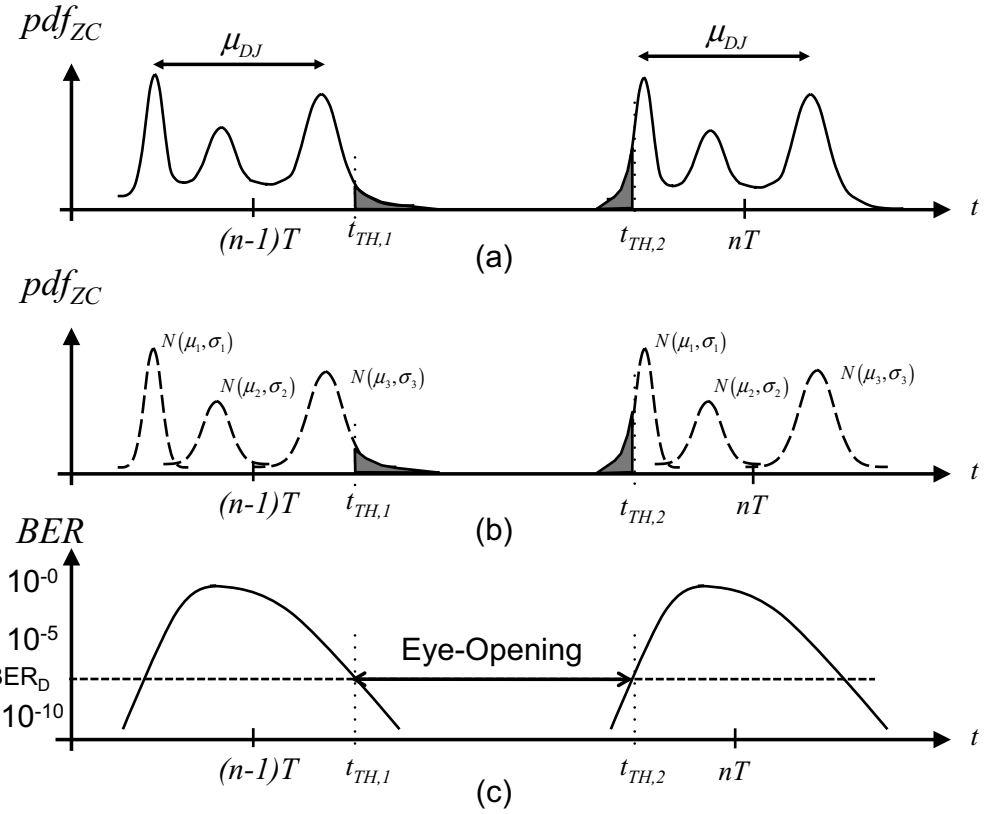

Another approach,[10] and one that tackles the general Gaussian mixture model, is the expectation maximum (EM) algorithm introduced back in Section 4.4.1. This algorithm assumes that G Gaussians are present and solves for the entire set of model parameters: $\mu_1, \mu_2, \ldots, \mu_G, \sigma_1, \sigma_2, \ldots, \sigma_G, \alpha_1, \alpha_2, \ldots, \alpha_G$ using an iteration approach.[11,12] The next two examples will help to illustrate the application of the EM algorithm to the general jitter decomposition problem.

EXAMPLE 14.17

The jitter distribution at the receiver end of a communication channel is to be collected and analyzed for its DJ, RJ, and TJ corresponding to a BER level of 10^{-12}. In order to extract the model parameters, use the EM algorithm and fit three Gaussian functions to the jitter data set. In order to generate the data set, create a routine that synthesizes a Gaussian mixture consisting of three Gaussians with means –0.02 UI, 0 UI, and 0.04 UI and standard deviations of 0.022 UI, 0.005 UI, and 0.018 UI and weighting factors 0.4, 0.2, and 0.4, respectively. Provide a plot of the jitter histogram. Also, how does the extracted model parameters compare with the synthesized sample set model parameters?

Solution:
A short routine was written in MATLAB that synthesizes a Gaussian mixture with the above mentioned model parameters. The routine was run and 1000 samples were collected and organized into a histogram as shown below:

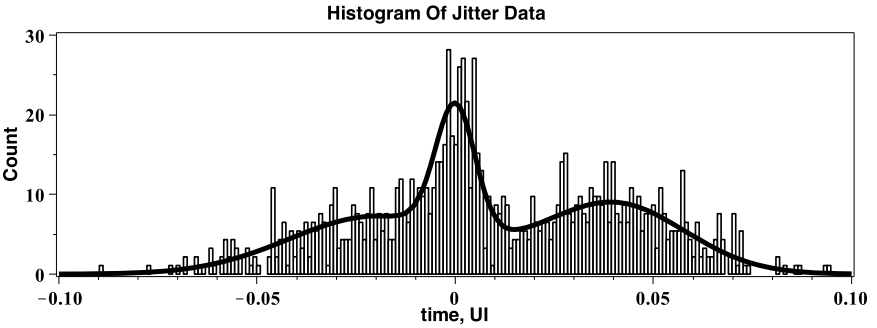

The PDF from which the samples were taken from is also superimposed on the above plot. We note that the general shape of this histogram reveals one Gaussian with a peak at about 0.04 UI, another with a peak at about 0, and the third may have a peak at about -0.03 UI. We estimate the standard deviation of the rightmost Gaussian at about 0.05 UI, the center one with about 0.01 UI, and the leftmost Gaussian with 0.05 UI. We will use these parameters as estimates for the Gaussian mixture curve fit algorithm. We will also assume that each Guassian component is equally important, and hence we assign a weight of 1/3 each. The better our estimate, the faster the algorithm will converge. A second MATLAB routinewas created based on the EM algorithm of Section 4.4.1. Using the above synthesized data, the Gaussian mixture curve-fitting algorithm was run. After 1000 iterations aiming for a root-mean-square error of less than 10^{-10}, the following model parameters were found:

$$\mu_1 = -0.018 \text{ UI}, \quad \sigma_1 = 0.0224 \text{ UI}, \quad \alpha_1 = 0.39$$
$$\mu_2 = 0.0007 \text{ UI}, \quad \sigma_2 = 0.0048 \text{ UI}, \quad \alpha_2 = 0.19$$
$$\mu_3 = 0.0398 \text{ UI}, \quad \sigma_3 = 0.0185 \text{ UI}, \quad \alpha_3 = 0.41$$

Substituting these parameters back into Eq. (14.101) and computing the value of this PDF over a range of –0.1 UI to 0.1 UI, we obtain the dashed line shown in the plot below. Also shown in the plot is a solid line that corresponds to the PDF from which the data set was derived. This is

the same line as in the figure above superimposed over the histogram of the data set. It is quite evident from this plot that the estimated PDF corresponds quite closely to the orginal one. We also include in the plot below a dot-dashed line corresponding to the PDF of our initial guess. In this case, the initial and final PDFs are clearly quite different from one another; this highlights the effectiveness of the EM algorithm.

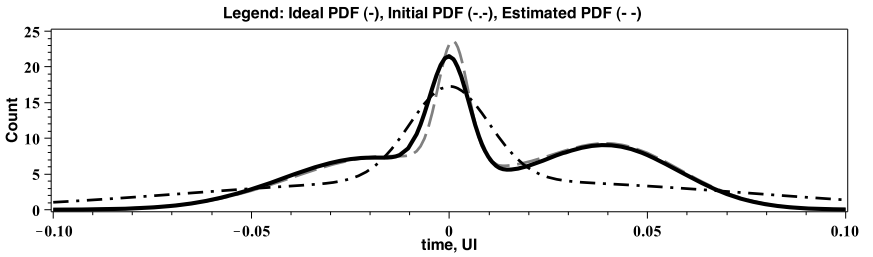

We can write an expression for the BER as a function of the normalized sampling instant, UI_{TH} as follows

$$\begin{aligned}\mathrm{BER}\left(\bar{t}_{TH}\right) = \frac{0.39}{2}\times\left[1-\Phi\left(\frac{UI_{TH}+0.018}{0.0224}\right)\right]+\frac{0.19}{2}\times\left[1-\Phi\left(\frac{UI_{TH}-0.0007}{0.0048}\right)\right]+\frac{0.41}{2}\\ \times\left[1-\Phi\left(\frac{UI_{TH}-0.0398}{0.0185}\right)\right]+\frac{0.39}{2}\times\Phi\left(\frac{UI_{TH}-1+0.018}{0.0224}\right)+\frac{0.19}{2}\\ \times\Phi\left(\frac{UI_{TH}-1-0.0007}{0.0048}\right)+\frac{0.41}{2}\times\Phi\left(\frac{UI_{TH}-1-0.0398}{0.0185}\right)\end{aligned}$$

After some further investigation we recongize that the negative tail of the jitter distrubution is dominated by $N(\mu_1, \sigma_1)$ and the postive tail region is dominated by $N(\mu_3, \sigma_3)$. We can therefore write the BER in the tail regions as

$$BER\left(\bar{t}_{TH}\right)\approx\begin{cases}\dfrac{0.41}{2}\times\left[1-\Phi\left(\dfrac{UI_{TH}-0.0398}{0.0185}\right)\right], & 0\ll UI_{TH}<\dfrac{1}{2}\\ \dfrac{0.39}{2}\times\Phi\left(\dfrac{UI_{TH}-1+0.018}{0.0224}\right), & \dfrac{1}{2}<UI_{TH}\ll 1\end{cases}$$

Finally, we compute the test metrics DJ and RJ and TJ(10^{-12}) from Eqs. (14.104) and (14.105) as follows:

$$\mathrm{DJ}=\mu_3-\mu_1=0.0398-(-0.018)=0.058\ \mathrm{UI}$$
$$\mathrm{RJ}=\frac{\sigma_1+\sigma_3}{2}=\frac{0.0224+0.0185}{2}=0.020\ \mathrm{UI}$$

and from Eq. (14.104), TJ at a desired BER of 10^{-12} can be written as

$$\mathrm{TJ}=0.0185\times\Phi^{-1}\left[1-\frac{2\times10^{-12}}{0.41}\right]+0.0224\times\Phi^{-1}\left[1-\frac{2\times10^{-12}}{0.39}\right]+0.0398-(-0.018)$$

which is further reduced to

$$TJ = 0.0185 \times \Phi^{-1}\left[1 - 4.89 \times 10^{-12}\right] + 0.0224 \times \Phi^{-1}\left[1 - 5.05 \times 10^{-12}\right] + 0.0398 - (-0.018)$$

Substituting $\Phi^{-1}[1 - 4.89 \times 10^{-12}] = 6.8096$ and $\Phi^{-1}[1 - 5.05 \times 10^{-12}] = 6.8051$ as found by a built-in routine in MATLAB, we write TJ = 0.337 UI.

EXAMPLE 14.18

The jitter distribution at the receiver end of a communication channel consisting of 10,000 samples was modeled by a four-term Gaussian mixture using the EM algorithm, and the following model parameters were found:

$$\begin{aligned} \mu_1 &= -0.03 \text{ UI}, & \sigma_1 &= 0.02 \text{ UI}, & \alpha_1 &= 0.4 \\ \mu_2 &= -0.02 \text{ UI}, & \sigma_2 &= 0.05 \text{ UI}, & \alpha_2 &= 0.2 \\ \mu_3 &= 0.03 \text{ UI}, & \sigma_3 &= 0.01 \text{ UI}, & \alpha_3 &= 0.1 \\ \mu_4 &= 0.04 \text{ UI}, & \sigma_4 &= 0.04 \text{ UI}, & \alpha_4 &= 0.3 \end{aligned}$$

Assuming that the unit interval is 1 ns and that the data eye sampling instant is half a UI, what is the BER associated with this system? Does the system behave with a BER less than 10^{-12}?

Solution:

Evaluating Eq. (14.102) a $UI_{TH} = 0.5$ UI and $T = 1$ UI, we write

$$\begin{aligned} \text{BER}(0.5\text{UI}) = {} & \frac{0.04}{2} \times \left[1 - \Phi\left(\frac{0.5 - \mu_1}{\sigma_1}\right)\right] + \frac{0.2}{2} \times \left[1 - \Phi\left(\frac{0.5 - \mu_2}{\sigma_2}\right)\right] + \frac{0.1}{2} \times \left[1 - \Phi\left(\frac{0.5 - \mu_3}{\sigma_3}\right)\right] + \frac{0.3}{2} \times \left[1 - \Phi\left(\frac{0.5 - \mu_4}{\sigma_4}\right)\right] \\ & + \frac{0.04}{2} \times \Phi\left(\frac{0.5 - 1 - \mu_1}{\sigma_1}\right) + \frac{0.2}{2} \times \Phi\left(\frac{0.5 - 1 - \mu_2}{\sigma_2}\right) + \frac{0.1}{2} \times \Phi\left(\frac{0.5 - 1 - \mu_3}{\sigma_3}\right) + \frac{0.3}{2} \times \Phi\left(\frac{0.5 - 1 - \mu_4}{\sigma_4}\right) \end{aligned}$$

Substituting the above Gaussian mixture parameters in normalized form, we find BER (0.5 UI) × 10^{-10}. Therefore, we can expect that the system theoretically will not operate with a BER less than 10^{-12}.

Exercise

14.24. The jitter distribution at the receiver end of a communication channel consisting of 10,000 samples was modeled by a four-term Gaussian mixture using the EM algorithm and the following model parameters were found:

$$0.25 \times N(-10 \text{ ps}, 10 \text{ ps}) + 0.25 \times N(-7 \text{ ps}, 7 \text{ ps}) + 0.25 \times N(4 \text{ ps}, 4 \text{ ps}) + 0.25 \times N(11 \text{ ps}, 11 \text{ ps})$$

Assuming the unit interval is 0.2 ns and that the data eye sampling instant is half a UI, what is the BER associated with this system? Does the system behave with a BER less than 10^{-12}?

ANS. $\text{BER}(UI/2) = 3.7 \times 10^{-17}$.

14.7 DETERMINISTIC JITTER DECOMPOSITION

Using either the dual-Dirac or Gaussian mixture jitter decomposition method, we can determine the random and deterministic components of the jittery signal. In order to further decompose the deterministic jitter component into its constitutive parts, such as periodic or sinusoidal, data-dependent, and bounded uncorrelated jitter, additional data capturing and signal processing is required. More specifically, we analyze the jitter samples as a time series, attempting to find underlying structure in the data. As we have done throughout this text, we shall rely heavily on an FFT analysis to help us identify this structure. Once the DJ components are identified, the goal is to construct their corresponding PDF and use these PDFs for diagnostic purposes.

14.7.1 Period and Sinusoidal Jitter (PJ/SJ)

Period jitter (PJ) of a serial communication link is defined as the deviation in the period time of a clock-like output signal. Usually, a PJ test is conducted when the input to the channel is driven with a small-amplitude sinusoidal phase-modulated signal, but PJ also arises from internal sources unrelated to the input as well.

Let us assume that a sequence of N time difference values for the signal in question and a reference clock corresponding to the zero crossing times is captured and stored in vector $J[n]$ for $n = 1, \ldots, N$ (see Figure 14.4 for greater clarification). If we assume that the PJ components are dominant (i.e., PJ is greater than RJ), then the standard deviation σ_J of this data set represents the RMS value of the PJ components and can be computed as follows:

$$\sigma_J = \sqrt{\frac{1}{N}\sum_{n=1}^{N}\left(J[n] - \frac{1}{N}\sum_{n=1}^{N}J[n]\right)^2} \tag{14.110}$$

Because DJ is expressed as a peak-to-peak quantity, PJ is described in the same peak-to-peak way by exploiting the relationship between the peak-to-peak value of a sine wave to its RMS value as follows

$$PJ \triangleq 2\sqrt{2} \times \sigma_J \tag{14.111}$$

The user of Eq. (14.111) should be aware that this formula is only approximate, because it has no information about the underlying nature of the periodic jitter and how separate sinusoidal signals combine.

There is another definition of period jitter that one finds in the literature. Digital system designers often use this definition when describing jitter. We briefly spoke about it in Section 14.2. Specifically, period jitter is defined as the first-order time difference between adjacent bit transitions given by the equation

$$J_{PER}[n] = J[n] - J[n-1] \tag{14.112}$$

The RMS value of this sequence (denoted by σ_{JPER}) would have a similar form to Eq. (14.110) above, except σ_{JPER} would replace σ_J. In the frequency domain, the period jitter sequence is related to the time jitter sequence by taking the z-transform of Eq. (14.112) and substituting for physical frequencies, that is, $z = e^{j2\pi fT}$, leading us to write

$$J_{PER}\left(e^{j2\pi fT}\right) = \left(1 - z^{-1}\right)J(z)\Big|_{z=e^{j2\pi fT}} = \left(1 - e^{-j2\pi fT}\right)J\left(e^{j2\pi fT}\right) \tag{14.113}$$

Clearly, the frequency description of the period jitter sequence J_{PER} is proportional to the time jitter sequence J in the frequency domain. However, we note that the proportionality constant is also a function of the test frequency. This means that the PJ metric computed from the time jitter sequence will be different from that obtained using the period jitter sequence. This can be source of confusion for many. To avoid this conflict, for the remainder of this text, we shall rely exclusively on the time jitter sequence to establish the PJ quantity. Example 14.9 will help to demonstrate this effect.

A more refined approach for identifying the PJ component that makes no assumption of the relative strength of the PJ component relative to the RJ component is to perform an FFT analysis of the jitter time series J. If coherency is difficult to achieve, a Hann or Blackman window may be necessary to reduce frequency leakage effects. If we denote the period jitter frequency transform with vector X_J (using our usual notation) and identify the FFT bin containing the fundamental of the periodic jitter as bin M_{PJ} and the corresponding number of harmonics H_{PJ}, then we can determine the RMS value of the PJ component from the following expression

$$\sigma_{PJ} = \sqrt{\sum_{p=1}^{H_{PJ}} c^2_{p\times M_{PJ},RMS}} \tag{14.114}$$

where

$$c_{k,RMS} = \begin{cases} \left|X_J[k]\right|, & k = 0 \\ \sqrt{2}\left|X_J[k]\right|, & k = 1,\ldots,N/2-1 \\ \dfrac{\left|X_J[k]\right|}{\sqrt{2}}, & k = N/2 \end{cases}$$

If PJ consists of a single tone, then using Eq. (14.111) with σ_{PJ} replacing $\sigma_{J_{PER}}$, we can estimate the peak-to-peak value of the PJ component. If PJ consists of more than one tone, then we must account for the phase relationship of each tone in the calculation of its peak-to-peak value. One approach is to perform an inverse-FFT (IFFT) on only the PJ components (remove all others) and extract the peak-to-peak value directly from the time-domain signal. Mathematically, we write

$$PJ \cong \max\{\text{IFFT}(J_{PJ,only})\} - \min\{\text{IFFT}(J_{PJ,only})\} \tag{14.115}$$

Correspondingly, we can also compute the samples of the time sequence $\text{IFFT}(J_{PJ,\text{only}})$ to construct a histogram of the PJ component. A mathematical formula can then be used to model the PDF for PJ. Because PJ is made up of harmonically related sinusoidal components, the PDF distribution will involve functions that appears in the general form as $1/\pi\sqrt{A^2 - t^2}$, where A is the amplitude of a single sine wave. In general, this is difficult to do and one general defers to thesingle tone case below.

As a special case of period jitter, if H_{PJ} is unity where only one tone is present, then PJ is sometimes referred to as sinusoidal jitter and is denoted with acronym SJ. Mathematically, we define SJ as

$$\text{SJ} \triangleq 2\sqrt{2} \times \sigma_{PJ} \tag{14.116}$$

where the corresponding period jitter PDF would be written as

$$pdf_{PJ} = \begin{cases} \dfrac{1}{\pi\sqrt{\left(\dfrac{SJ}{2}\right)^2 - t^2}}, & -\dfrac{\text{SJ}}{2} \le t \le \dfrac{\text{SJ}}{2} \\ 0, & \text{otherwise} \end{cases} \tag{14.117}$$

SJ plays an important role in jitter tolerance and transfer function tests of the next section.

EXAMPLE 14.19

A time jitter sequence *J[n]* can be described by the following discrete-time equation:

$$J[n] = 0.001\sin\left(2\pi\frac{11}{1024}n\right)$$

Here A_J is the amplitide of the phase modulated sequence and M_J is the number of cycles completed in N sample points. Compute the period jitter sequence and compare its amplitude to the time jitter sequence amplitude.

Solution:
The period jitter sequence is computed from time jitter sequence according to

$$J_{PER}[n] = J[n] - J[n-1] = 0.001\sin\left[2\pi\frac{11}{1024}n\right] - 0.001\sin\left[2\pi\frac{11}{1024}(n-1)\right]$$

Running through a short for loop, we obtain a plot of the period jitter together with the time jitter sequence below:

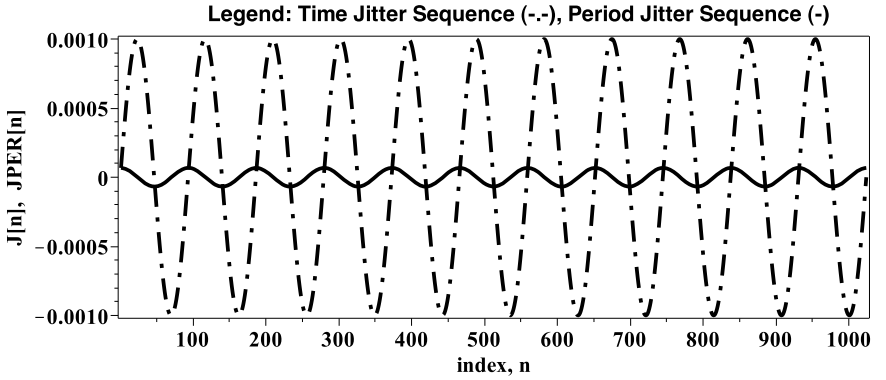

The plot clearly reveals that the amplitudes of the two sequences are quite different. In fact, the analysis shows that the amplitude of the time jitter sequence is 10^{-3} and the amplitude of the period jitter sequence is 6.7×10^{-5}. In fact, the ratio of these two amplitudes is equal to

$$\frac{\hat{J}_{PER}}{\hat{J}_P} = \left|1 - e^{-j2\pi M_J/N}\right| = 0.0067 \text{ with } M_J = 11 \text{ and } N = 1024.$$

EXAMPLE 14.20

The SJ component of a jitter distribution was found to be 0.1 UI for a receiver operating at a bit rate of 1 GHz. Estimate the shape of the histogram that one would expect from this jitter component alone.

Solution:
Denormalizing the SJ component, we write its peak-to-peak value as $0.1/10^9$ or 10^{-10} s. Substituting this result back into Eq. (14.117), we write the PDF for this jitter component between -0.1 UI $< t < 0.1$ UI as

$$pdf_{SJ} = \frac{1}{\pi\sqrt{\left(\frac{10^{-10}}{2}\right)^2 - t^2}}$$

and everywhere else as 0. The following plot of this distrubtion would resemble the general shape of any particular histogram captured from this random distribution.

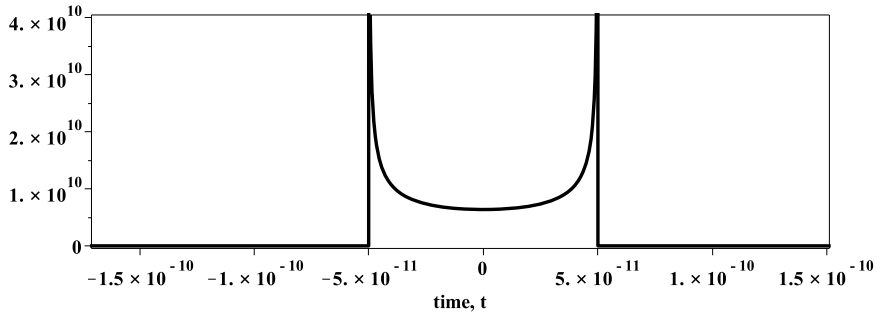

As is evident from the plot above, adual-Dirac like behavior results.

Exercises

14.25. A time jitter sequence can be described by the following discrete-time equation: J[n] = 10 sin (2π 13/1024 n). What is the probability density function for this sequence?

ANS. $f_j = \{1/\pi\sqrt{(10)^2 - J^2}$, $-10 \le J \le 10$ otherwise

14.7.2 Data-Dependent Jitter (DDJ)

When a serial communication link is driven by random data pattern, channel dispersion causes inter-symbol interference (ISI) to occur (see Figure 14.17). In addition, a transmitter may transmit a logic high value with different bit duration than a logic low value. Collectively, these two effects limitations give rise to data-dependent jitter (DDJ). Typically, a *P*-bit PRBS data pattern is used to

excite a system by repeating this pattern throughout the duration of the test. Due to the repetition of this pattern, additional periodic jitter is produced that is harmonically related to this repletion frequency. For a *P*-bit PRBS pattern with bit duration *T*, the pattern repetition rate is *P* x *T* so that the fundamental frequency of the DDJ component will appear at 1/(*P* x *T*) Hz. Assuming the harmonics of PJ and DDJ are different, then we can compute the RMS of the DDJ components using the exact same spectrum approach for PJ, except we drive the channel with a P-bit PRBS pattern. Assuming an *N*-point period jitter vector J, the fundamental component of DDJ will appear in bin M_{DDJ}= *N/P*, whence we write the RMS value of the DDJ component as

$$\sigma_{DDJ} = \sqrt{\sum_{p=1}^{H_{DDJ}} c_{p\times M_{DDJ}}^2} \tag{14.118}$$

where we assume that H_{DDJ} represent the number of harmonics associated with the DDJ jitter component. Once again, it is best to isolate the DDJ components so that an inverse FFT can be run and the peak-to-peak values extracted using the following expression:

$$\text{DDJ} \cong \max\{\text{IFFT}(J_{DDJ,only})\} - \min\{\text{IFFT}(J_{DDJ,only})\} \tag{14.119}$$

Correspondingly, we can also the samples of the time sequence IFFT($J_{DDJ,\text{only}}$) to construct the histogram of the DDJ component. In order to determine the mathematical form of this jitter distribution, we need to further decompose DDJ into ISI and DCD components.

In the case of DCD, the input is driven by a clock-like data pattern so that the effects of ISI are eliminated. The time difference between the zero crossings for a 0-to-1 bit transition and a reference clock are collected from which the average time offset value $t_{DCD,01,av}$ is found. Likewise, this procedure is repeated for the 1–0 bit transitions and the $t_{\text{DCD},10,av}$ value is found. These two results are then combined to form the PDF for the DCD using the dual-Dirac function, accounting for the asymmetry about the ideal zero crossing point as illustrated in Figure 14.19a, as follows

$$pdf_{DCD} = \frac{1}{2}\delta\left(t + \frac{t_{DCD,10,av}}{2}\right) + \frac{1}{2}\delta\left(t - \frac{t_{DCD,01,av}}{2}\right) \tag{14.120}$$

The DCD test metric expressed as a peak-to-peak quantity is defined as follows

$$\text{DCD} = t_{DCD,01,av} - t_{DCD,10,av} \tag{14.121}$$

When only the DCD metric is provided, we can approximate the PDF of the DCD as a dual-Dirac function as follows:

$$pdf_{DCD} \approx \frac{1}{2}\delta\left(t + \frac{\text{DCD}}{2}\right) + \frac{1}{2}\delta\left(t - \frac{\text{DCD}}{2}\right) \tag{14.122}$$

To identify the ISI distribution, a test very similar to DCD is performed but the input is driven with a specific data pattern other than a clock-like pattern. The zero crossings for the 0–1 bit transitions are collected and the extremes are identified, say $t_{ISI,01,\min}$ and $t_{ISI,01,\max}$. The process is repeated for the 1–0 zero crossings and, again, the extremes are identified as $t_{ISI,10,\min}$ and $t_{ISI,10,\max}$. The ISI test metric is then defined as the average of these two peak-to-peak values as follows

$$\text{ISI} \cong \frac{\left(t_{ISI,01,\max} - t_{ISI,01,\min}\right) + \left(t_{ISI,10,\max} - t_{ISI,10,\min}\right)}{2} \tag{14.123}$$

A first-order estimate of the PDF of the ISI can be written as another dual-Dirac function as follows:

$$pdf_{ISI} \approx \frac{1}{2}\delta\left(t+\frac{\text{ISI}}{2}\right)+\frac{1}{2}\delta\left(t-\frac{\text{ISI}}{2}\right) \tag{14.124}$$

As ISI and DCD convolve together to form the DDJ distribution, that is,

$$pdf_{DDJ} = pdf_{ISI} \otimes pdf_{DCD} \tag{14.125}$$

Substituting Eqs. (14.122) and (14.124) into Eq. (14.125), we write

$$pdf_{DDJ} = \left[\frac{1}{2}\delta\left(t+\frac{\text{ISI}}{2}\right)+\frac{1}{2}\delta\left(t-\frac{\text{ISI}}{2}\right)\right]\otimes\left[\frac{1}{2}\delta\left(t+\frac{\text{DCD}}{2}\right)+\frac{1}{2}\delta\left(t-\frac{\text{DCD}}{2}\right)\right] \tag{14.126}$$

Further expansion leads to the general form of the DDJ distribution as

$$\begin{aligned} pdf_{DDJ} = {} & \frac{1}{4}\delta\left(t+\frac{\text{DCD}}{2}+\frac{\text{ISI}}{2}\right)+\frac{1}{4}\delta\left(t-\frac{\text{DCD}}{2}+\frac{\text{ISI}}{2}\right) \\ & +\frac{1}{4}\delta\left(t+\frac{\text{DCD}}{2}-\frac{\text{ISI}}{2}\right)+\frac{1}{4}\delta\left(t-\frac{\text{DCD}}{2}-\frac{\text{ISI}}{2}\right) \end{aligned} \tag{14.127}$$

14.7.3 Bounded and Uncorrelated Jitter (BUJ)

During a data pattern test, additional tones unrelated to the test pattern can appear in the PSD of the jitter sequence; also the noise floor may rise. Firstly, for an alternating sequence of 1's and 0's, the PSD would contain the only the PJ and RJ components, as shown in Figure 14.34a. Here we illustrate the PJ component with a sine tone in bin M_{PJ}. When a PRBS pattern is applied to the channel input, theoretically, one would expect to continue to see the PJ component, as well as harmonics that are related to the repetition period of the PRBS pattern. In Figure 14.34b we depict this situation with three tones harmonically related to one another beginning with the fundamental in bin M_{DDJ}. In some situations, when testing with a PRBS sequence, additional tones may appear; also, the noise floor may increase. Because these signals have no theoretical relationship to the PRBS data pattern, these jitter components are classified as bounded and uncorrelated jitter (BUJ). It is essentially a catchall term that accounts for jitter that does not fit into PJ, DDJ, or RJ categories. DUJ generally arises from crosstalk and electromagnetic interference sources. It is important to note that BUJ jitter is bounded and its peak-to-peak value does not increase with more measurement samples.

Given measurements of the RMS value of PJ, DDJ, and RJ, together with the RMS value of the jitter sequence, denoted as σ_J, we can estimate the RMS value of the total BUJ component as

$$\sigma_{BUJ} = \sqrt{\sigma_J^2 - \sigma_{PJ}^2 - \sigma_{DDJ}^2 - \sigma_{RJ}^2} \tag{14.128}$$

where we assume that the powers of the individual components of BUJ add, that is, $(\sigma_{BUJ} = \sqrt{\sigma_{BUJ}^2 + \sigma_{BUJ,2}^2})$. We do not attempt to list the PDF for BUJ, because we need more information about the source of this jitter.

Figure 14.34. Power spectral density plot of a period jitter sequence with input: (a) alternating 1's and 0's pattern, (a) PRBS data sequence and (b) PRBS data sequence, but an additional tone and noise level is unaccounted for.

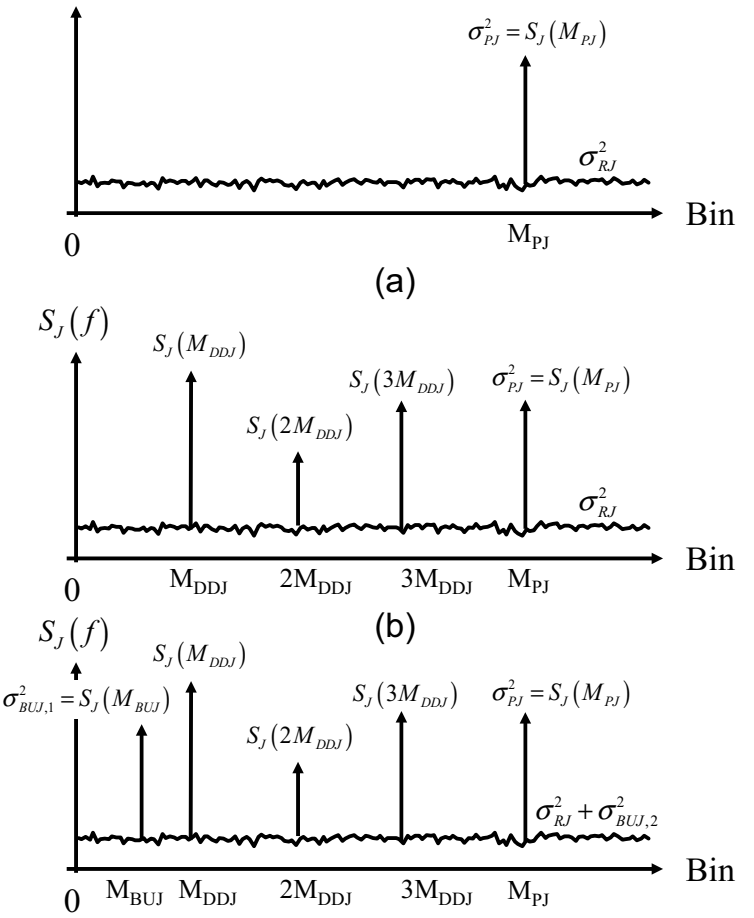

The following example will help to illustrate the deterministic jitter decomposition method described above.

EXAMPLE 14.21

A jitter sequence consisting of 1024 samples was captured from a serial I/O channel driven by two separate data patterns. In one case, an alternating sequence of 1's and 0's was used, in the other, a PRBS pattern was used. An FFT analysis performed on the two separate sets of jitter data, as well as with the PRBS sequence,resulted in the information below. Determine the test metrics: PJ, DDJ, BUJ.

Spectral Bin In Nyquist Interval	|XJ| Complex Spectral Coefficients (UI)		
	1010 clock-like Input	PRBS Input	
		Theory	Actual
0	0.001	0	6×10^{-4}
1, ..., 512 except	~1×10^{-4}	0	~2×10^{-4}
55	0	0.021 – *j* 0.028	0.02 – *j* 0.03
110	0	0.002 + *j* 0.003	0.001 + *j* 0.002
165	0	0.006 – *j* 0.007	0.005 – *j* 0.006
193	0	0	0.01 – *j* 0.02
201	0.02 + j 0.05	0	0.018 + *j* 0.053

Solution:
Using the spectral data from the alternating 1010 data pattern, we find from the FFT data set above that a tone is present in bin 201 with an RMS value of

$$\sigma_{PJ} = \sqrt{2}\sqrt{0.02^2 + 0.05^2} = 0.076 \text{ UI}$$

For a single tone, the peak-to-peak value denoted by PJ or SJ is simply

$$\text{PJ} = \text{SJ} = 0.215 \text{ UI}$$

We also notice that from the spectral data for the clock-like input, the RJ noise component can be estimated to be

$$\sigma_{RJ} = \sqrt{\sum_{k=0}^{512} c_{k,RMS}^2 - c_{0,RMS}^2 - c_{201,RMS}^2} \approx \sqrt{512 \times \left(\sqrt{2} \times 10^{-4}\right)^2 - \sqrt{2}\left(0.02^2 + 0.05^2\right)} = 3.18 \times 10^{-3} \text{UI}$$

Next, as is evident from the middle column of data, through ideal simulation we expect to see harmonics related to the PRBS data pattern in bins 55, 110, and 165. Tones falling in any other bin is deemed unrelated to DDJ. Tonal components, other than those related to PJ, would be considered as being part of BUJ. Using the data from the rightmost column, we find that the RMS value of DDJ is

$$\sigma_{DDJ} = \sqrt{c_{55,RMS}^2 + c_{110,RMS}^2 + c_{165,RMS}^2} = \sqrt{2}\sqrt{\left(0.21^2 + 0.13^2\right) + \left(0.02^2 + 0.03^2\right) + \left(0.06^2 + 0.07^2\right)} = 50.6 \times 10^{-3}$$

To obtain the peak-to-peak value of DDJ, we notch out all bins other than those related to DDJ and perform an inverse FFT. This is achieved by setting bins 0–512 to zero except bins 55, 110, and 165 (as well as its first image). Next we scale these three bins by the factor *N* (=1024) and perform an inverse FFT, according to

$$d_{DDJ} = 1024 \times \text{IFFT}\left\{ \begin{bmatrix} 0,\ldots,0,\left(0.02 - j0.03\right),0,\ldots,0,\left(0.001 + j0.002\right),0,\ldots,0,0,\left(0.005 - j0.006\right),0,\ldots,0,0 \\ 0,\ldots,0,\left(0.005 + j0.006\right),0,\ldots,0,\left(0.001 - j0.002\right),0,\ldots,0,0,\left(0.02 + j0.03\right),0,\ldots,0 \end{bmatrix} \right\}$$

On doing this, the following DDJ jitter sequence results:

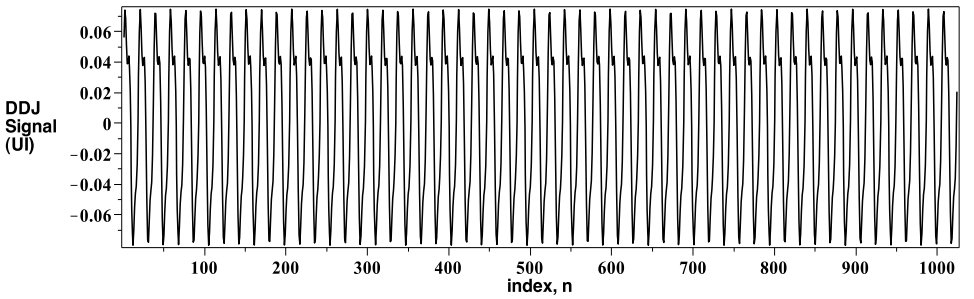

As is evident, the peak-to-peak value of DDJ is about

$$\text{DDJ} = 0.154 \text{ UI}$$

What remains now is the identification of the BUJ components. From the right-most column we recognize that a tone is present in bin 193 having an RMS value of

$$\sigma_{BUJ,1} = \sqrt{2}\sqrt{0.01^2 + 0.02^2} = 31.6 \times 10^{-3} \text{ UI}$$

We also recognize that the noise floor has increased when the data pattern changed. We attribute this increase to some bounded but uncorrelated jitter source. We quantify its value by taking the power difference between the two noise floors associated with the two different data patterns, that is,

$$\sigma_{BUJ} = \sqrt{\sigma_{BUJ,1}^2 + \sigma_{BUJ,2}^2} = \sqrt{\left(31.6 \times 10^{-3}\right)^2 + \left(5.4 \times 10^{-3}\right)^2} = 5.4 \times 10^{-3} \text{ UI}$$

To estimate the peak-to-peak value of the BUJ component, we note that the sinusoidal component is about four times larger in amplitude, so as a first estimate we obtain

$$\text{BUJ} \approx 2\sqrt{2\sigma}_{BUJ,1} = 2\sqrt{2} \times 31.6 \times 10^{-3} = 89.4 \times 10^{-3} \text{ UI}$$

Because this term does not include the correlated and bounded noise components evident in the noise floor, it underestimates the level of BUJ. A better estimate would be to repeat the test several times and average out the random noise leaving only the correlated signals.

EXAMPLE 14.22

A serial I/O channel was characterized for its RJ and DJ components resulting in the following table of measurements. Estimate the shape of the histogram of the total jitter distribution that would result? From this distribution, relate the peak-to-peak levels to the underlying test

metrics found below. Also, plot the corresponding PDF of the zero-crossing distribution across two consectutive bit transitions assuming a bit duration of 100 ps.

Jitter Metrics			
RJ (rms ps)	DJ		
	SJ (pp ps)	ISI (pp ps)	DCD (pp ps)
2	25	14	2

Solution:

Given the above metrics, we can represent each jitter distribution mathematically and pictorially as follows:

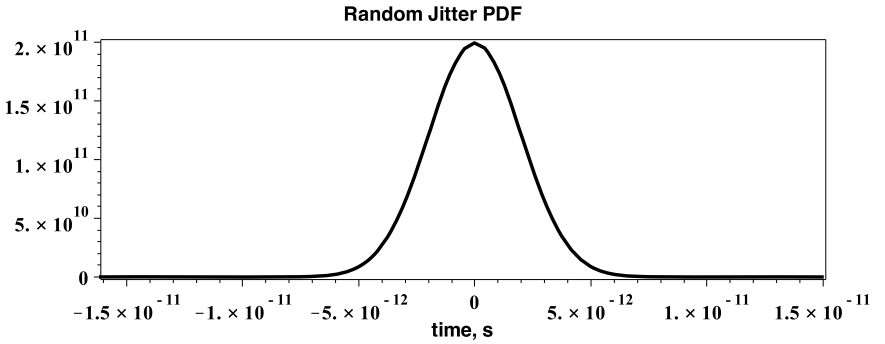

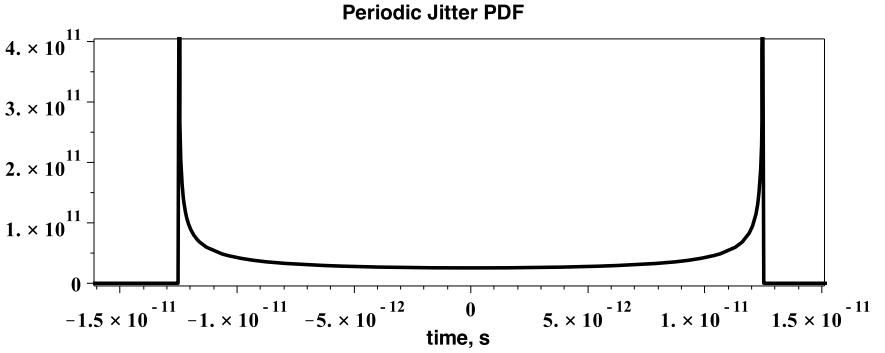

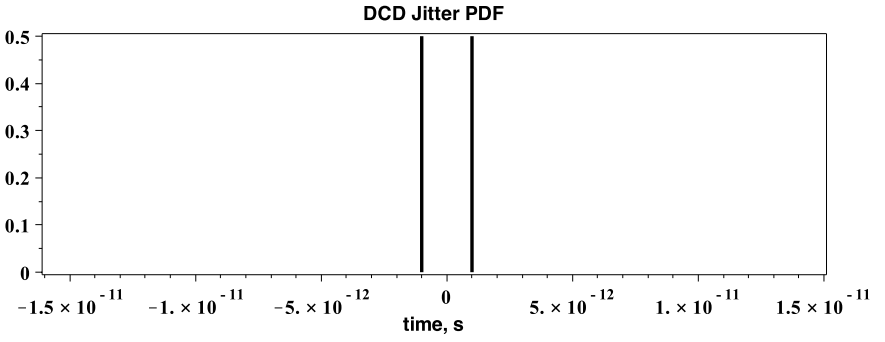

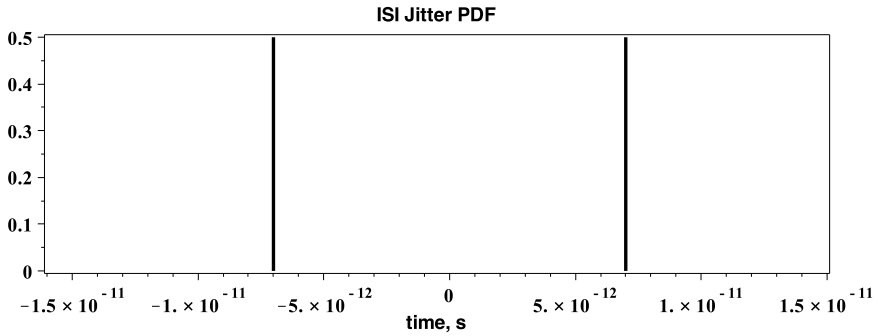

The total jitter distribution is a convolution of individual PDFs as follows:

$$pdf_{TJ} = pdf_{RJ} \otimes pdf_{PJ} \otimes pdf_{ISI} \otimes pdf_{DCD}$$

Using a computer program, we solved the above multiple kernel convolution for the total jitter distribution using a numerical integration routine. The numerical solution is found below:

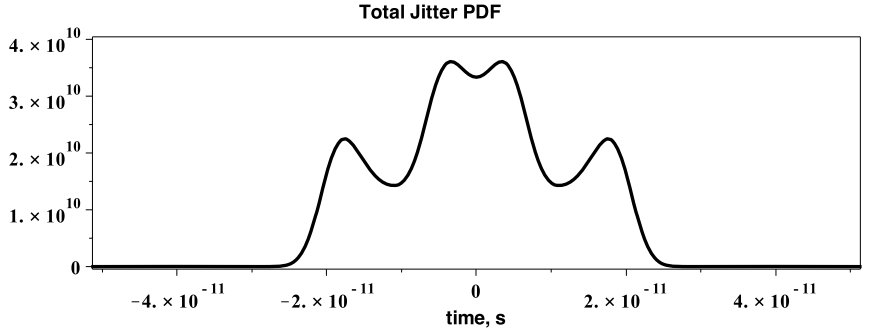

Here we see a multimodal distribution with four peaks, located at approximately -18 ps, -4 ps, 4 ps, and 18 ps. If we treat the sinusoidal distribution as a dual-Dirac density, then together with the other two Dirac distributions for ISI and DCD, we will end up with eight impulses located at ±12.5 ±7 ±1 ps or ±4.5, ±6.5, ±18.5 and ±20.5 ps. While these numbers are close to the peak locations, they do not coincide exactly, owing to the many interactions with the Gaussian distribution. Care must be exercised carefully when attempting to de-correlate jitter behavior from the total jitter distribution.

Finally, the PDF of the jitter distribution across two consectutive bit transitions separated by 100 ps is found by convolving the PDF of the total jitter with a dual-Dirac distribution with centers located at 0 and 100 ps, that is,

$$pdf_{ZC} = pdf_{TJ} \otimes \left[\frac{1}{2}\delta(t) + \frac{1}{2}\delta\left(t - 1\times 10^{-10}\right)\right]$$

The resulting zero-crossing PDF is shown plotted below:

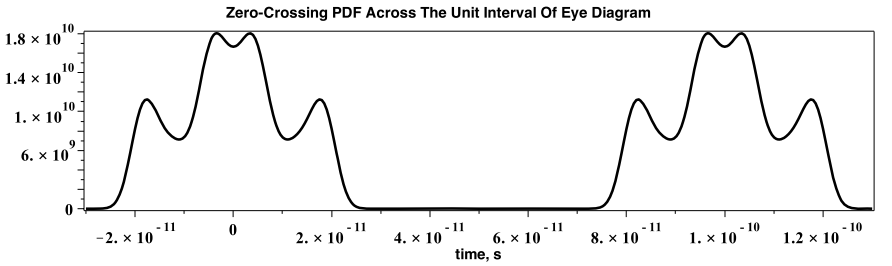

14.8 JITTER TRANSMISSION TESTS

Up to this point in this chapter we have been discussing the properties of jitter present at the transmitter or received output. In this section we shall address the sensitivity of a system to jitter imposed at its input and the effect that it has on its output. Two measures of jitter transmission are used: (1) jitter transfer and (2) jitter tolerance. We shall define these two terms and how to make their measurement below.

14.8.1 Jitter Transfer Test

Jitter transfer is a measurement of the amount of jitter present at the output of the digital channel relative to a particular amount of jitter applied to its input. The ratio is usually specified as a function of frequency, as the channel is generally frequency sensitive. Generally, a jitter transfer test uses a clock-like input data pattern to avoid ISI issues. In much the same way as we did for measuring the gain of an analog or sampled data channel, a sinusoidal phase modulated signal having specific amplitude and frequency is applied to the input of a device or system and the corresponding output sinusoidal phase modulated response is measured. Assuming the peak-to-peak value of the input phase modulated signal is SJ_{IN} and the peak-to-peak value of the output is SJ_{OUT} then we define the jitter transfer at frequency ω as

$$G_J(\omega) \triangleq \frac{SJ_{OUT}}{SJ_{IN}} \tag{14.129}$$

or, equivalently, in dB, as

$$G_{J,dB}(\omega) = 20\log_{10} G_J(\omega) \tag{14.130}$$

Repeating this measurement for a range of input frequencies and comparing the jitter gain to a jitter transfer compliance mask, such as that shown in Figure 14.35, we would have a complete jitter transfer test. Any data point that falls inside of the hashed region would result in a failed test.

Figure 14.35. An example jitter transfer compliance mask with measured data superimposed. This particular data set passes the test as all the data points fall inside the acceptable region (as shown).

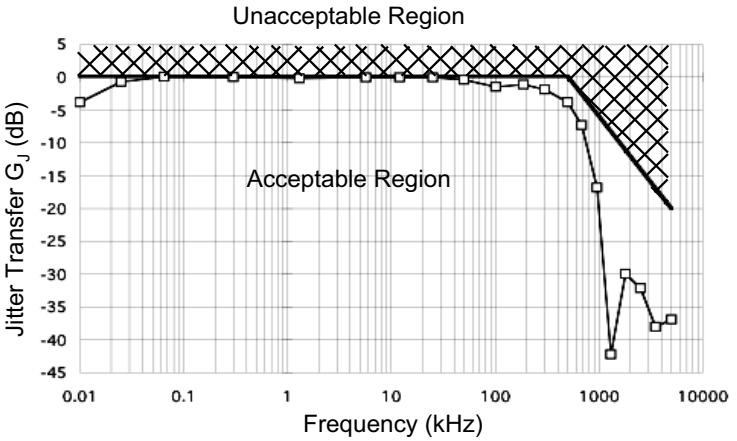

While we could measure both the input and output jitter level using the power spectral method described above for computing PJ, a more efficient method is to use coherent signal generation and sampling, in much the same way we did for the analog and sampled data channel measurements using the AWG and digitizer. Let us explain this more fully below.

Coherent Jitter Generation

As jitter transfer is based on injecting a known sinusoidal jitter signal at a particular frequency, we can use coherency to set up the test so that the spectrum of the samples of the output signal that is collected and processed with an *N*-point FFT falls in the appropriate bin. This avoids the need for any additional post-processing or windowing.

Mathematically, a clock-like digital signal can be described by a sinusoidal with unity amplitude and frequency f_c, followed by a squaring operation as follows

$$d(t) = \text{sgn}\left\{\sin\left[2\pi f_c t\right]\right\} \tag{14.131}$$

where sgn{.} represents the signum function. Now, if we argument the phase of the sinusoidal function by adding a phase term J(t), to represent the jitter signal as a function of time, we would write the digital signal as follows

$$d(t) = \text{sgn}\left\{\sin\left[2\pi f_c t + J(t)\right]\right\} \tag{14.132}$$

Furthermore, if we assume the phase function is sinusoidal, with amplitude A_J and frequency f_J, that is,

$$J(t) = A_J \sin\left(2\pi f_J t\right) \tag{14.133}$$

then Eq. (14.132) can be written as

$$d(t) = \text{sgn}\left\{\sin\left[2\pi f_c t + A_J \sin\left(2\pi f_J t\right)\right]\right\} \tag{14.134}$$

The units of $J(t)$ are expressed in radians, but one often see this jitter signal expressed in terms of seconds,

$$J(t)\ \left[\text{seconds}\right] = \frac{1}{2\pi f_c} \times J(t)\ \left[\text{radians}\right] \tag{14.135}$$

or in terms of unit intervals (UI) as

$$J(t)\ \left[UI\right] = \frac{1}{2\pi} \times J(t)\ \left[\text{radians}\right] \tag{14.136}$$

If we assume that this signal is sampled at sampling rate F_s, then we can write the sampled form of Eq. (14.134) as

$$d[n] = \text{sgn}\left\{\sin\left[2\pi \frac{f_c}{F_S} n + A_J \sin\left(2\pi \frac{f_J}{F_S} n\right)\right]\right\} \tag{14.137}$$

In order to maintain coherency, we impose the conditions

$$\frac{f_c}{F_S} = \frac{M_c}{N} \text{ and } \qquad \frac{f_J}{F_S} = \frac{M_J}{N} \tag{14.138}$$

where N, M_c, and M_J are integers. In the usually way, N represents the number of samples obtained from $d(t)$, and M_c and M_J represent the number of cycles the clock and jitter signal complete in N points, respectively. This allows us to rewrite Eq. (14.137) as

$$d[n] = \text{sgn}\left\{\sin\left[2\pi\frac{M_c}{N}n + A_J \sin\left(2\pi\frac{M_J}{N}n\right)\right]\right\} \tag{14.139}$$

Deriving N points from Eq. (14.139) and storing them in the source memory of the arbitrary waveform generator (AWG) would provide a means to create a sinusoidal jitter signal with amplitude A_J riding on the clock-like data signal. A simple test setup illustrating this approach is shown in Figure 15.36a. For very-high-frequency data rates, an AWG would not be available to synthesis such waveforms directly. Instead, the digitally synthesized jitter signal would phase modulate a reference clock signal using some phase modulation technique such as the Armstrong phase modulator as shown in Figure 14.36b. A third technique is the method of data edge placement as shown in Figure 14.36c. This technique uses a digital-to-time converter (DTC) to place the data edges at specific points along the UI of the data eye according to an input digital code. The phase-lock loop removes high-frequency images, so it is essentially the reconstruction filter of this digital-to-time conversion process. A variant of this approach is one that makes use of a periodic sequence of bits together with a phase lock loop to synthesize a sinusoidal jitter signal.[14,15] The DTC is essentially realized with a set of digital codes.

Figure 14.36. Generating a phase modulated clock signal: (a) a direct digital synthesis method involving an AWG, (b) an indirect method using the Armstrong phase modulator technique and a low-frequency AWG, (c) edge-placement technique using a digital-to-time converter followed by a PLL.

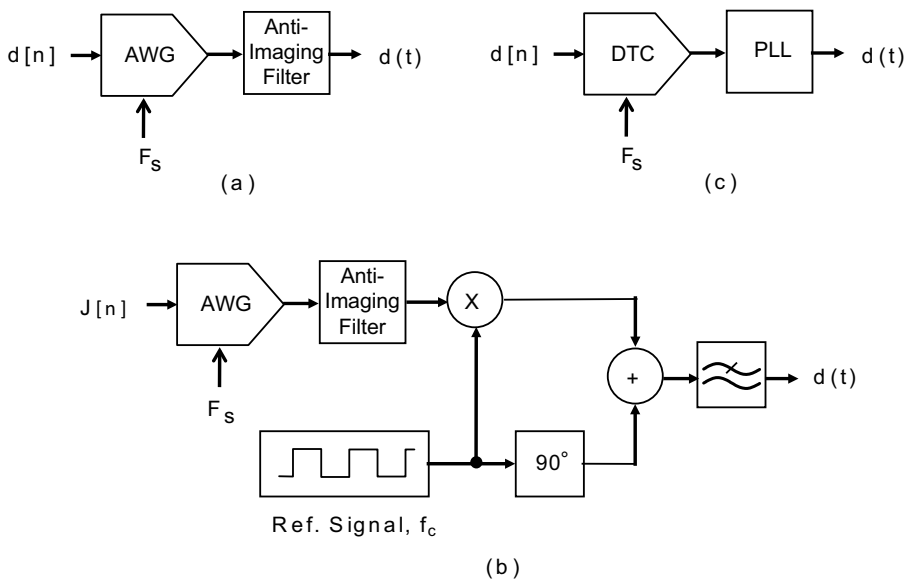

EXAMPLE 14.23

A digital receiver operates at a clock rate of 100 MHz. A jitter transfer test needs to be performed with a 10-kHz phase-modulated sinusoidal signal having an amplitude of 0.5 UI. Using an AWG with a sampling rate of 1 GHz, write a short routine that generates the AWG samples.

Solution:

Our first task is to detemine the number of samples and cycles used in the waveform sythesis. Substituting the given data in the coherency expressions, we write

$$\frac{100\,\text{MHz}}{1\,\text{GHz}} = \frac{M_c}{N} \quad \text{and} \quad \frac{10\,\text{kHz}}{1\,\text{GHz}} = \frac{M_J}{N}$$

Simplifying and isolating the two M terms, we write

$$M_c = \frac{1}{10} \times N \quad \text{and} \quad M_J = \frac{1}{10^5} \times N$$

As M_c, M_J and N are all integers, we immediately recongize that N must contain the factor 10^5. This makes it impossible for N to be expressed solely as a power of two. This leaves us with three options: (1) Alter the data rate f_c and/or the frequency of the modulating sinewave f_J such that N is a power of two, (2) work with a non-power-of-two vector length and use a window function together with the radix-2 FFT, or (3) work with a non-power-of-two vector length and assume that the jitter sequence consists of a single sine wave from which its RMS value is computed directly from the time sequence. We will select the latter two approaches and select $N = 3 \times 10^5$. Substituting N back into the above expressions, we obtain

$$M_c = 3 \times 10^4 \quad \text{and} \quad M_J = 3$$

As far as the jitter amplitude is concerned, we want a 0.5-UI amplitude but we need to convert between UI and radians. To do this, we use

$$A_J[\text{radians}] = 2\pi \times A_J[\text{UI}] = \pi$$

Using Eq. (14.137), M_J, M_c, and N, together with A_J = π radians, the waveform synthesis routine can be written using a programming for loop as follows:

$$\begin{aligned} &\text{for } n = 1 \text{ to } 3 \times 10^5 \\ &d[n] = \text{sign}\left\{ \sin\left[2\pi \frac{1}{10}(n-1) + 3.1415 \times \sin\left[2\pi \frac{1}{10^5}(n-1) \right] \right] \right\} \\ &\text{end} \end{aligned}$$

Running this procedure results in the following plot of a short portion of the sequence between n = 15,000 to 15,100 where the modulating signal is near its peak, and again between n = 50,000 and 50,100 where the modulating signal is near zero:

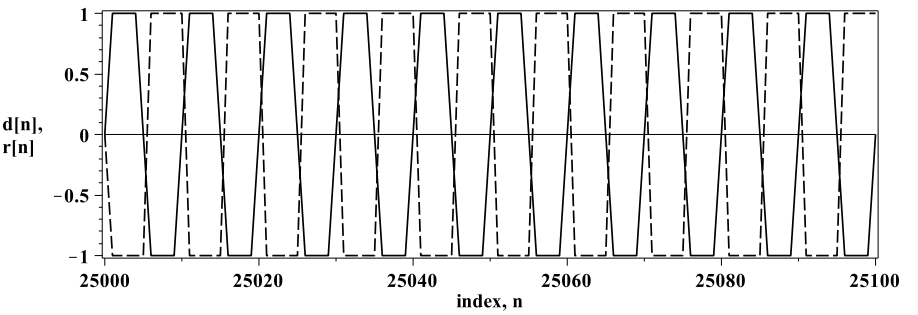

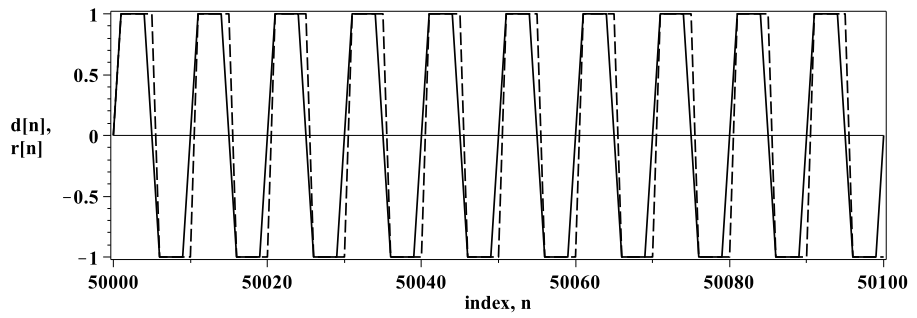

Clearly, the jitter sequence goes through a maximum phase shift of 3.14 radians or 0.5 UI as expected.

Exercises

14.26. A digital receiver operates at a clock rate of 600 MHz. A jitter transfer test needs to be performed with a 1-kHz phase-modulated sinusoidal signal having an amplitude of 10^{-8} s. Select the values of M_c, M_J and N such that the samples are coherent with a 4-GHz sampling rate.

ANS. $M_c = 1.8 \times 10^6$, $M_J = 3$, $N = 1.2 \times 10^7$.

Coherent Phase Extraction Using Analytic Signal Representation

In terms of extracting the sinusoidal phase-modulated response of the device or system, again, we can describe three approaches. The first method to be described is based on the analytic signal extraction method presented in references 16 and 17. This method uses a fast digitizer operating at a sampling rate of F_S, whereby the channel output signal is sampled and the data are collected and stored in vector d_{OUT}. In order to ensure that Shannon's sampling theorem is respected, the incoming digital signal must be band-limited so that only the fundamental components of the incoming signal are presented to the digitizer. Next, an analytic or complex signal representation of collected data d_{OUT} is created using the discrete Hilbert transform according to the following:

$$d_{OUT,\,analytic} = d_{OUT} + j\hat{d}_{OUT} \tag{14.140}$$

where the discrete-time sequence $\hat{d}_{OUT}$ is related to the original time series through the discrete Hilbert transform[18] (DTH) as follows

$$\hat{d}_{OUT}[n] = \mathrm{DHT}\{d_{OUT}\} = \frac{2}{\pi}\begin{cases} \displaystyle\sum_{k=odd} \frac{d_{OUT}(k)}{n-k}, & n \text{ even} \\ \displaystyle\sum_{k=even} \frac{d_{OUT}(k)}{n-k}, & n \text{ odd} \end{cases} \tag{14.141}$$

In general, the DHT defined above is computationally inefficient. Instead, one can work in the frequency domain using the spectral coefficients of d_{OUT}, that is,

$$D_{OUT}(k) = \mathrm{FFT}\{d_{OUT}\}, \quad k = 0, \ldots, N-1 \tag{14.142}$$

and obtain the spectral coefficients of the analytic signal $D_{OUT,analytic}$ as

$$D_{OUT,\,analytic}(k)=\begin{cases} D_{OUT}(k), & k=0 \\ 2D_{OUT}(k), & k=1,2,\ldots,\dfrac{N}{2}-1 \\ 0, & k=\dfrac{N}{2},\ldots,N-1 \end{cases} \tag{14.143}$$

Through the application of the inverse FFT, we obtain the N-point Hilbert transform of the N-point sequence d_{OUT} as follows

$$\hat{d}_{OUT}[n]=\mathrm{Im}\left\langle \mathrm{IFFT}\left\{D_{OUT,analytic}\right\}\right\rangle, \quad n=0,\ldots,N-1 \tag{14.144}$$

Of course, the real part of $\left\langle \mathrm{IFFT}\{D_{OUT,analytic}\}\right\rangle$ is the original data sequence d_{OUT}.

The discrete-time total instantaneous phase from the complex signal using the following recursive equation:

$$\theta_i[n]=\theta_i[n-1]+\tan^{-1}\left(\frac{\hat{d}_{OUT}[n]}{d_{OUT}[n]}\right)-\tan^{-1}\left(\frac{\hat{d}_{OUT}[n-1]}{d_{OUT}[n-1]}\right) \tag{14.145}$$

Because this phase term includes both the phase of the carrier and the jitter-injected signal, we need to determine the instantaneous phase of the carrier and subtract it from Eq. (14.145) to obtain the effect of the phase-modulated jitter signal alone. To begin, let us recognize that the sequence of phase samples corresponding to the reference signal varies proportionally with the sample time [argument term of Eq. (14.139) when A_j is zero], according to

$$\theta_{REF}[n]=2\pi\frac{M_c}{N}n \tag{14.146}$$

or in recursive form as

$$\theta_{REF}[n]=\theta_{REF}[n-1]+2\pi\frac{M_c}{N} \tag{14.147}$$

The phase-modulated jitter sequence would then be recovered by subtracting Eq. (14.146) from Eq. (14.145) to obtain

$$J[n]=\theta_i[n]-\theta_{REF}[n] \tag{14.148}$$

or simply as

$$J[n]=\theta_i[n]-2\pi\frac{M_c}{N}n \tag{14.149}$$

Note that great care must be exercised when using the inverse-tangent operation associated with Eq. (14.145). Normally the built-in inverse-tangent operation of a tester or computer routine, such as MATLAB or Excel, limits its range to two quadrants of the complex plane, that is, $\pm\pi$.

Moreover, extension to four-quadrant operation does not solve the problem completely. We will address this issue shortly.

While the reference phase term is known at the AWG output, it may experience phase shift through the digital channel, so one should not rely on the generated signal properties alone. Instead, it is always best to extract the reference signal phase behavior from the measured data at the receiver end. There are at least two ways in which to do this. The first method is to fit a straight line through the instantaneous phase signal $\theta_i[n]$ using linear regression analysis (similar to the best-fit line method used in DAC/ADC testing), such as

$$\theta_{REF}[n] = \lambda n + \beta \tag{14.150}$$

Subsequently, the instantaneous excess phase sequence would then be found from Eq. (14.148).

A second approach is to work with the frequency information associated with the captured digital sequence d_{OUT}. Let us begin by taking the FFT of d_{OUT} and denote the result as D_{OUT}, that is,

$$D_{OUT} = \text{FFT}(d_{OUT}) \tag{14.151}$$

Next, set all bins to zero except bins M_c and N-M_c and perform an inverse FFT according to

$$d_{REF} = \text{IFFT}\left\{[0,\ldots,0,D_{OUT}(M_c),0,\ldots,0,D_{OUT}(N-M_c),0,\ldots,0]\right\} \tag{14.152}$$

Subsequently, perform a discrete Hilbert transform on d_{REF} and obtain the analytic signal representation of the reference signal as follows:

$$d_{REF,analytic} = d_{REF} + j\hat{d}_{REF} \tag{14.153}$$

The instantaneous phase behavior of the reference signal is then found using the following recursive equation:

$$\theta_{REF}[n] = \theta_{REF}[n-1] + \tan^{-1}\left(\frac{\hat{d}_{REF}[n]}{d_{REF}[n]}\right) - \tan^{-1}\left(\frac{\hat{d}_{REF}[n-1]}{d_{REF}[n-1]}\right) \tag{14.154}$$

The analytic signal representation for the reference signal in the time domain would then be described using the inverse FFT as follows:

$$d_{REF,analytic} = d_{REF} + j\hat{d}_{REF} = IFFT\left\{[0,\ldots,0,2D_{OUT}(M_c),0,\ldots,0]\right\} \tag{14.155}$$

Similarly, the analytic signal representation for the d_{OUT} sequence is found from

$$\begin{aligned} d_{OUT,analytic} &= d_{OUT} + j\hat{d}_{OUT} \\ &= \text{IFFT}\left\{[D_{OUT}(0),2D_{OUT}(1),\ldots,2D_{OUT}(M_c),\ldots,2D_{OUT}\left(\frac{N}{2}-1\right),0,0,\ldots,0]\right\} \end{aligned} \tag{14.156}$$

Before we move on to the calculation of jitter transfer gain, we need to close off the issue of unwrapping the phase function of the various complex signals. At the heart of this difficulty is the

mathematical behavior of the inverse-tangent operation. While the trigonometric tangent maps one value to another, the inverse tangent operation maps one value to many values separated by multiples of ±2π. This creates discontinuities in the computed phase behavior of the complex signal and renders the analytic signal analysis method useless.

To get around the computational difficulties of unwrapping a phase function, we must keep track of the phase changes as a function of the sampling instant, in particular as we move from either the third or fourth quadrant of the complex place into the first or second quadrant, we must add 2π to the instantaneous phase function. Here we are assuming that a step change in phase is never greater than π. A condition that is met when the sampling process respects Shannon's sampling constraint (i.e., no less than 2 points per period on the highest frequency component). Following this process, assuming we have an analytic signal defined as $z[n] = x[n] + j\hat{x}[n]$, the instantaneous unwrapped phase function would be written as

$$\theta_i[n] = \begin{cases} \theta_i[n-1] + 2\pi + \tan 4\mathrm{q}^{-1}\left(\dfrac{\hat{x}[n]}{x[n]}\right) - \tan 4\mathrm{q}^{-1}\left(\dfrac{\hat{x}[n-1]}{x[n-1]}\right) & \hat{x}[n-1] < 0, x[n] > 0, \hat{x}[n] > 0 \\ & \text{or} \\ & x[n-1] > 0, \hat{x}[n-1] < 0, \hat{x}[n] > 0 \\ \theta_i[n-1] + \tan 4\mathrm{q}^{-1}\left(\dfrac{\hat{x}[n]}{x[n]}\right) - \tan 4\mathrm{q}^{-1}\left(\dfrac{\hat{x}[n-1]}{x[n-1]}\right) & \text{otherwise} \end{cases} \tag{14.157}$$

where the four-quadrant inverse-tangent function $\tan 4q^{-1}(.)$ is defined as follows

$$\tan 4q^{-1}\left(\frac{y}{x}\right) = \begin{cases} \tan^{-1}\left(\dfrac{y}{x}\right), & x \geq 0, y \geq 0 \\ \pi - \tan^{-1}\left(\dfrac{y}{-x}\right), & x < 0, y \geq 0 \\ \pi + \tan^{-1}\left(\dfrac{-y}{-x}\right), & x < 0, y < 0 \\ 2\pi - \tan^{-1}\left(\dfrac{-y}{x}\right), & x \geq 0, y < 0 \end{cases} \tag{14.158}$$

The following example will help to illustrate this jitter extraction technique on a multitone phase modulated signal.

EXAMPLE 14.24

A 4096-point data set is collected from the following two-tone unity-amplitude phase-modulated jitter sequence:

$$d_{OUT}[n] = \sin\left[2\pi\frac{1013}{4096}(n-1) + 1\times\sin\left[2\pi\frac{57}{4096}(n-1)\right] + 1\times\sin\left[2\pi\frac{23}{4096}(n-1)\right]\right]$$

Extract the jitter sequence using the analytic signal approach and compare this sequence to the ideal result.

Solution:
The first step to the analytic signal extraction method is to obtain the FFT of the sampled sequence. Let us denote the FFT of the data sequenceas follows:

$$D_{OUT} = FFT\left(d_{OUT}\right)$$

A plot of the magnitude response corresponding to the spectral coefficients of this data sequence is shown below over the Nyquist and its first image band:

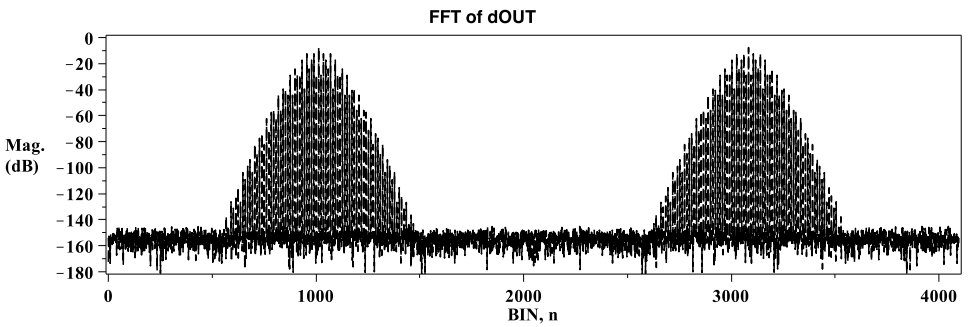

Here we see a very rich spectral plot with most of the power of the signal concentrated around the carrier located in bin 1013. We also notice that the magnitude response is symmetrical about the 2048 bin. Next, we perform the Hilbert transform of the data sequence in the frequency domain, resulting in the magnitude response shown below:

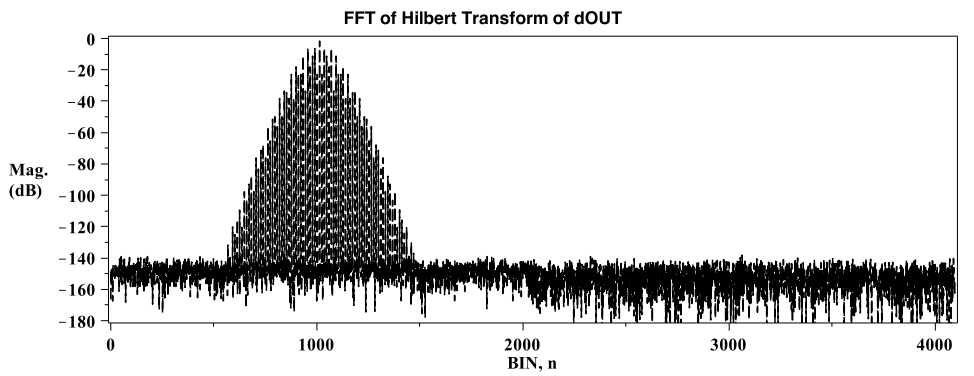

Here we see magnitude response in the Nyquist interval increase by 3 dB and the level of the first image reduced to the noise floor of the FFT. We can also extract the reference signal from the above spectral plot and obtain the spectral coefficients of the Hilbert transform of the reference signal as follows:

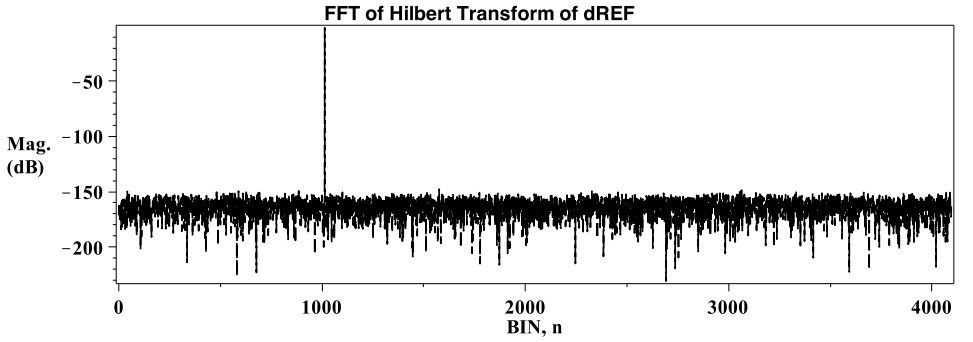

The inverse FFT of the Hilbert transform of D_{OUT} results in the complex sequence whose real and imaginary parts are plotted below for n between 0 and 150:

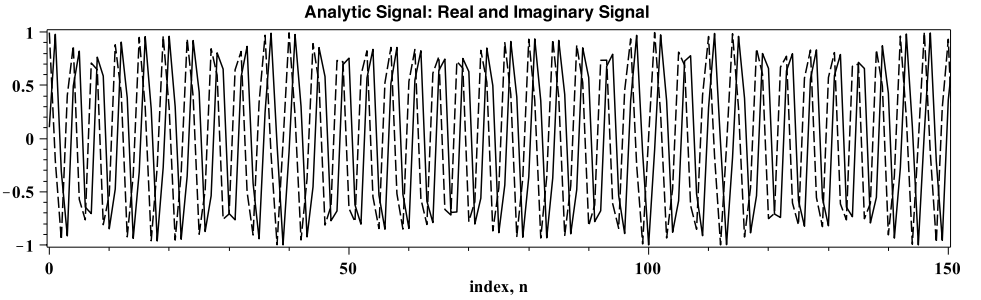

The reader can see two identical signals, one shifted slightly with respect to the other. In fact, the phase offset is exactly π/2, as defined by the Hilbert transform. Using the analytic signal representation for d_{OUT} and the reference, we extract the following two instantaneous phase sequences:

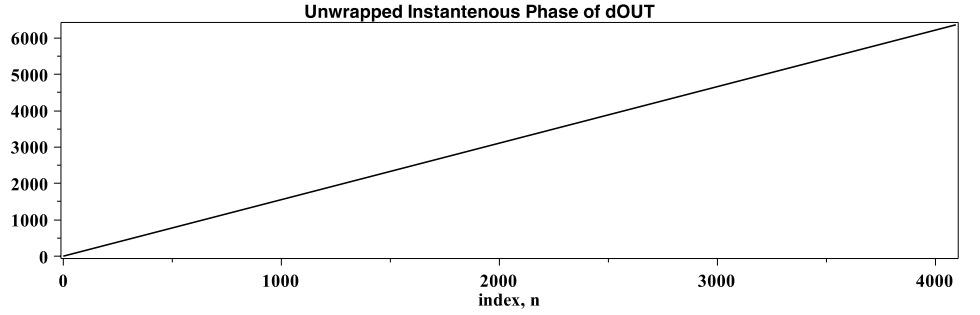

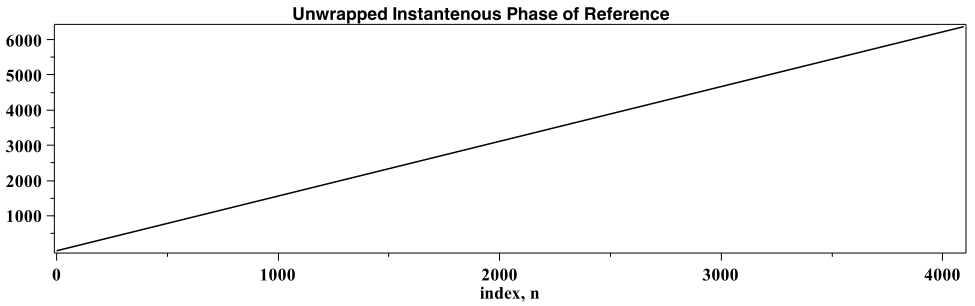

Here both phase sequences increase monotonically with index, *n*. In fact, both plots look identical. However, taking their difference reveals the key information that we seek, that being the phase-modulated jitter sequence as shown below:

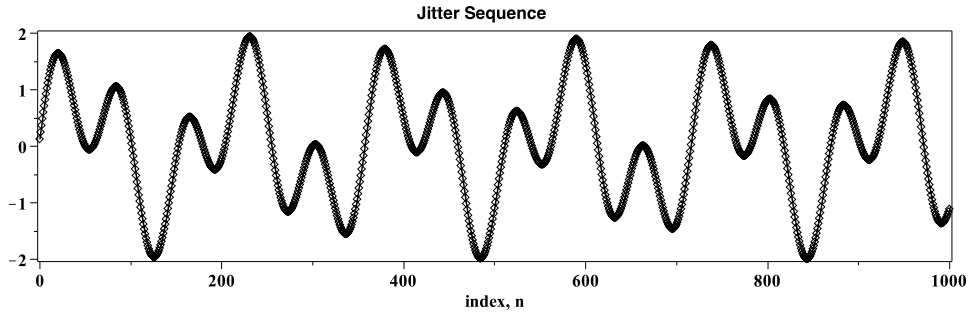

Superimposed on this plot is the expected jitter sequence taken from the given phase-modulating data sequence (shown as circles).

We conclude that the analytic signal extraction method was effective in extracting the two-tone phase modulated signal. It is interesting to note from this example that if we take the FFT of the extracted jitter sequence we can obtain a spectral plot that separates the two tones in the usual DSP-based manner as follows:

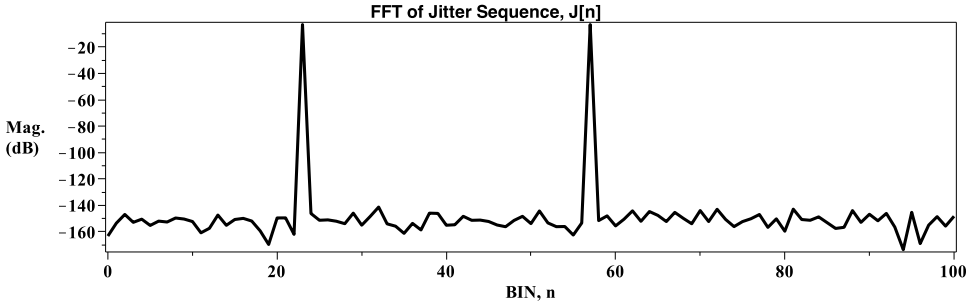

It should be clear from the above example that all DSP-based methods of previous chapters are directly applicable to a jitter sequence.

Final Comments

The objective of this section was to measure the sinusoidal phase-modulated response of a device or system so that the jitter transfer gain could be computed. We now are equipped with the DSP-based techniques in which to extract this information from a time sequence. If we define the jitter sequence at the output of the system as $J_{OUT}[n]$, then we can obtain the peak-to-peak value from the M_J bin using the spectral coefficient notation as follows:

Figure 14.37. Extracting the phase component of a digital signal: (a) indirect method involving a high-speed digitizer, (b) a direct method using a heterodyning technique, (c) another direct method involving a TDC.

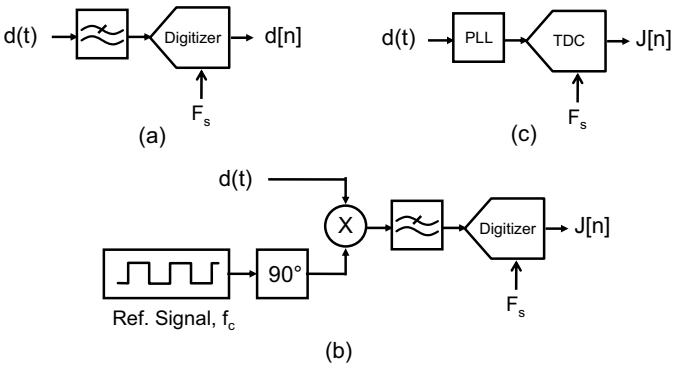

$$SJ_{OUT} = 2\sqrt{2} \times c_{M_J - RMS, J_{OUT}} \tag{14.159}$$

Likewise, the input sinusoidal phase-modulated sequence, denoted as $J_{IN}[n]$, is analyzed in the exact same way leading to

$$SJ_{IN} = 2\sqrt{2} \times c_{M_J - RMS, J_{IN}} \tag{14.160}$$

Finally, we combine Eqs. (14.159) and (14.160) and substitute into Eq. (14.129) to find the jitter transfer gain corresponding to Bin M_J as

$$G_J(M_J) = \frac{c_{M_J - RMS, J_{OUT}}}{c_{M_J - RMS, J_{IN}}} \tag{14.161}$$

The process can be repeated across a band of frequencies or one can create a multitone jitter signal and capture the entire jitter transfer over a band of frequencies.

To close this section, we point out through Figure 14.37 that there are several other ways in which to extract the jitter sequence of a phase-modulated signal. Figure 14.37a illustrates the high-speed sampling method just described. The setup in part Figure 14.37b illustrates a heterodyning approach whereby the system output is mixed with a reference signal and the low-frequency image is removed by filtering and then digitized. The test setup of Figure 14.37c makes use of a PLL and time-to-digital (TDC) converter arrangement to obtain the jitter sequence directly. A TDC essentially measures the time difference between the reference and the digital signal to produce $J[n]$. For the latter two test setups, regular FFT post-processing, together with Eq. (14.161), can be used to obtain the jitter transfer gain.

14.8.2 Jitter Tolerance Test

A jitter tolerance test measures the level of jitter that can be applied to the input to a device or system while maintaining a specific BER level at its output. This test generally requires a data source with controllable jitter, a means to verify the characteristics of the jittered input signal, and a means to detect whether the device or system is meeting its BER requirement. The general jitter

Figure 14.38. A general jitter tolerance test setup illustrating the different source conditions.

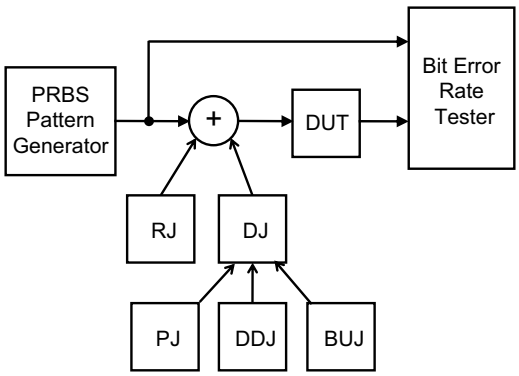

Figure 14.39. A jitter tolerance compliance mask for the SONET OC-12 specification.

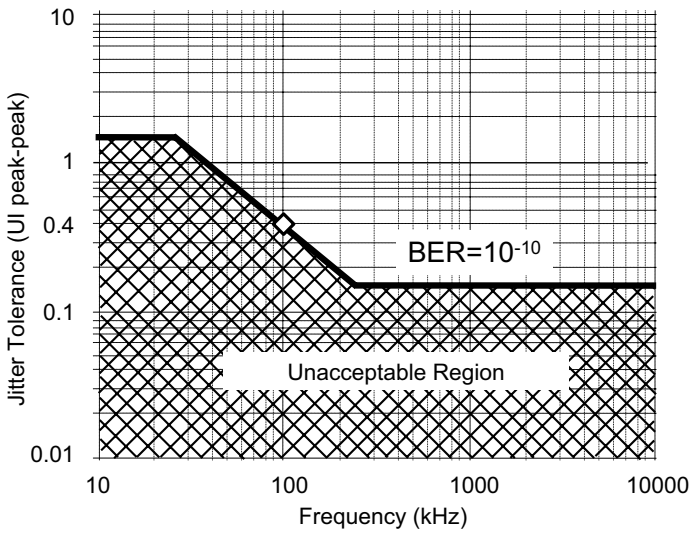

tolerance test setup is shown in Figure 14.38. Depending on the standard, the jitter on the input signal can take various forms. For example, SONET testing requires jitter in the form of a sinusoidal phase modulation, which is swept or stepped across a prescribed frequency band while the amplitude is adjusted so that a specific BER level is maintained. The input amplitude of the jitter is then compared against a frequency template, such as that shown in Figure 14.39 for the SONET OC-12 transmission specification. As an example, at an input sinusoidal frequency of 100 kHz, the device or system must be capable of handling an injected peak-to-peak sinusoidal jitter of no less than of 0.4 UI while maintaining a BER of 10^{-10} or smaller. It is important that the input signal have little RJ component, at least negligible when compared to the SJ component. In contrast to SONET testing, the SATA specification requires a test signal bearing a wide variety of both random and deterministic jitter down to a BER level of 10^{-12} or smaller. Great care must be exercised when selecting the jitter source, especially in light of the very high demands on its performance.

Figure 14.40. (a) Relating the input and output jitter behavior through a linear system function $G(j\omega)$. (b) Input-output PDFs for a sinusoidal input signal and its relationship to $G(j\omega)$.

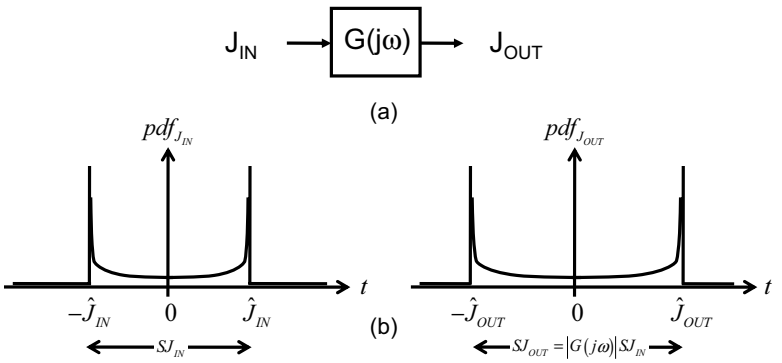

To gain a better understanding of a jitter tolerance test under sinusoidal input conditions, let us assume that the input and output phase or jitter behavior of a system is linearly related by some transfer function $G(j\omega)$ as depicted in Figure 14.40a. Such a transfer function arises naturally from the underlying mathematical description of a clock recovery circuit. If the input to the system is described by the equation $J_{IN}\sin(\hat{\omega}t)$, then the output can be described as $|G(j\omega)|\hat{J}_{IN}\sin(\omega t + \angle G(j\omega))$. Equally, we can relate the PDFs of the input and output distributions as shown in Figure 14.40b with peak-to-peak values of SJ_{IN} and $SJ_{OUT} = |G(j\omega)|SJ_{IN}$, respectively. Clearly, the larger the gain of the system at a particular frequency, the larger the output peak-to-peak jitter. Assuming that sinusoidal jitter is the only jitter present, then we can describe the PDF of the zero-crossings of two consecutive bits as shown in Figure 14.41a. Superimposed on this plot is the ideal sampling instant at $t_{SH} = T/2$. This threshold sits midway between the two ideal bit transitions. As is evident from this figure, the jitter is bounded and much less than the sampling threshold so that no transmission errors are expected. As the input peak-to-peak value increases, as shown in Figure 14.41b, the peak value of the output jitter distribution gets closer to the sampling instant, but again, no errors are expected. However, once the amplitude of the jitter exceeds the sampling threshold [i.e., $\hat{J}_{IN}|G(j\omega)| > T/2$], errors are expected as illustrated in Figure 14.41c. We can quantify the BER level by integrating the areas beyond the threshold on each side and write

$$\text{BER} = \frac{1}{2}P_e\Big|_{t>t_{SH}} + \frac{1}{2}P_e\Big|_{t<t_{SH}} = \frac{1}{2}\times\int_{T/2}^{\infty} pdf_{J_{OUT}}\Big|_{t=0}\,dt + \frac{1}{2}\times\int_{-\infty}^{T/2} pdf_{J_{OUT}}\Big|_{t=T}\,dt \qquad \textbf{(14.162)}$$

where

$$pdf_{J_{OUT}} = \begin{cases} \dfrac{1}{\pi\sqrt{\left(\dfrac{SJ_{OUT}}{2}\right)^2 - t^2}}, & -\dfrac{SJ_{OUT}}{2} \le t \le \dfrac{SJ_{OUT}}{2} \\ 0 & \text{otherwise} \end{cases} \qquad \textbf{(14.163)}$$

Substituting and using the integral relationship $\int \dfrac{1}{\sqrt{a^2 - x^2}}dx = -\cos^{-1}\left(\dfrac{x}{a}\right),\ (a^2 > x^2)$, we write

$$\text{BER} = \int_{T/2}^{SJ_{OUT}/2} \frac{1}{\pi\sqrt{\left(\dfrac{SJ_{OUT}}{2}\right)^2 - t^2}}dt = \frac{1}{\pi}\cos^{-1}\left(\frac{T}{SJ_{OUT}}\right), \qquad SJ_{OUT} > T \qquad \textbf{(14.164)}$$

Figure 14.41. Illustrating the zero-crossing PDF for two consecutive bit transitions when the system is excited by a sinusoidal signal: (a) $\hat{J}_{OUT} < T/2$ no bit errors, (b) $\hat{J}_{OUT} < T/2$ but larger than situation in part (a) but again no bit errors, (c) $\hat{J}_{OUT} < T/2$ with bit errors.

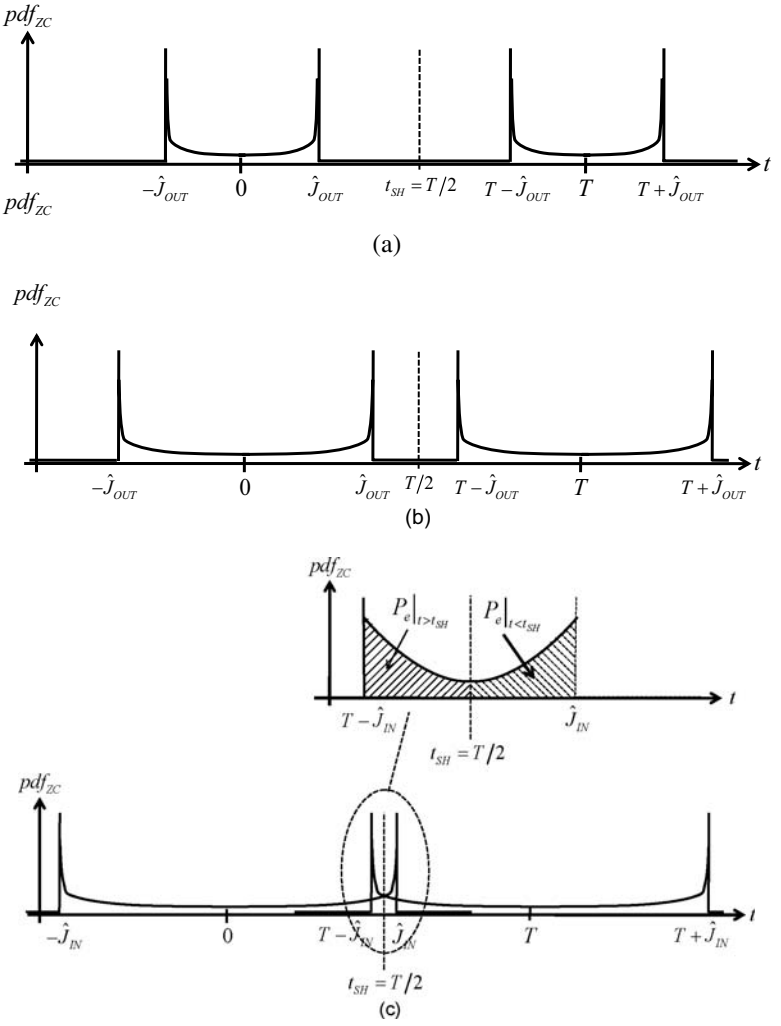

Rearranging and using the trigonometric power series expansion around $x = 0$ $\left(\text{i.e., } \cos x \approx 1 - \frac{x^2}{2}\right)$, we write the BER as

$$\text{BER} = \frac{2}{\pi}\sqrt{1 - \frac{T}{SJ_{OUT}}}, \qquad SJ_{OUT} > T \tag{14.165}$$

or expressing SJ_{OUT} in terms of UIs, we write

$$\text{BER} = \frac{2}{\pi}\sqrt{1 - \frac{1}{SJ_{OUT}}}, \qquad SJ_{OUT} > 1 \text{ UI} \tag{14.166}$$

Replacing the output SJ term by the input *SJ* term and system function $G(j\omega)$, we finally write

$$\text{BER} = \frac{2}{\pi}\sqrt{1-\frac{1}{|G(j\omega)|SJ_{IN}}}, \quad |G(j\omega)|SJ_{IN} > 1 \text{ UI} \tag{14.167}$$

This equation provides the key insight into the jitter tolerance test. It shows how the peak-to-peak input jitter level, the system transfer function, and the BER performance are all interrelated. For instance, if $G(j\omega)$ has a low-pass nature whereby at DC, $G(j\omega) = 1$ and for $f > f_B$, $G(j\omega) = 0$, then the BER performance will have a value of $\frac{2}{\pi}\sqrt{1-\frac{1}{SJ_{IN}}}$ for $f > f_B$ and a very large value of $2/\pi$ for $f > f_B$.

For a particular BER performance, we can rearrange Eq. (14.167) and write the input *SJ* as follows:

$$SJ_{IN} = \frac{1}{|G(j\omega)|\left[1-\left(\frac{\pi}{2}\times \text{BER}\right)^2\right]} \tag{14.168}$$

The above expression reveals the nature of the mask that separates the acceptable region from the unacceptable region as illustrated in the jitter tolerance plot of Figure 14.39. The shape of this mask follows the inverse of the system transfer function $|G(\text{j}\omega)|^{-1}$. In order to clearly identify the points on this mask, let us denote these points as $SJ_{IN}|_{GOLDEN}$ and the corresponding system gain as $G_{GOLDEN}(j\omega)$, then we can write

$$SJ_{IN}|_{GOLDEN} = \frac{1}{|G_{GOLDEN}(j\omega)|\left[1-\left(\frac{\pi}{2}\times \text{BER}\right)^2\right]} \tag{14.169}$$

Any measured SJ_{IN} that is above $SJ_{IN}|_{GOLDEN}$ will fall in the acceptable region. To understand why this is so, consider a situation where the input *SJ* at a particular frequency to a DUT is adjusted so that the BER at the output reaches the desired level. If $SJ_{IN}|_{DUT} > SJ_{IN}|_{GOLDEN}$, then we can write

$$\frac{1}{|G_{DUT}(j\omega)|\left[1-\left(\frac{\pi}{2}\times \text{BER}\right)^2\right]} > \frac{1}{|G_{GOLDEN}(j\omega)|\left[1-\left(\frac{\pi}{2}\times \text{BER}\right)^2\right]} \tag{14.170}$$

which leads to

$$|G_{GOLDEN}(j\omega)| > |G_{DUT}(j\omega)| \tag{14.171}$$

This expression suggests that the DUT gain is less than the golden device gain and hence can tolerate a greater level of jitter at its input before reaching the same output level or, equivalently, the same BER level. It should be noted here that the jitter tolerance test is much more than just a measurement of the gain of the system transfer function, because it includes nonlinear and noise effects not modeled by the above equations.

EXAMPLE 14.25

A jitter tolerance test was performed on a digital receiver that must conform to the SONET OC-12 specification shown in Figure 14.39. The following table lists the results of this test. Does the receiver meet the OC-12 specification? What is the gain of the measured device relative to the golden device gain at 300 kHz?

Input SJ (pp)	Input Frequency	Measured BER
2.2 UI	10 kHz	10^{-10}
2.3 UI	30 kHz	10^{-10}
1.1 UI	100 kHz	10^{-10}
0.11 UI	300 kHz	10^{-10}
0.21 UI	1,000 kHz	10^{-10}
0.32 UI	3,000 kHz	10^{-10}
0.32 UI	10,000 kHz	10^{-10}

Solution:
To see clearly the results of the test, we superimposed the data points from the table on a frequency plot with the OC-12 compliance mask superimposed. All points but one at 300 kHz appear above the BER = 10^{-10} line, hence this device does not pass the test.

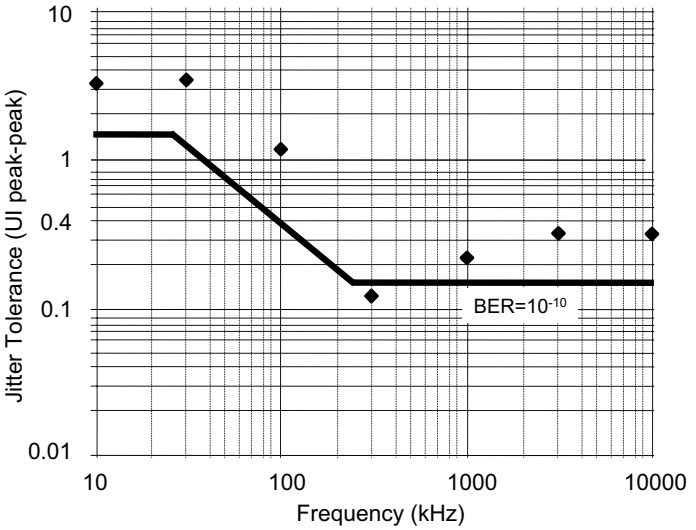

The gain of the DUT relative to the golden device gain is found from Eq. (14.167) as

$$\frac{2}{\pi}\sqrt{1-\frac{1}{\left|G_{GOLDEN}(j\omega)\right|SJ_{IN}\big|_{GOLDEN}}}=\frac{2}{\pi}\sqrt{1-\frac{1}{\left|G_{DUT}(j\omega)\right|SJ_{IN}\big|_{DUT}}}$$

which reduces to

$$\frac{\left|G_{DUT}(j\omega)\right|}{\left|G_{GOLDEN}(j\omega)\right|}=\frac{SJ_{IN}\big|_{GOLDEN}}{SJ_{IN}\big|_{DUT}}$$

Substituting the appropriate measured and golden device values leads to

$$\frac{\left|G_{DUT}\left(j2\pi \times 300\text{ kHz}\right)\right|}{\left|G_{GOLDEN}\left(j2\pi \times 300\text{ kHz}\right)\right|} = \frac{0.15\text{ UI}}{0.11\text{ UI}} = 1.36$$

Here we see the DUT has a gain that is 1.36 times larger than the golden device gain at 300 kHz.

EXAMPLE 14.26

A golden device operating at a bit rate of 100 MHz has an input–output phase transfer function described as follows:

$$G(s) = 50\frac{s+50}{s+5000}$$

Plot the expected jitter tolerance mask for a sinusoidal phase-modulated inputsignal with a BER of 10^{-10}.

Solution:
According to Eq. (14.169), the expected input SJ mask level can be written as

$$SJ_{IN}\big|_{GOLDEN}(f) = \frac{1}{\left|50\frac{j2\pi f+50}{j2\pi f+5000}\right|\left[1-\left(\frac{\pi}{2}\times 10^{-10}\right)^2\right]}$$

The corresponding jitter tolerance plot becomes

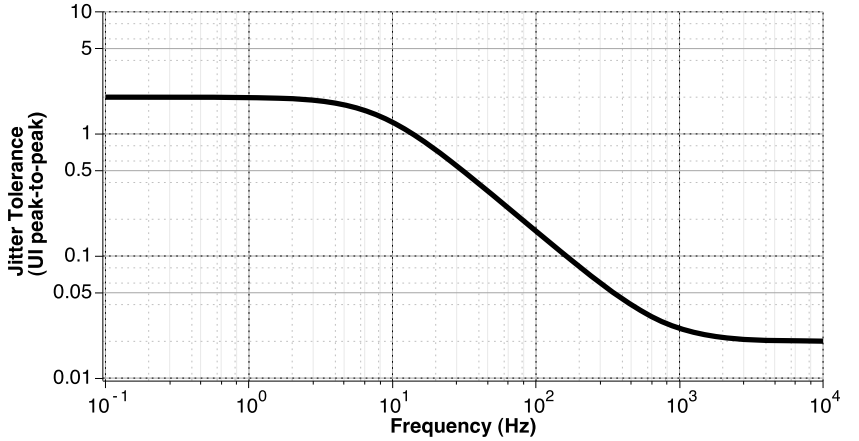

Exercises

14.27. Repeat the development of the BER expression shown in Eq. (14.162) for a sinusoidal jitter tolerance test but this time assume the PDF of output jitter is described by a uniform PDF from -SJ/2 to SJ/2.

ANS. $$\text{BER} = \frac{1}{2}\left[1 - \frac{1}{|G(j\omega)|SJ_{IN}}\right], \quad |G(j\omega)|SJ_{IN} > 1\ \text{UI}$$

14.28. Repeat the development of the BER expression shown in Eq. (14.162) for a sinusoidal jitter tolerance test but this time assume the normalized sampling instant is an arbitray point between 0 and *T*.

ANS. $$\text{BER} = \frac{1}{2}\left[1 + \frac{1}{\pi}\cos^{-1}\left(\frac{2\text{UI}_{TH}}{|G(j\omega)|SJ_{IN}}\right) - \frac{1}{\pi}\cos^{-1}\left(\frac{2(\text{UI}_{TH} - 1)}{|G(j\omega)|SJ_{IN}}\right)\right], \quad |G(j\omega)|SJ_{IN} > 1\ \text{UI}$$

The above jitter tolerance test was developed from the perspective of a sinusoidal phase-modulated stimulus such as that used for SONET. One can just as easily develop the idea of a golden device behavior with respect to other types of input distributions. The reader can find several examples of this in the problem set at the end of this chapter.

During production a jitter tolerance test is conducted in a go/no-go fashion whereby the input DJ and RJ are first established by way of the transmission compliance mask, combined with the appropriate PRBS data pattern, and then applied to the device or system. The corresponding BER performance is then measured and compared to the expected level as specified in the communication standard (say BER_D). If the BER is less than or equal to BER_D over the entire frequency band, the device will pass the test. Owing to the number of BER measurements required during a jitter tolerance test, methods that speed up this test are often critical for a product's commercial success.

14.9 SUMMARY

In this chapter, we have reviewed the test principles related to clock and serial communication channel measurements. We began by studying the noise attributes of a clock signal in the time domain and then in the frequency domain. As with any noise process, statistical methods were used to quantify the level of noise present with the clock signal. This included some discussion on accumulated jitter, a concept related to the autocorrelation function of the jitter time sequence, and an aggregate power spectral density metric based on the average spectral behavior of the clock signal. Subsequently, the remainder of the chapter focused on measurement principles related to serial data communications. It began by introducing the concept of an eye diagram from which the idea of a zero crossing probability distribution was introduced. This was then expanded to include the effects of a real channel, such as noise and dispersion, leading to a classification of the various types of jitter one encounter in practice. Using a probabilistic argument, the probability of transmission error was introduced in terms of a probability density function for a jitter mechanism. The concept of bit error rate (BER) was introduced as the average probability of transmission error. Subsequently, the BER was modeled as a binomial distribution from which confidence intervals could be computed and related to test time. At this point in the chapter it became evident that a BER test requires excessive test time and the following section outlined different strategies to reduce the time of a BER test. All of these methods involved expressing the BER as a function of a model of the underlying jitter process and then solving for the parameters of this model at a low BER level where test time can be made short. A general method of modeling a Gaussian mixture

was outlined and shown to be a powerful method of modeling various sources of jitter. Commonly used test metrics like random jitter (RJ), deterministic jitter (DJ), and total jitter (TJ) were defined. Methods to further decompose deterministic jitter were outlined. These methods were based on DSP techniques similar to the techniques used for analog and sampled-data channels. The chapter concluded with a short discussion on jitter transmission test whereby a jitter signal is injected into the channel and its effect on the output is quantified. This included a discussion on jitter transfer and jitter tolerance type tests.

PROBLEMS

14.1. A time jitter sequence is described by $J[n] = 0.001 \sin^2(14\pi/1024n) + 0.001$ for n = 0,1,…, 1023. What is the mean, standard deviation, and peak-to-peak value of this time jitter sequence. Plot the histogram of this data sequence over a range of 0 to 0.002.

14.2. A time jitter sequence is described by $J[n] = 0.001 \sin(14\pi/1024n)$ for n = 0,1,…, 1023. What is the period jitter and cycle-to-cycle jitter of this time jitter sequence.

14.3. A time jitter sequence is described by $J[n] = 0.001 \sin(14\pi/1024\ n) + \left[1 - e^{-\left(\frac{3}{64}n\right)}\right]$ for all n. Plot and observe the behavior of the accumulated jitter sequence corresponding to this signal over a range of 64 delay instants using a sample set of 128.

14.5. A time jitter sequence is described by $J[n] = 0.001 \times \text{randn}() + 0.001 \times \left[1 - e^{-\left(\frac{3}{128}n\right)}\right]$ for all n. Here randn() represents a Gaussian random number with zero mean and unity standard deviation. Plot and observe the behavior of the accumulated jitter sequence for this signal over a range of 128 delay instants using a sample set of 256.

14.6. The PSD of the voltage level of a 100-MHz clock signal is described by $S_v(f) = 10^{-4}/10^4 + (f - 10^8) + 0.5 \times \delta(f - 10^{-8})$ in units of V²/Hz. What is the RMS noise level associated with this clock signal over a 1000-Hz bandwidth center around the first harmonic of the clock signal?

14.7. The PSD of the instantaneous phase of a 2.5-GHz clock signal is described by $S_\phi(f) = 4 \times 10^{-4}/10^4 + f^2$ in units of rad²/Hz. What is the RMS level associated with the phase of this clock signal over a 1000-Hz bandwidth?

14.8. The PSD of the voltage level of a 100-MHz clock signal is described by $S_v(f) = 10^{-4}/10^4 + (f - 10^8)^2 + 0.5 \times \delta(f - 10^8)$ in units of V²/Hz. What is the phase noise of the clock at a 10,000-Hz offset in dBc/Hz?

14.9. The PSD of the instantaneous phase of a 2.5-GHz clock signal is described by $S_\phi(f) = 4 \times 10^{-4}/10^4 + f^2$ in units of rad²/Hz. What is the phase noise of the clock at 10,000-Hz in dBc/Hz?

14.10. The PSD of the instantaneous phase of a 10-GHz clock signal is described by $S_\phi(f) = 10^{-5}/10^6 + f^2$ in units of rad²/Hz. What is the spectrum of a jitter sequence derived from this clock signal in s²/Hz? How about when expressed in UI²/Hz?

14.11. A phase jitter sequence expressed in radians can be described by the equation $\phi[n] = 0.1\sin(50\pi/1024n)$ for n = 0,…,1023 was extracted from a 100-MHz clock signal using a 10-GHz sampling rate. Plot the phase spectrum in UI²/Hz.

14.12. A time jitter sequence expressed in nanoseconds can be described by the equation $J[n] = 0.1\sin(14\pi/1024n) + 0.1\sin 50\pi/1024n + 0.1\sin 124\pi/1024n$ for n = 0,…,1023

was extracted from a 100-MHz clock signal using a 10-GHz sampling rate. Plot the phase spectrum in s^2/Hz.

14.13. Determine the following list of convolutions:

(a) $\delta(t-a)\otimes\frac{1}{\sigma\sqrt{2\pi}}e^{-t^2/2\sigma^2}$,

(b) $\delta(t-a)\otimes\frac{1}{\sigma\sqrt{2\pi}}e^{-(t-\mu)^2/2\sigma^2}$,

(c) $\left[\frac{1}{2}\delta(t+a)+\frac{1}{2}\delta(t-a)\right]\otimes\left[\frac{1}{2}\delta(t+b)+\frac{1}{2}\delta(t-b)\right]$, and

(d) $\left[\frac{1}{4}\delta(f+a)+\frac{1}{4}\delta(f-a)+\frac{1}{4}\delta(f+2a)+\frac{1}{4}\delta(f-2a)\right]\otimes\left[\frac{1}{2}\delta(f+b)+\frac{1}{2}\delta(f-b)\right]$.

14.14. The PDF for the ideal zero crossings of an eye diagram can be described by $\frac{1}{2}\delta(t)+\frac{1}{2}\delta(t-10^{-8})$. If the PDF of the random jitter present at the receiver is $10^{-9}/\sqrt{2\pi}\ e^{-t^2/2\times10^{-18}}$, what is the PDF of the actual zero crossings?

14.15. The PDF for the zero crossings at a receiver due to inter-symbol interference can be described by $\frac{1}{4}\delta\left(t+10^{-9}\right)+\frac{1}{4}\delta\left(t-10^{-9}\right)+\frac{1}{4}\delta\left(t-10^{-8}+10^{-9}\right)+\frac{1}{4}\delta\left(t-10^{-8}-10^{-9}\right)$. If the PDF of the random jitter present at the receiver is $10^{9}/\sqrt{2\pi}\ e^{-t^2/2\times10^{-18}}$, what is the PDF of the zero crossings?

14.16. In Chapter 5 we learned that the standard Gaussian CDF can be approximated by

$$\Phi(z)\approx\begin{cases}1-\left(\frac{1}{(1-\alpha)z+\alpha\sqrt{z^2+\beta}}\right)\frac{1}{\sqrt{2\pi}}e^{\frac{-z^2}{2}} & 0\le z<\infty\\ \left(\frac{1}{-(1-\alpha)z+\alpha\sqrt{z^2+\beta}}\right)\frac{1}{\sqrt{2\pi}}e^{\frac{-z^2}{2}} & -\infty<z<0\end{cases}$$

where

$$\alpha=\frac{1}{\pi}\quad\text{and}\quad\beta=2\pi$$

Compare the behavior of this function to the exact CDF function using a built-in routine found in MATLAB, Excel or elsewhere defined by

$$\Phi(z)=\frac{1}{\sqrt{2\pi}}\int_{-\infty}^{z}e^{\frac{-u^2}{2}}du$$

How well does these function compare for very small values of $\Phi(z)$? How about large values? Plot the difference between these two functions for -10 < z < 10. What is the maximum error in percent?

14.17. A logic 0 is transmitted at a nominal level of 0 V and a logic 1 is transmitted at a nominal level of 1.2 V. Each logic level has equal probability of being transmitted. If a 100-mV RMS Gaussian noise signal is assumed to be present at the receiver, what is the probability of making an single trial bit error if the detector threshold is set at 0.6 V. Repeat for a detector threshold of 0.75 V.

14.18. A logic 0 is transmitted at a nominal level of -1.0 V, and a logic 1 is transmitted at a nominal level of 1.0 V. If a 250-mV RMS Gaussian noise signal is assumed to be present at the receiver, what is the probability of making an single trial bit error if the detector threshold is set at 0.0 V. Assume that a logic one has twice the probability of being transmitted than a logic zero.

14.19. Data are transmitted to a receiver at a data rate of 2 Gbits/s through a channel that causes the zero crossings to vary according to a Gaussian distribution with zero mean and a 50-ps standard deviation. Assume that the 0 to 1 transitions are equally likely to occur as the 1 to 0 transitions. What is the probability of error of a single event if the sampling instant is set midway between bit transitions? What about if the sampling instant is set at 0.4 ns?

14.20. Describe the PDF of the zero crossings of an ideal receiver operating at a data rate of 1 Gbps when twice the number of logic 0's are transmitted than the logic 1's.

14.21. The set of zero crossings appearing on an oscilloscope corresponding to an eye diagram measurement is described by the following dual-Gaussian PDF:

$$pdf = \frac{1}{4}\frac{1}{\sigma\sqrt{2\pi}}e^{-t^2/2\sigma^2} + \frac{3}{4}\frac{1}{\sigma\sqrt{2\pi}}e^{1(t-1000\,\text{ps})^2/2\sigma^2}$$

where $\sigma = 50$ ps. What is the probability of error of a single event if the normalized sampling instant is set at UI/4.

14.22. Data are transmitted to a receiver at a data rate of 2 Gbits/s through a channel that causes the zero crossings to vary according to a multi-Gaussian distribution described by

$$pdf = \frac{1}{4}\frac{1}{\sigma\sqrt{2\pi}}e^{-(t+5\,\text{ps})^2/2\sigma^2} + \frac{1}{4}\frac{1}{\sigma\sqrt{2\pi}}e^{-(t-4\,\text{ps})^2/2\sigma^2} + \frac{1}{4}\frac{1}{\sigma\sqrt{2\pi}}e^{-(t-500\,\text{ps}+5\,\text{ps})^2/2\sigma^2}$$
$$+ \frac{1}{4}\frac{1}{\sigma\sqrt{2\pi}}e^{-(t-500\,\text{ps}-5\,\text{ps})^2/2\sigma^2}$$

What is the probability of error of a single event if the sampling instant is set midway between bit transitions when $\sigma = 10$?

14.23. A series of 10 transmission measurements was conducted involving 10^{10} bits operating at a data rate of 600 Mbits/s resulting in the following list of transmisson errors: 5, 6, 4, 6, 3, 7, 3, 6, 1, 0. What is the 95% confidence interval for BER associated with this transmission system? How long in seconds did the test take to complete?

14.24. Data are transmitted at a rate of 5 Gbps over a channel with a single-bit error probability of 10^{-8}. If 10^9 bits are transmitted, what is the probability of no bit errors, one bit error, two bit errors, and ten bit errors. What is the average number of errors expected?

14.25. Data are transmitted at a rate of 10 Gbps over a channel with a single-bit error probability of 10^{-11}. If 10^{12} bits are transmitted, what is the probability of less than or equal to one bit error, less than or equal to two bit errors, and less than or equal to ten bit errors?

14.26. Demonstrate that the Possion approximation for the binomial distribution is valid over the range of N_T between 10^9 to 10^{14} for a BER of 10^{-12}:

$$\sum_{k=0}^{N_E}\left(\frac{N_T!}{k!(N_T-k)!}\right) BER^k(1-\text{BER})^{N_T-k} \approx \sum_{k=0}^{N_E}\frac{1}{k!}(N_T\text{BER})^k e^{-N_T\text{BER}}$$

14.27. A system transmission test is to be run whereby a BER < 10^{-12} is to be verified. How many samples should be collected such that the desired BER is met with a CL of 97% when no more than 10 errors are deemed acceptable. What is the total test time if the data rate is 4 Gbps?

14.28. A system transmission test is to be run whereby a BER < $10^{-11}$is to be verified at a confidence level of 99% when 3 or less bit errors are deemed acccptable. What are the minimum and maximum bit lengths required for this test? Also, what is the minimum and maximum time for this test if the data rate is 1 Gbps? Does testing for a fail part prior to the end of the test provide significant test time savings?

14.29. Draw the schematic diagram of a 5-stage LFSR that realizes a primitive generating polynomial.

14.30. Write a computer program to generate a maximum length sequence corresponding to a 5-stage LFSR. What is the expected length of the repeating pattern produced by this LFSR? Is the sequence periodic? How do you check?

14.31. Draw the schematic diagram of a 12-stage LFSR that realizes a primitive generating polynomial.

14.32. Write a computer program to generate a maximum length sequence corresponding to a 12-stage LFSR. What is the expect length of the repeating pattern produced by this LFSR? What is the value of the seed used to generate this sequence? Is the sequence periodic?

14.33. A PRBS sequence of degree 3 is required for a BER test. Determine the unique test pattern for a seed of 101. Compare this pattern to one generated with a seed of 001. Are there any common attributes?

14.34. A system transmission test is to be run whereby a BER < 10^{-12} is to be verified using the amplitude-based scan test method. The threshold voltage of the receiver was adjusted to the levels –200, –100, 100 and 200 mV, and the corresponding BER levels were measured: 5×10^{-6}, 5×10^{-9}, 5×10^{-9}, and 5×10^{-6}. What are the levels of the received logic values? Does the system meet the BER requirements if the reciever threshold is set at 10 mV?

14.35. A digital system is designed to operate at 2.5 Gbps and have a nominal logic 1 level of 3.3 V and a logic 0 at 0.1 V. If the threshold of the receiver is set at 1.65 V and the noise present at the receiver is 180 mV RMS, select the levels of the amplitude scan test method so that the system can be verified for a BER < 10^{-12} at a confidence level of 99.7% and that the total test time is less than 0.5 s.

14.36. A digital sampling oscilloscope obtained the following eye diagram while observing the characteristics of a 1-Gbps digital signal. Histograms were obtain using the built-in function of the scope at a sampling instant midway between transitions (i.e., at the maximum point of eye opening). Detailed analysis revealed that each histogram is Gaussian. One histogram has a mean value of 2.8 V and a standard deviation of 150 mV. The other has a mean of 120 mV and a standard deviation of 75 mV. Estimate the BER level when the threshold level is set at 2.0 V.

14.37. A digital sampling oscilloscope was used to determine the zero crossings of an eye diagram. At 0 UI, the histogram is Gaussian distributed with zero mean and a standard deviation of 80 ps. At unity UI, the histogram is again Gaussian distributed with zero mean value and a standard deviation of 45 ps. If the unit interval is equal to 1 ns, what is the expected BER associated with this system at a normalized sampling instant of 0.5 UI?

14.38. The BER performance of a digital receiver was measured to be 10^{-16} at a bit rate of 20 Gbps having a sampling instant at one-half the bit duration. If the sampling instant can vary by ±10% from its ideal position, what is the range of BER performance expected during production?

14.39. A digital system operates with a 20-GHz clock. How much RJ can be tolerated by the system if the BER is to be less than 10^{-14} and the DJ is no greater than 3 ps? Assume that the sampling instant is in the middle of the data eye and the total jitter is modeled as a dual-Dirac PDF.

14.40. A digital system operates with a 10-GHz clock. How much DJ can be tolerated by the system if the BER is to be less than 10^{-14} and the RJ is no greater than 5 ps? Assume that the sampling instant is in the middle of the data eye. Assume that the sampling instant is in the middle of the data eye and the total jitter is modeled as a dual-Dirac PDF.

14.41. A system transmission test is to be run whereby a BER < 10^{-14} is to be verified using the dual-Dirac jitter-decomposition test method. The system operates with a 10-GHz clock, and the following BER measurements are at two different sampling instances: BER = 0.25×10^{-5} at 29 ps, and BER = 0.25×10^{-7} at 34 ps. Assume that the digital system operates with a sampling instant in the middle of the data eye. Does the system meet spec?

14.42. A system transmission test was run and the RJ and DJ components were found to be 100 ps and 75 ps, respectively. What is the TJ component at a BER level of 10^{-12}?

14.43. A system transmission test was run and the RJ and DJ components were found to be 100 ps and 75 ps, respectively. What is the TJ component at a BER level of 10^{-14}?

14.44. A system transmission test was run where the RJ component was found to be 10 ps and the TJ component at a BER level of 10^{-12} was found to be 150 ps. What is the DJ component?

14.45. The PDF for total jitter is described by the three-term Gaussian model as follows:

$$pdf = \frac{1}{4}\frac{1}{(2\,\text{ps})\sqrt{2\pi}}e^{-(t+5\text{ps})^2/2(2\text{ps})^2} + \frac{1}{2}\frac{1}{(3\ \text{ps})\sqrt{2\pi}}e^{-(t-1\text{ps})^2/2(3\ \text{ps})^2} + \frac{1}{4}\frac{1}{(4\,\text{ps})\sqrt{2\pi}}e^{-(t-5\text{ps})^2/2(4\ \text{ps})^2}$$

For low BER levels, write an expression of the BER level as a function of the sampling instant. What is the BER at a sampling instant of 30 ps, assuming a 1-Gbps data rate?

14.46. The PDF for total jitter is described by the three-term Gaussian model as follows:

$$pdf = \frac{1}{4}\frac{1}{(2\,\text{ps})\sqrt{2\pi}}e^{-(t+5\text{ps})^2/2(2\text{ps})^2} + \frac{1}{2}\frac{1}{(3\ \text{ps})\sqrt{2\pi}}e^{-(t-1\text{ps})^2/2(3\ \text{ps})^2} + \frac{1}{4}\frac{1}{(4\,\text{ps})\sqrt{2\pi}}e^{-(t-5\text{ps})^2/2(4\ \text{ps})^2}$$

What are the DJ, RJ, and TJ metrics at a desired BER of 10^{-12}?

14.47. The jitter distribution at the transmit side of a communication channel can be described by a four-term Gaussian mixture having the following parameters:

$$0.3 \times N(-100\text{ ps}, 50\text{ ps}) + 0.2 \times N(-10\text{ ps}, 60\text{ ps}) + 0.2 \times N(50\text{ ps}, 60\text{ ps}) + 0.3 \times N(120\text{ ps}, 50\text{ ps})$$

What is the RJ, DJ, and TJ at a BER of 10^{-12} assuming a bit rate of 600 Mbps?

14.48. The jitter distribution at the receiver side of a communication channel can be described by a four-term Gaussian mixture having the following parameters:

$$0.2 \times N(-12\text{ ps}, 5\text{ ps}) + 0.3 \times N(-5\text{ ps}, 6\text{ ps}) + 0.3 \times N(4\text{ ps}, 6\text{ ps}) + 0.2 \times \text{N}(11\text{ ps}, 7\text{ ps})$$

What is the RJ, DJ, and TJ at a BER of 10^{-12}, assuming a bit rate of 2 Gbps?

14.49. Extract a Gaussian mixture model using the EM algorithm from a data set synthesized from a distribution consisting of three Gaussians with means –0.04 UI, 0.01 UI, and 0.1 UI, standard deviations of 0.05 UI, 0.03 UI, and 0.04 UI and weighting factors 0.4, 0.2, and 0.4, respectively. How does extracted models compare with the original data set?

14.50. The jitter distribution at the receiver end of a communication channel consisting of 10,000 samples was modeled by a four-term Gaussian mixture using the EM algorithm and the following model parameters were found:

$$0.2 \times N(-12\text{ ps}, 5\text{ ps}) + 0.3 \times N(-5\text{ ps}, 6\text{ ps}) + 0.3 \times N(4\text{ ps}, 6\text{ ps}) + 0.2 \times N(11\text{ ps}, 7\text{ ps})$$

Assuming that the unit interval is 0.12 ns and that the data eye sampling instant is half a UI, what is the BER associated with this system? Does the system behave with a BER less than 10^{-12}?

14.51. A time jitter sequence can be described by the following discrete-time equation: $J[n] = 2\sin(2\pi\ 51/1024n)$. Sketch the probability density function for this sequence.

14.52. A PRBS sequence of degree 5 is required to excite a digital communication channel. Using a sequence length of 1024 bits, together with a periodic PRBS sequence, what is the spectrum of this pattern? If any tonal behavior is present, what are the RMS values and in which bins of the FFT do these tones appear?

14.53. A jitter sequence consisting of 512 samples was captured from a serial I/O channel driven by two separate data patterns, in one case, an alternating sequence of 1's and 0's was used, and in the other a PRBS pattern was used. An FFT analysis performed on the two separate sets of jitter data, as well as with the PRBS sequence, resulted in the information below. Determine the test metrics: PJ, DDJ, BUJ.

	|X| Complex Spectral Coefficients (UI)		
		PRBS Input	
Spectral Bin in Nyquist Interval	1010 Clock-like Input	Theory	Actual
0	0.01	0	5×10^{-3}
1, ..., 256 except	$\sim 1 \times 10^{-5}$	0	$\sim 4 \times 10^{-4}$
33	0	0.041 – j 0.026	0.05 – j 0.03
91	0	0.01 + j 0.02	0.03 + j 0.03
153	0	0.006 – j 0.007	0.005 – j 0.006
211	0	0	0.001 – j 0.02
251	0.03 – j 0.09	0	0.028 + j 0.033

14.54. The RJ, SJ, ISI, and DCD metrics are 5 ps rms, 20 ps pp, 6 ps pp, and 3 ps pp, respectively. Write an expression for the PDF for each jitter component. Provide a sketch of the total jitter distribution and the zero-crossing PDF assuming a bit duration of 200 ps.

14.55. The RJ, ISI, and DCD metrics are 5 ps rms, 6 ps pp, and 3 ps pp, respectively. Write an expression for the PDF of the total jitter distribution.

14.56. A digital receiver operates at a clock rate of 800 MHz. A jitter transfer test needs to be performed with a 3-kHz phase-modulated sinusoidal signal having an amplitude of 0.001 radians. Select the values of M_c, M_f, and N such that the samples are coherent with a 5-GHz sampling rate.

14.57. A digital receiver operates at a clock rate of 500 MHz. A jitter transfer test needs to be performed with a 5-kHz phase modulated sinusoidal signal having an amplitude of 1.0 UI. Using an AWG with a sampling rate of 10 GHz, write a short routine that generates the AWG samples.

14.58. Compute the discrete Hilbert transform of the sequence: $d[n] = 1 \times \sin(2\pi\ 11/1024)n$. Plot each sequence on the same time axis and compare.

14.59. A 2048-point data set is collected from the following two-tone unity-amplitude phase-modulated jitter sequence:

$$d_{OUT}[n] = \sin\left[2\pi\frac{601}{2048}(n-1) + 1\times\sin\left[2\pi\frac{51}{2048}(n-1)\right] + 1\times\sin\left[2\pi\frac{11}{2048}(n-1)\right]\right].$$

Extract the jitter sequence using the analytic signal approach and compare this sequence to the ideal result.

14.60. A golden device operating at a bit rate of 100 MHz has an input–output phase transfer function described as follows: $\Phi(s) = s(s + 18849.55)/s^2 + 18849.55s + 1.184352 \times 10^8$. Plot the expected jitter tolerance mask for a sinusoidal phase-modulated input signal with a BER of 10^{-12}.

REFERENCES

1. M. P. Li, *Jitter, Noise, and Signal Integrity at High-Speed*, Prentice Hall, Pearson Education, Boston, 2008.
2. Application Note, *Advanced Phase Noise and Transient Measurement Techniques*, Agilent Technologies, 2007, 5989-7273EN.
3. J. A. McNeil, *A simple method for relating time- and frequency-domain measures* of *oscillator performance*, in *2001 IEEE Southwest Symposium on Mixed Signal Design*, Austin, TX, February, pp. 7–12, 2001.
4. Maxim Application Note: Statistica; Confidence Levels for Estimating Error Probability, download, at http://pdfserv.maxim-ic.com/en/an/AN1095.pdf.
5. T. O. Dickson, E. Laskin, I. Khalid, R. Beerkens, J. Xie, B. Karajica, and S. P. Voinigescu, An 80-Gb/s 231-1 pseudo-random binary sequence generator in SiGe BiCMOS technology," *IEEE Journal of Solid-State Circuits*, **40**(12), pp. 2735–2745, December 2005.
6. M. Rowe, BER measurements reveal network health, *Test & Measurement World*, July 1, 2002.
7. K. Willox, Q factor: The wrong answer for service providers and equipment manufacturers, *IEEE Communications Magazine*, **41**(2), pp. S18–S21, February 2003.
8. Application Note, *Jitter Analysis: The Dual-Dirac Model, RJ/DJ, and Q-Scale*, Agilent Technologies, December 2004, http://cp.literature.agilent.com/litweb/pdf/5989-3206EN.pdf.
9. M. P. Li, J. Wilstru, R, Jessen, and D. Petrich, A new method for jitter decomposition through its distribution tail fitting, in *IEEE Proceedings, International Test Conference Proceedings*, pp. 788–794, October 1999.
10. A. P. Dempster, N. M. Laird, and D. B. Rubin, Maximum likelihood from incomplete data via the EM algorithm. *Journal of the Royal Statistical Society: Series B*, **39**(1), pp. 1–38, November 1977.
11. F. Nan, Y. Wang, F. Li, W. Yang, and X. Ma, Better method than tail-fitting algorithm for jitter separation based on gaussian mixture model, *Journal of Electronic Testing*, **25**(6), pp. 337–342, Dec. 2009.
12. N. Vlassis and A. Likas, A kurtosis-based dynamic approach to Gaussian mixture modeling, *IEEE Trans. on Systems, Man, and Cybernetics—Part A: Systems and Humans*, **29**(4), pp. 393–399, July 1999.
13. S. Aouini, *Gaussian Mixture Parameter Estimation Using the Expectation-Maximization Algorithm*, ECSE 509 Technical Report, McGill University, November 2004.
14. B. Veillette and G. W. Roberts, Reliable analog bandpass signal generation, in *proceedings of the IEEE International Symposium on Circuits and Systems*, Monterey, CA, June 1998.
15. S. Aouini, K. Chuai and G. W. Roberts, A low-cost ATE phase signal generation technique for test applications, in *Proceedings of the 2010 IEEE International Test Conference*, Austin, TX, November 2010.
16. C. M. Miller and D. J. McQuate, Jitter analysis of high-speed digital systems, *Hewlett-Packard Journal*, pp. 49–56, February 1995.
17. T. J. Yamaguchi, M. Soma, M. Ishida, T. Watanabe and T. Ohmi, Extraction of instantaneous and RMS sinusoidal jitter using an analytic signal method, *IEEE Transactions on Circuits and Systems II: Analog and Digital Signal Processing*, **50**(6), pp. 288–298, June 2003.
18. S. C. Kak, The discrete Hilbert transform, *Proceedings of the IEEE*, **58**(4), pp. 585–586, April 1970.